Exocytosis and polarity in plant cells: insights by studying cellulose synthase complexes and the exocyst

Ying Zhang

Thesis committee

Thesis supervisor
Prof. dr. A.M.C. Emons
Professor of Plant Cell Biology
Wageningen University

Thesis co-supervisors
Dr. ir. M.J. Ketelaar
Assistant professor, Laboratory of Cell Biology
Wageningen University
Prof. dr. C.M. Liu
Director of Key Laboratory of Plant Molecular Physiology, Institute of Botany
Chinese Academy of Sciences

Other members
Prof. dr. ir. F.P.M. Govers, Wageningen University
Prof. dr. ir. G.H. Immink, Wageningen University
Prof. dr. C. Mariani, Radboud University, Nijmegen
Prof. dr. V. Zarsky, Charles University, Prague, Czech Republic

Exocytosis and polarity in plant cells: insights by studying cellulose synthase complexes and the exocyst

Ying Zhang

Contents

Background and outline of this thesis

Background and outline of this thesis

The contents of this thesis cover different processes involved in secretion of plant cells. Secretion in walled plant cells is required for a wide range of processes, such as cell wall formation, plant defense, homeostasis and mucilage and nectar production. All secretion involves exocytosis, which is the fusion of Golgi-derived vesicles with the plasma membrane that surrounds the cytoplasm. During exocytosis, the contents of vesicles are released into the space between the plasma membrane and the cell wall. The membrane of vesicles fuses with the plasma membrane by which the plasma membrane increases in size and integral membrane proteins are inserted. Here we focus on the regulation of exocytosis involved in plant cell growth and cell wall formation.

The cell wall of plants consists of two components, cell wall matrix and the load bearing cellulose microfibrils. Cell wall matrix consists of amongst others, pectin, hemicellulose and glycoproteins. Cell wall matrix is delivered against the existing cell wall as content of exocytotic vesicles. It can be compared to concrete in reinforced concrete. The load-bearing component of the plant cell wall, the cellulose microfibrils can be compared to the steel rods in reinforced concrete. They are produced by CESA complexes that reside in the plasma membrane and are propelled through that membrane by the force of cellulose production. It is thought that the orientation of cellulose microfibrils in the cell wall of growing cells (at least) co-determines the direction of cell expansion. This implies that intracellular mechanisms must be in place that guide the movement direction of CESA complexes that deposit cellulose microfibrils.

The plant cytoskeleton consists of actin filaments and microtubules. In interphase cells, microtubules have a cortical localization. In growing cells their organization is transverse to the growth axis, the same direction as the cellulose microfibrils. For decades it has been hypothesized that cortical microtubules (CMTs) are involved in orienting cellulose microfibrils, the product of the CESA complexes, but only over recent years, live cell co-localization studies using fluorescently tagged CESA complexes and microtubules have proven that CMTs can guide CESA complexes. Besides guiding CESA complexes, CMTs also serve as a preferential location for insertion of CESA complexes into the plasma membrane. Although CMTs determine the direction of cellulose microfibril deposition and the direction of cell growth in axially or diffuse growing cells, other mechanisms must be present to target exocytotic

vesicles to specific locations of cells, for example during cytokinesis, where they are targeted to the developing cell plate, and during tip growth, where they are targeted to the expanding tip.

In yeast and mammalian cells, a protein complex involved in regulating polar exocytosis has been identified: the exocyst. This protein complex is conserved in plants and does indeed localize to developing cell plates, indicating that it may play a role in polarized secretion. Little is known about the role of the exocyst in polarized secretion in interphase cells.

In chapter 1 of this thesis we review the current knowledge about the exocyst in plant cells. Although conserved, the plant exocyst has unique features that diverge from the exocyst in other eukaryotes. Mainly the number of genes that encode the subunit EXO70 is much larger than in vertebrates and fungi. We hypothesize that the large number of EXO70 genes has acquired plant-specific functions in for example cell wall deposition and defense.

In chapter 2 we have studied the exocyst subunit SEC3 in Arabidopsis. In this plant, SEC3 is encoded by 2 virtually identical, tandemly organized genes. We show that embryo development in a T-DNA insertional mutant in SEC3A is arrested; the embryo fails to acquire a heart shape. A similar sec3b mutant is gametophytically defective. We have used a functional SEC3A:GFP fusion to study SEC3A localization and show that SEC3 is present in blinking puncta at the plasma membrane. These puncta have average lifetimes of 6-12 seconds and could represent exocytotic events. In tip growing cells, these puncta do not have a polar localization and do not co-localize with CMTs and CESA complex insertion events. While we did not observe large differences in lifetime and density of SEC3 puncta in growing and fully-grown cells, the amount of SEC3a puncta dropped during treatment with the exocytosis inhibitor brefeldin A.

Chapter 3 focuses on the relationship between CMTs and CESA complexes. To address this, we used root hair cells. These are tubular cells that expand by tip growth. In the root hair tube, the density of CMTs decreases gradually during ageing of the cell, of which we took advantage to obtain insight in the role of CMTs in organizing CESA complexes and thus cellulose microfibrils. Firstly we show that CESA complexes are inserted and present in the plasma membrane of both tube and tip of both growing and fully-grown root hairs. Secondly, we study the consequences of different densities of CMTs on insertion and guidance of CESA complexes. We show that CMTs not only

change the movement direction of CESA complexes, they also decrease the variation in movement direction, which produces a cell wall with more tightly packed cellulose microfibrils.

In chapter 4 we investigate how CESA complexes that track widely spaced CMTs can produce a uniform cell wall texture of cellulose microfibrils with a much smaller spacing. We hypothesize that this could be either caused by CESA complexes that do not track CMTs, or by constant reorganization of cortical microtubules and show that the latter is the case.

Chapter 5 is a discussion in which we link the results from the previous chapters and provide a framework within the existing literature.

Chapter 1

The plant exocyst

**Ying Zhang [1], Chun-Ming Liu [2],
Anne Mie C. Emons [1, 3], Tijs Ketelaar [1]**

[1] Laboratory of Cell Biology, Wageningen University,
Building 107, Radix W1, Drovendaalsesteeg 1,
6708 PB Wageningen, The Netherlands

[2] Key Laboratory of Plant Molecular Physiology,
Institute of Botany, Chinese Academy of Sciences,
Nanxincun 20, Fragrant Hill, Beijing 100093, China

[3] Department of Biomolecular Systems, FOM Institute
for Atomic and Molecular Physics, Science Park 104,
1098 XG Amsterdam, The Netherlands

Abstract

The exocyst is an octameric vesicle tethering complex that functions upstream of SNARE mediated exocytotic vesicle fusion with the plasma membrane. All proteins in the complex have been conserved during evolution, and genes that encode the exocyst subunits are present in the genomes of all plants investigated to date. Although the plant exocyst has not been studied in great detail, it is likely that the basic function of the exocyst in vesicle tethering is conserved. Nevertheless, genomic and genetic studies suggest that the exocyst complex in plants may have more diversified roles than that in budding yeast. In this review, we compare the knowledge about the exocyst in plant cells to the well-studied exocyst in budding yeast, in order to explore similarities and differences in expression and function between these organisms, both of which have walled cells.

Introduction

Exocytosis is the fusion of Golgi-derived, exocytotic vesicles with the plasma membrane, where the vesicle membrane is inserted into the plasma membrane and the contents of the vesicles are deposited into the extracellular matrix. Exocytosis is a fundamental process in all eukaryotic cells and is vital for cell growth, cell polarity establishment, neurotransmission in animal cells, cell wall formation in plants and fungi, and numerous other processes that require delivery of components to the plasma membrane or to the extracellular environment. In most cell types, if not all, exocytosis is localized; it does not occur equally over the cell surface, but preferentially at specific locations.

In cell-wall forming plant cells, exocytotic vesicles contain cell-wall matrix precursors in their interior and cellulose synthase complexes in their membrane. Upon exocytosis, the matrix materials are deposited into the existing cell wall and cellulose synthase complexes inserted into the plasma membrane (Lindeboom et al. 2008). This makes the Golgi vesicle the unit, the building stones for cell growth. Most plant cells expand by intercalary growth; i.e., some cell wall facets expand more than others, for instance, the longitudinal ones in root epidermal cells. Since the cell wall of rapidly expanding facets does not become thinner and the wall of the slowly expanding facets does not get thicker, this suggests that the exocytosis in intercalary growing cells is polarized. In tip growing cells, e.g., root hairs and pollen tubes, where expansion takes place over a small surface area, the tip, exocytosis clearly is polarized (Miller et al. 1997; Geitmann and Emons 2000; Ketelaar et al. 2003).

During exocytosis, specific SNARE proteins, present on the vesicle (v-SNAREs) and the plasma membrane (t-SNAREs), are essential for membrane fusion. Tethering proteins are thought to form a connection between the vesicle and target membranes (Sztul and Lupashin 2006). Some of these tethering proteins bind directly to SNAREs and may play a critical role in the spatio-temporal regulation of SNARE complex assembly before membrane fusion (Cai et al. 2007; Kummel and Heinemann 2008). Many different tethering factors have been identified. Some of these factors are conserved over a wide range of organisms; others are specific for single trafficking pathways. Examples of these tethering factors are the exocyst, GARP (Golgi-associated retrograde protein), COG (conserved oligomeric Golgi), and Dsl1 complexes (Songer and Munson 2009).

The exocyst, an evolutionarily conserved protein complex, is required for tethering and fusion of the vesicles and plasma membrane at the sites of polarized exocytosis (Munson and Novick 2006). The exocyst is comprised of eight subunits: SEC3, SEC5, SEC6 SEC8, SEC10, SEC15, EXO70, and EXO84 (Boyd et al. 2004; Hsu et al. 2004; Tsuboi et al. 2005). Homologues of all exocyst subunits have been identified in the genome of *Arabidopsis* (Elias et al. 2003) rice, poplar and the moss *Physcomitrella patens* (Chong et al. 2009). In yeast and mammalian cells, each exocyst subunit is encoded by a single gene (Elias et al. 2003; Table 1). In *Arabidopsis*, SEC6 and SEC8 are encoded by a single gene, SEC3, SEC5, SEC10 and SEC15 are encoded by two genes, EXO84 is encoded by 3 genes and EXO70 by 23 genes (Table 1). The plant specific expansion of the number of *EXO70* genes suggests either that different *EXO70* genes are expressed during development and/or in different tissues that perform identical functions or that different *EXO70* genes may function in different, most likely plant specific types of exocytosis.

Table 1. The number of genes encoding different exocyst subunits in yeast, human and *Arabidopsis*

Exocyst genes	S.cerevisiae	Homo sapiens	Arabidopsis
SEC3	1	1	2
SEC5	1	1	2
SEC6	1	1	1
SEC8	1	1	1
SEC10	1	1	2
SEC15	1	1	2
EXO70	1	1	23
EXO84	1	1	3

Although very little is known about the plant exocyst, recent evidence indicates that it is essential for plant survival (Cole et al. 2005; Hála et al. 2008). It is likely that in plants, like in a wide range of other organisms, the exocyst plays a role in targeted exocytosis. However, much work is needed to generate a coherent picture of the function of the plant exocyst. In this review, we will compare the knowledge of the exocyst in the model organism budding yeast, which is a walled, unicellular organism, with results that have been obtained for the plant exocyst, in order to speculate about its functions in plants, multi-cellular walled organisms.

The structure and function of the budding yeast exocyst

The budding yeast, *Saccharomyces cerevisiae*, serves as a model system for polarized exocytosis, in which many of the components involved in both cell polarity and exocytosis have been well investigated (Brennwald and Rossi 2007). *S. cerevisiae* cells undergo a budding process, which requires polarized exocytosis to deliver newly synthesized materials to the daughter cell (Zhang et al. 2008). In budding yeast, the exocyst is essential for the polarized exocytosis. Loss of function of different exocyst subunits inhibits exocytosis and causes accumulation of secretory vesicles in the cytosol close to the budding region (bud tips and mother-bud necks (Hsu et al. 2004; Munson and Novick 2006; Zhang et al. 2008; Songer and Munson 2009). All of these 8 exocyst subunits accumulate at the sites where the active exocytosis takes place during budding and cell growth: the sites of bud emergence, the tips of the forming daughter cells and the mother-daughter connection (Zhang et al. 2005). The accumulation of the exocyst at the mother-daughter bud neck in *S. cerevisiae* is thought to be related to a function in cytokinesis. Although all the subunits have the same localization on membrane areas where active exocytosis takes place during the final stages of vesicle tethering, they achieve this localization via at least two different mechanisms: most exocyst subunits (SEC5, SEC6, SEC8, SEC10, SEC15 and EXO84) are delivered to the exocytosis sites through their attachment to the secrerory vesicles. This transport is dependent on actin cables which serve as tracks for the vesicle delivery (Hutagalung et al. 2009).

In contrast, SEC3 is localized to the active growing sites independent of actin cables and the ongoing secretion events. Hence, SEC3 is regarded as a spatial landmark for defining of the sites of secretion and for the recruitment of other exocyst subunits to the exocytotic sites. Polarized localization of Exo70 to the plasma membrane is partially actin-dependent (Finger et al. 1998; Wiederkehr et al. 2003; He and Guo 2009; Hutagalung et al. 2009). From the knowledge mentioned above it is expected that, in yeast, disruption of exocyst function will lead to defects in processes that depend on polarized exocytosis.

How does the exocyst recognize a specific membrane domain and bring the vesicles to this location for exocytosis? In yeast, the recruitment of SEC3 and EXO70 to the plasma membrane is mediated by both binding of these two subunits to inner plasma membrane leaflet phosphatidylinositol 4,5-bisphosphate ($PI(4,5)P_2$) (He et al. 2007; Liu et al. 2007; Zhang et al. 2008) and Rho family GTPases. Disruption of the

interaction of SEC3 and EXO70 with PI(4,5)P$_2$ (He et al. 2007; Zhang et al. 2008) or reduction of cellular PI(4,5)P$_2$ levels (He et al. 2007) inhibits the assembly of the yeast exocyst at the plasma membrane. It is certain that PI(4,5)P$_2$ binding is not sufficient for polar localization of the yeast exocyst, since PI(4,5)P$_2$ is not polarly distributed in the plasma membrane (He et al. 2007). Most likely the positional information for polar localization of the exocyst to the budding site is provided by Rho family GTPases. Such interactions with PI(4,5)P$_2$ are conserved in mammals (Liu et al. 2007), while in plants, PI(4,5)P$_2$ binding by exocyst subunits has not yet been studied. In addition, SEC3 is a downstream effector of activated Rho family GTPases CDC42 and RHO1. In *cdc42* or *rho1* mutants, the polarity of the exocyst localization at the plasma membrane is abolished (Guo et al. 2001; Zhang et al. 2001). In addition, Exo70 interacts with another Rho family GTPase, activated Rho3 (Robinson et al. 1999); however, since disruption of the interaction by mutations in EXO70 does not cause exocyst mis-localization or malfunction, it is not clear what kind of role this interaction plays (He et al. 2007; Hutagalung et al. 2009). There are indications that CDC42 acts as an upstream activator of EXO70 (Adamo et al. 2001). Taken together, these data clearly show that the regulation of the yeast exocyst by Rho family GTPases is poorly understood (He and Guo 2009). Besides Rho family GTPases, interactions with other GTPases have also been found. The interaction between SEC15 and the Rab GTPase SEC4 is essential for exocyst assembly (Guo et al. 1999). Vesicle tethering by the exocyst is followed by SNARE-mediated vesicle fusion with the plasma membrane. In this review, we will not focus on these interactions, as none of them have been identified in plants yet. We refer the reader to He and Guo (2009) for more information.

To gain insight into the function of the exocyst in exocytosis, knowledge about the exocyst structure and assembly, i.e. the spatial-temporal interaction patterns between the different exocyst subunits, is crucial. Protein-protein interactions within the exocyst complex have been identified in yeast (and animal) cells which were determined using various approaches, including yeast two hybrid experiments, co-immunoprecipitation and pull-down assays (reviewed by Munson and Novick 2006). The results of these interaction analyses are summarized in Figure 1.

Besides the above experiments, protein crystallography studies have given insight in the exocyst structure. The crystal structure of the large domains of three yeast exocyst subunits have been determined: nearly full-length budding yeast EXO70p (Dong et al. 2005; Hamburger et al. 2006), the C-terminal domain of budding yeast
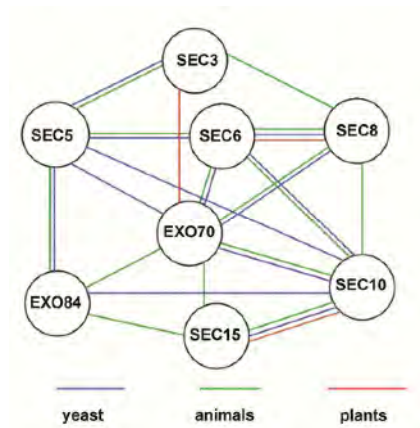
Figure 1. Interactions among different exocyst subunits. A comparison between yeast, animal and plants (the interactions in yeast and animals are reviewed by Munson and Novick 2006; The plant specific interactions are described in Hála et al. 2008).

EXO84p (Dong et al. 2005) and the C-terminal domain of budding yeast SEC6p (Sivaram et al. 2006). All these proteins contain multiple helical bundles, which are reflected in a similar, long, rod-like shape, with identical topology (Munson and Novick 2006; Sivaram et al. 2006; Songer and Munson 2009). Full length EXO70 consists of four bundles, and the C-terminal domains of EXO84 and SEC6 each consist of two bundles (Munson and Novick 2006). These bundles can pack together in an elongated side-to-side manner to form an elongated rod-like shape (Munson and Novick 2006). Recently, Croteau et al. (2009) employed hidden Markov models combined with secondary structure predictions to examine the sequence of each exocyst subunit. They showed that all exocyst subunits contain helical bundles, even though different exocyst subunits only share less than 10% of similarity at the primary sequence level. Using quick freeze/deep-etch cryo-electron microscopy of the chemically unfixed exocyst complex and exocyst complex prefixed with glutaraldehyde, a similar rod-like shape has been found, suggesting that this is the predominant structure of the exocyst. The unfixed complex appears as a flower with four to six 'petals' (4–6 nm wide × 10–30 nm long; Hsu et al. 1998). In contrast, the prefixed complex is a 13 nm × 30 nm structure with a couple of small appendages, which may more closely resemble the native exocyst structure (Munson and Novick 2006). Munson et al. (2006) suggested that the extended shape of unfixed complexes in the electron microscope might represent the structure of exocyst complexes bound

to Rab, Rho and Ral small GTPases, while connecting the vesicle and plasma membrane when they are relatively distant from each other. The closed structure of the fixed complex may represent the shape of the exocyst during later steps of membrane fusion. Undoubtedly, more evidence is needed to test this hypothesis.

Exocytosis in Plants and the Plant Exocyst

Exocytosis is probably used in a more diverse set of processes in multi-cellular plants, relative to budding yeast. Similar to budding yeast, exocytosis in plants functions during cell growth and cell division. However, numerous other processes also require polarized exocytosis in plants. Examples are the production of nectar by nectar-producing glands in flowers attracting bees (review: Nepi and Stpiczynska 2007), mucilage secretion by root cap cells (Wen et al. 2007), and secretion for secondary cell wall thickening. Besides these processes, polarized exocytosis has also been implicated in the positioning of PIN proteins to certain sides of the plasma membrane, which plays an important role in controlling the direction in which the plant growth regulator auxin leaves the cell (for review see: Vanneste and Friml 2009). PIN proteins are the first class of plant proteins shown to be associated with differential localization at plasma membrane and are the efflux carriers mediating directional transport of auxin. It is likely that many other processes require (polarized) exocytosis in plants. In other multicellular organisms such as insects and mammals, in which also exocytosis for different types of secretion occurs, the exocyst is involved in some, but not all types of polarized exocytosis (for review see: He and Guo 2009). Indeed, alternative tethering factors are available in fungi and animals. In plants, to our knowledge, only the exocyst genes have been proposed as a tethering complex. If the plant exocyst is involved in exocytosis for various types of secretion, the plant specific expansion of the EXO70 family of genes (Table 1) may represent a means of regulation of the plant exocyst during exocytosis processes for different purposes. From the evolutionary point of view, this hypothesis is plausible. Phylogenetic analyses suggest that, although the basic exocytosis machinery is established in the common eukaryotic ancestor and conserved among fungi, plants and animals, organisms in different kingdoms have apparently evolved different strategies to cope with trafficking the endomembrane and cellular components (Vernoud et al. 2003; Mouratou et al. 2005; Cole and Fowler 2006; Synek et al. 2006; Dacks et al. 2008; Chong et al. 2009; Zarsky et al. 2009). The use of T-DNA insertions in genes of

the large EXO70 family in *Arabidopsis* offer an opportunity to determine whether the plant exocyst plays a role in exocytosis in different types of processes.

Different plant exocyst subunits have been knocked out and the consequences on plantd evelopment have been studied. Lines with T-DNA insertions that disrupt expression of *Arabidopsis* exocyst subunits encoded by single genes such as SEC6 and SEC8 (see Table 1) invariably fail to produce progeny homozygous forthese T-DNA insertion (Cole et al. 2005; Hála et al. 2008). Also insertion in some subunits that are encoded by two genes fail to produce progeny that is homozygous for the T-DNA insertion (double mutants with both disrupted SEC5A and SEC5B; SEC15A). The failure to produce homozygous knockouts for these insertions can be traced to a male transmission defect, caused by defects in pollen tube germination and/or pollen tube growth (Cole et al. 2005; Hála et al. 2008). Due to the failure to produce homozygous plants with the above mentioned exocyst genes it is only feasible to study the role of the exocyst in pollen using T-DNA insertion lines. However, the prominent defects in pollen tube growth strongly suggest that the exocyst in *Arabidopsis* plays an essential role in polar exocytosis, a requirement for tip growth of pollen tubes.

Besides these pollen lethal mutants, a T-DNA insertion in AtEXO70A1, causes the disruption of root hair growth and the formation of the stigmatic papillae. Plants with homozygous T-DNA insertions in AtEXO70A1 also have shortened hypocotyls in etiolated seedlings, smaller organs, loss of apical dominance and reduced fertility (Synek et al. 2006). The shortened etiolated hypocotyl phenotype of the AtEXO70A1mutant was enhanced in double mutants with sec8 or sec5 alleles that normally do not display vegetative phenotypic defects (Hála et al. 2008).

Recently, it was showed that AtEXO70A1 plays critical role in self-imcompatibility in crucifer species (Samuel et al. 2009). In *Brassica napus*, the self-incompatibility is mediated through the interaction of S-locus Cys-rich/S-locus protein 11 (SCR/SP11) carried by pollen coat and the stigma-specific S Receptor Kinase (SRK; Schopfer et al. 1999; Takasaki et al. 2000; Silva et al. 2001). Following the attachment of self pollen to the stigma, SCR/SP11 binds to the membrane-localized SRK, activates SRK, which then interacts with and phosphorylates the ARM-repeat containing 1 (ARC1), an E3 ubiquitin ligase, to trigger rejection of self pollen (Goring and Walker 2004; Murase et al. 2004; Kakita et al. 2007). ARC1 interacts directly with Axo70A1 in vitro, and thus could trigger inhibition of EXO70A1 via degradation in a self-incompatible response (Samuel et al. 2009). Consistent with this idea, additional experiments showed that

EXO70A1 can be considered to be a compatibility factor in the stigma. Both *Brassica* and *Arabidopsis* lines with reduced EXO70A1 in the stigma (by RNAi or mutation) are incapable of accepting compatible pollen. By contrast, overexpression of EXO70A1 in *Brassica* is sufficient to partially overcome the self pollen rejection response in self-incompatible *Brassica* plants. These experiments for the first time bring the exocyst to the context of protein degradation-based self-imcompatibility response in the stigma (Samuel et al. 2009). Of course whether EXO70A1 participates in pollen-stigma interactions through a role in exocytosis, and which cellular materials could be exported during this process remain to be studied.

Known phenotypes of T-DNA insertions in *Arabidopsis* genes that encode exocyst subunits and a list of the other *Arabidopsis* exocyst genes are given in Table 2. Interestingly, disruption of the Roothairless1 (RTH1) gene in maize, which encodes a homologue of SEC3, resulted in defects in root hair elongation (Wen et al. 2005). Since there are at least SEC3 genes present in the genome of maize, this mild phenotype in comparison to that of sec3b knockout lines in *Arabidopsis* possibly is likely to reflect redundancy with the other SEC3 isoforms. Even so, the tip growth of root hairs is a clear type of polarized exocytosis (Emons AMC 2009), in which the exocyst is involved in *Arabidopsis* (the AtEXO70A1 mutant has a root hair growth phenotype (Synek et al. 2006)) and also in maize.

Hála et al. (2008) performed yeast two hybrid assays to assess interactions between different subunits within the plant exocyst, and showed that SEC6 interacts with SEC8, SEC10 interacts with SEC15B and SEC3A interacts with EXO70A1. The interactions between SEC6 and SEC8 and the interaction between SEC10 and SEC15 are conserved, but the interaction between SEC3 and an EXO70 subunit appears to be unique for plants. Besides interactions conserved in yeast and mammals, unique interactions have also been found in these organisms (Figure 1). These non-conserved interactions may reflect differences in for example exocyst aggregation in different organisms (see below). When compared to animal cells and yeast, the number of interactions between different exocyst subunits in *Arabidopsis* found by Hála et al. (2008) seems low (Figure 1). It is likely that this reflects the limited amount of research into the plant exocyst rather than major differences in exocyst functioning between plants and other species.

The function of the plant exocyst in polarized exocytosis in tip growing pollen tubes suggests its presence in the tips of growing pollen tubes. Hála et al. (2008) used

Table 2. List of *Arabidopsis* exocyst genes

Gene	Protein	Developmental defects in knockout lines	Reference
At1g47550	SEC3A	unknown	
At1g47560	SEC3B	unknown	
At1g76850	SEC5A	Defects in pollen germination and pollen tube growth in sec5a and sec5b double mutant	Hála et al. 2008
At1g21170	SEC5B	Defects in pollen germination and pollen tube growth in in sec5a and sec5b double mutant	Hála et al. 2008
At1g71820	SEC6	Defects in pollen germination and pollen tube growth	Hála et al. 2008
At3g10380	SEC8	Defects in pollen germination and pollen tube growth	Cole et al. 2005
At5g12370*	SEC10	unknown	
At3g56640	SEC15A	Defects in pollen germination	Hála et al. 2008
At4g02350	SEC15B	unknown	
At1g10385	EXO84A	unknown	
At5g49830	EXO84B	unknown	
At1g10180	EXO84C	unknown	
At5g03540	EXO70A1	Defects in polarized cell growth and plant development (see text)	Synek et al. 2006
At5g52340	EXO70A2	unknown	
At5g52350	EXO70A3	unknown	
At 5g58430	EXO70B1	unknown	
At1g07000	EXO70B2	unknown	
At 5g13150	EXO70C1	unknown	
At5g13990	EXO70C2	unknown	
At1g72470	EXO70D1	unknown	
At1g54090	EXO70D2	unknown	
At3g14090	EXO70D3	unknown	
At3g29400	EXO70E1	unknown	
At5g61010	EXO70E2	unknown	
At5g50380	EXO70F1	unknown	
At4g31540	EXO70G1	unknown	
At1g51640	EXO70G2	unknown	
At3g55150	EXO70H1	unknown	
At2g39380	EXO70H2	unknown	
At3g09530	EXO70H3	unknown	
At3g09520	EXO70H4	unknown	
At2g28640	EXO70H5	unknown	
At1g07725	EXO70H6	unknown	
At5g59730	EXO70H7	unknown	
At2g28650	EXO70H8	unknown	

*The *At5g12370* locus contains two tandemly repeated *SEC10* genes (Hála et al. 2008).
The table gives AGI numbers, exocyst subunit names, developmental defects in knockout lines and references to this work.

antibodies against SEC6, SEC8 and EXO70 A1 for an immunolocalisation study in Tobacco pollen tubes. Although all these exocyst subunits examined localized to the

tip-region of growing pollen tubes, it appears that none of them are really localized locally to the expanding membrane. However, the imaging/sample preparation techniques that were used in these experiments do not adequately assess this protein localization; the samples were fixed in paraformaldehyde (and not by rapid freeze fixation), and examined only at the light microscope level (Zonia and Munnik 2009). Nevertheless, SEC6 and SEC8 do preferentially associate with the membrane fractionin Tobacco pollen (Hála et al. 2008). Even so, it is still not clear which protein(s) define the target of the exocytosis for pollen tube tip growth. Even so, the apical localization of exocyst subunits in pollen tubes fits with its putative role in polarized secretion in plants and is very similar to the accumulation of the exocyst in the bud region in budding yeast. Chong et al. (Chong et al. 2009) studied the localization globular-like structures in the perinuclear region of the cell. These structures included TGN/early endosomes membranes as well as late endosome membranes. AtSEC6, AtSEC8 and AtEXO70A1 showed a diffuse cytosolic distribution. Chong et al. (2009) suggest that the equal cytoplasmic fluorescence may be caused by the undifferentiated and unpolarized state of BY-2 cells. However, since these cells elongate, they are polarized cells. AtEXO70E2 and AtEXO70G1 localized to TGN/early endosome markers and late endosome/prevacuolar compartment markers labeled punctuate structures throughout the cytoplasm. Co-expression with other fluorescently tagged exocyst subunits (AtSEC5a, AtSEC8, AtSEC15a, AtSEC15b and AtEXO84b) recruited these proteins to the same locations. This suggests thatAtEXO70E2 and AtEXO70G1 may be triggering the formation of high-order complexes at these locations. However, one has to realize that all the above localization studies have been carried out by overexpression of exocyst subunits, which may cause localization artifacts. Structural studies on the plant exocyst have not been performed so far. However, electron tomographs of high-pressure-frozen cells at the post-meiotic cytokinesis during pollen development and cell plate formation of the somatic cells in *Arabidopsis* revealed 24 nm-long structures tethering the membrane vesicles (Otegui and Staehelin 2004; Segui-Simarro et al. 2004), which resemble the mammalian exocyst complex visualized by transmission electron microscopy (Hsu et al. 1998). If these structures observed in plants represent the plant exocyst, the exocyst in plant cells has a similar rod-shaped structure with helical bundles as the yeast exocyst. Furthermore, showing that these structures are indeed the plantexocyst would also suggest that the conserved rod-shape is required for exocyst complex function.

Co-purification experiments provide additional evidence that the different plant

exocyst subunits function as a complex. Hála et al. (2008) found that most ofthe *Arabidopsis* exocyst subunits are present in high molecular mass fractions. It is worth noting that Hála et al. (2008) estimated the molecular mass of the exocyst at 900 kD, larger than the predicted mass of 760 kD when each subunit is represented as a single protein. It is possible that non-exocyst proteins co-purify with the exocyst, a phenomenon which is also observed in mammals (Yeaman et al. 2004). Alternatively, due to the shape of the complexes, their mobility may be decreased. Hála et al. (2008) found that seven plant exocyst subunits (SEC3, SEC5, SEC6, SEC8, SEC10, SEC15 and EXO70A1) co-fractionated during a purification procedure that iscommonly used for non-plant exocyst purification. A reduction in the amount of and SEC15 in relation to the other exocyst subunits was found after the purification procedure, which suggests that these subunits are loosely associated with the exocyst, whereasother subunits serve as a more tightly associated core of the exocyst. Hála et al. (2008) were not able to detect EXO84 in their experiments, but suggest that it will be in the same fractions. Once the structure and interaction patterns within the plant exocyst have been determined, a more comprehensive comparisonbetween the exocyst complexes of yeast, mammals and plants can be made.

Although in *Arabidopsis*, it has been shown that Rab GTPase RabA4b localizes to the tips of growing root hair cells (Preuss et al. 2004) and RabA4d to the tips of growing pollen tubes, where it has a clear role in pollen tube growth (Szumlanski and Nielsen 2009), direct interactions between exocyst subunits and small GTPases have not been reported yet. However, Lavy et al. (2007) showed that ICR1, a novel effector of an activated ROP (Rho of Plants) GTPase interacts with SEC3A. Ectopic expression of ICR1 causes similar growth defects as expression of constitutively active ROPs, such as changes in the cellular morphology of leaf-epidermis-pavement and root-hair cells. This phenotype may well be caused by ectopic activation of the exocyst. The interaction of Sec3A with the ROP effector ICR1 and unique plant specific interactions between the plant exocyst and the exocyst in other organisms shows that, although conserved instructure and very likely in its general function (exocytotic vesicle tethering to the plasma membrane), the plant exocyst may have unique features. Unique features, both in terms of exocytosis for a variety of processes in which it is involved, and in terms of assembly and activation and localization. It is likely that over the coming years, the exciting, novel features of the plant exocyst will be the focal point of numerous studies and more and more detailed information about the plant exocyst and plant polarized exocytosis in general will become available. Especially live cell imaging of the localization of different plant exocyst subunits will give valuable information about exocyst functioning in secretion for different purposes.

Acknowledgements

References

- Adamo JE, Moskow JJ, Gladfelter AS, Viterbo D, Lew DJ, Brennwald PJ (2001) Yeast Cdc42 functions at a late step in exocytosis, specifically during polarized growth of the emerging bud. *J. Cell Biol.* **155**, 581–592.

- Boyd C, Hughes T, Pypaert M, Novick P (2004) Vesicles carry most exocyst subunits to exocytic sites marked by the remaining two subunits, Sec3p and Exo70p. *J. Cell Biol.* **167**, 889–901.

- Brennwald P, Rossi G (2007) Spatial regulation of exocytosis and cell polarity: yeast as a model for animal cells. *FEBS Lett.* **581**,2119–2124.

- Cai H, Reinisch K, Ferro-Novick S (2007) Coats, tethers, Rabs, and SNAREs work together to mediate the intracellular destination of a transport vesicle. *Dev. Cell* **12**, 671–682.

- Chong YT, Gidda SK, Sanford C, Parkinson J, Mullen RT, Goring DR (2009) Characterization of the *Arabidopsis thaliana* exocyst complex gene families by phylogenetic, expression profiling, and subcellular localization studies. *New Phytol.*

- Cole RA, Fowler JE (2006) Polarized growth: maintaining focus on the tip. *Curr. Opin. Plant Biol.* **9**, 579–588.

- Cole RA, Synek L, Zarsky V, Fowler JE (2005) SEC8, a subunit of the putative *Arabidopsis* exocyst complex, facilitates pollen germination and competitive pollen tube growth. *Plant Physiol.* **138**, 2005–2018.

- Croteau NJ, Furgason ML, Devos D, Munson M (2009) Conservation of helical bundle structure between the exocyst subunits. *PLoS One***4**, e4443.

- Dacks JB, Poon PP, Field MC (2008) Phylogeny of endocytic components yields insight into the process of nonendosymbiotic organelle evolution. *Proc. Natl. Acad. Sci. USA* **105**, 588–593.

- Dong G, Hutagalung AH, Fu C, Novick P, Reinisch KM (2005) The structures of exocyst subunit Exo70p and the Exo84p C-terminal domains reveal a common motif. *Nat. Struct. Mol. Biol.* **12**, 1094–1100.

- Elias M, Drdova E, Ziak D, Bavlnka B, Hála M, Cvrckova F, Soukupova H, Zarsky V (2003) The exocyst complex in plants. *Cell Biol. Int.* **27**,199–201.

- Emons AMC KT (2009) *Intracellular Organization: A Prerequisite for Root Hair Elongation and Cell Wall Deposition*, vol. **12**. Springer, Berlin, Heidelberg, New York .

- Finger FP, Hughes TE, Novick P (1998) Sec3p is a spatial landmark for polarized secretion in budding yeast. *Cell* **92**, 559–571.

- Geitmann A, Emons AMC (2000) The cytoskeleton in plant and fungal cell tip growth. *J. Microsc. Oxford* **198**, 218–245.

- Goring DR, Walker JC (2004) Plant sciences. Self-rejection–a new kinase connection. *Science* **303**, 1474–1475.

- Guo W, Roth D, Walch-Solimena C, Novick P (1999) The exocyst is an effector for Sec4p, targeting secretory vesicles to sites of exocytosis. *EMBO J.* **18**, 1071–1080.

- Guo W, Tamanoi F, Novick P (2001) Spatial regulation of the exocyst complex by Rho1 GTPase. *Nat. Cell Biol.* **3**, 353–360.

- Hála M, Cole R, Synek L, Drdova E, Pecenkova T, Nordheim A, Lamkemeyer T, Madlung J, Hochholdinger F, Fowler JE, Zarsky V (2008)An exocyst complex functions in plant cell growth in *Arabidopsis* and tobacco. *Plant Cell* **20**, 1330–1345.

- Hamburger ZA, Hamburger AE, West AP Jr. , Weis WI (2006) Crystal structure of the S.cerevisiae exocyst component Exo70p. *J. Mol. Biol.***356**, 9–21.

- He B, Guo W (2009) The exocyst complex in polarized exocytosis. *Curr. Opin. Cell Biol.* **21**, 537–542.

- He B, Xi F, Zhang X, Zhang J, Guo W (2007) Exo70 interacts with phospholipids and mediates the targeting of the exocyst to the plasma membrane. *EMBO J.* **26**, 4053–4065.

- Hsu SC, Hazuka CD, Roth R, Foletti DL, Heuser J, Scheller RH (1998) Subunit composition, protein interactions, and structures of the mammalian brain sec6/8 complex and septin filaments. *Neuron* **20**, 1111–1122.

- Hsu SC, TerBush D, Abraham M, Guo W (2004) The exocyst complex in polarized exocytosis. *Int. Rev. Cytol.* **233**, 243–265.

- Hutagalung AH, Coleman J, Pypaert M, Novick PJ (2009) An internal domain of Exo70p is required for actin-independent localization and mediates assembly of specific exocyst components. *Mol. Biol. Cell* **20**, 153–163.

- Kakita M, Murase K, Iwano M, Matsumoto T, Watanabe M, Shiba H, Isogai A, Takayama S (2007) Two distinct forms of M-locus protein kinase localize to the plasma membrane and interact directly with S-locus receptor kinase to transduce self-incompatibility signaling in*Brassica rapa*. *Plant Cell* **19**, 3961–3973.

- Ketelaar T, De Ruijter NC, Emons AM (2003) Unstable F-actin specifies the area and microtubule direction of cell expansion in *Arabidopsis*root hairs. *Plant Cell* **15**, 285–292.

- Kummel D, Heinemann U (2008) Diversity in structure and function of tethering complexes: evidence for different mechanisms in vesicular transport regulation. *Curr. Protein Pept. Sci.* **9**, 197–209.

- Lavy M, Bloch D, Hazak O, Gutman I, Poraty L, Sorek N, Sternberg H, Yalovsky S (2007) A Novel ROP/RAC effector links cell polarity, root-meristem maintenance, and vesicle trafficking. *Curr. Biol.* **17**, 947–952.

- Lindeboom J, Mulder BM, Vos JW, Ketelaar T, Emons AM (2008) Cellulose microfibril deposition: coordinated activity at the plant plasma membrane. *J. Microsc.* **231**, 192–200.

- Liu J, Zuo X, Yue P, Guo W (2007) Phosphatidylinositol 4,5-bisphosphate mediates the targeting of the exocyst to the plasma membrane for exocytosis

- in mammalian cells. *Mol. Biol. Cell* **18**, 4483–4492.

- Miller DD, DeRuijter NCA, Emons AMC (1997) From signal to form: aspects of the cytoskeleton plasma membrane cell wall continuum in root hair tips. *J. Exp. Bot.* **48**, 1881–1896.

- Mouratou B, Biou V, Joubert A, Cohen J, Shields DJ, Geldner N, Jurgens G, Melancon P, Cherfils J (2005) The domain architecture of large guanine nucleotide exchange factors for the small GTP-binding protein Arf. *BMC Genomics* **6**, 20.

- Munson M, Novick P (2006) The exocyst defrocked, a framework of rods revealed. *Nat. Struct. Mol. Biol.* **13**, 577–581.

- Murase K, Shiba H, Iwano M, Che FS, Watanabe M, Isogai A, Takayama S (2004) A membrane-anchored protein kinase involved in*Brassica* self-incompatibility signaling. *Science* **303**, 1516–1519.

- Nepi M, Stpiczynska M (2007) Nectar resorption and translocation in *Cucurbita* pepo L. and *Platanthera chlorantha* Custer (Rchb.). *Plant Biol. (Stuttg.)* **9**, 93–100.

- Otegui MS, Staehelin LA (2004) Electron tomographic analysis of post-meiotic cytokinesis during pollen development in *Arabidopsis thaliana.* *Planta* **218**, 501–515.

- Preuss ML, Serna J, Falbel TG, Bednarek SY, Nielsen E (2004) The *Arabidopsis* Rab GTPase RabA4b localizes to the tips of growing root hair cells. *Plant Cell* **16**, 1589–1603.

- Robinson NG, Guo L, Imai J, Toh EA, Matsui Y, Tamanoi F (1999) Rho3 of *Saccharomyces cerevisiae*, which regulates the actin cytoskeleton and exocytosis, is a GTPase which interacts with Myo2 and Exo70. *Mol. Cell Biol.* **19**, 3580–3587.

- Samuel MA, Chong YT, Haasen KE, Aldea-Brydges MG, Stone SL, Goring DR (2009) Cellular pathways regulating responses to compatible and self-incompatible pollen in *Brassica* and *Arabidopsis* stigmas intersect at Exo70A1, a putative component of the exocyst complex. *Plant Cell*

- Schopfer CR, Nasrallah ME, Nasrallah JB (1999) The male determinant of self-incompatibility in *Brassica*. *Science* **286**, 1697–1700.

- Segui-Simarro JM, Austin JR 2nd , White EA, Staehelin LA (2004) Electron tomographic analysis of somatic cell plate formation in meristematic cells of *Arabidopsis* preserved by high-pressure freezing. *Plant Cell* **16**, 836–856.

- Silva NF, Stone SL, Christie LN, Sulaman W, Nazarian KA, Burnett LA, Arnoldo MA, Rothstein SJ, Goring DR (2001) Expression of the S receptor kinase in self-compatible *Brassica napus* cv. Westar leads to the allele-specific rejection of self-incompatible *Brassica napus* pollen. *Mol. Genet. Genomics* **265**, 552–559.

- Sivaram MV, Furgason ML, Brewer DN, Munson M (2006) The structure of the exocyst subunit Sec6p defines a conserved architecture with diverse roles. *Nat. Struct. Mol. Biol.* **13**, 555–556.

- Songer JA, Munson M (2009) Sec6p anchors the assembled exocyst complex at sites of secretion. *Mol. Biol. Cell* **20**, 973–982.

- Synek L, Schlager N, Elias M, Quentin M, Hauser MT, Zarsky V (2006) AtEXO70A1, a member of a family of putative exocyst subunits specifically expanded in land plants, is important for polar growth and plant development. *Plant J.* **48**, 54–72.

- Sztul E, Lupashin V (2006) Role of tethering factors in secretory membrane traffic. *Am. J. Physiol. Cell Physiol.* **290**, C11–26.

- Szumlanski AL, Nielsen E (2009) The Rab GTPase RabA4d regulates pollen tube tip growth in *Arabidopsis thaliana*. *Plant Cell* **21**, 526–544.

- Takasaki T, Hatakeyama K, Suzuki G, Watanabe M, Isogai A, Hinata K (2000) The S receptor kinase determines self-incompatibility in *Brassica stigma*. *Nature* **403**, 913–916.

- Tsuboi T, Ravier MA, Xie H, Ewart MA, Gould GW, Baldwin SA, Rutter GA (2005) Mammalian exocyst complex is required for the docking step of insulin vesicle exocytosis. *J. Biol. Chem.* **280**, 25565–25570.

- Vanneste S, Friml J (2009) Auxin, a trigger for change in plant development. *Cell* **136**, 1005–1016.

- Vernoud V, Horton AC, Yang Z, Nielsen E (2003) Analysis of the small GTPase gene superfamily of *Arabidopsis*. *Plant Physiol.* **131**, 1191–1208.

- Wen F, VanEtten HD, Tsaprailis G, Hawes MC (2007) Extracellular proteins in pea root tip and border cell exudates. *Plant Physiol.* **143**, 773–783.

- Wen TJ, Hochholdinger F, Sauer M, Bruce W, Schnable PS (2005) The roothairless1 gene of maize encodes a homolog of sec3, which is involved in polar exocytosis. *Plant Physiol.* **138**, 1637–1643.

- Wiederkehr A, Du Y, Pypaert M, Ferro-Novick S, Novick P (2003) Sec3p is needed for the spatial regulation of secretion and for the inheritance of the cortical endoplasmic reticulum. *Mol. Biol. Cell* **14**, 4770–4782.

- Yeaman C, Grindstaff KK, Nelson WJ (2004) Mechanism of recruiting Sec6/8 (exocyst) complex to the apical junctional complex during polarization of epithelial cells. *J. Cell Sci.* **117**, 559–570.

- Zarsky V, Cvrckova F, Potocky M, Hála M (2009) Exocytosis and cell polarity in plants – exocyst and recycling domains. *New Phytol.* **183**, 255–272.

- Zhang X, Bi E, Novick P, Du L, Kozminski KG, Lipschutz JH, Guo W (2001) Cdc42 interacts with the exocyst and regulates polarized secretion. *J. Biol. Chem.* **276**, 46745–46750.

- Zhang X, Orlando K, He B, Xi F, Zhang J, Zajac A, Guo W (2008) Membrane association and functional regulation of Sec3 by phospholipids and Cdc42. *J. Cell Biol.* **180**, 145–158.

- Zhang X, Zajac A, Zhang J, Wang P, Li M, Murray J, TerBush D, Guo W (2005) The critical role of Exo84p in the organization and polarized localization of the exocyst complex. *J. Biol. Chem.* **280**, 20356–20364.

- Zonia L, Munnik T (2009) Uncovering hidden treasures in pollen tube growth mechanics. *Trends Plant Sci.* **14**, 318–327.

Chapter 2

The exocyst subunit SEC3A is essential for embryo development and accumulates in transient puncta at the plasma membrane

Ying Zhang [a], Richard Immink [b], Chun-Ming Liu [c],

Anne Mie Emons [a,d], Tijs Ketelaar [a]

[a] Laboratory of Cell Biology, Wageningen University, Building 107, Radix W1, Drovendaalsesteeg 1, 6708 PB Wageningen, The Netherlands

[b] Bioscience, Plant Research International, Wageningen University and Research Center, Building 107, Radix W1, Drovendaalsesteeg 1, 6708 PB Wageningen, The Netherlands

[c] Key Laboratory of Plant Molecular Physiology, Institute of Botany, Chinese Academy of Sciences, Nanxincun 20, Fragrant Hill, Beijing 100093, China

[d] Department of Biomolecular Systems, FOM Institute for Atomic and Molecular Physics, Science Park 104, 1098 XG Amsterdam, The Netherlands

Abstract

SEC3 is one of the subunits of the exocyst, a conserved octameric protein complex that is essential for polarized secretion in mammals and fungi. Although the exocyst is essential for plant development, its precise function has not been elucidated. Arabidopsis possesses two *SEC3* genes, *SEC3A* and *SEC3B*. We have analysed plants mutated in these genes. *sec3b* mutants are gametophytically lethal, whereas *sec3a* mutants are defective in the globular to the heart stage transition in embryogenesis. Expression of SEC3A:GFP complements the *sec3a* mutant phenotype and confocal microscopy reveals that the fusion protein localizes to the initial cell plate during early stages of cell plate formation and to the division wall from 30 min after cytokinesis onwards, while it is absent from the expanding cell plate, similar to the other plant exocyst subunits.

In interphase cells SEC3A:GFP localizes to the cytoplasm and to the plasma membrane, where it forms immobile, punctuate structures with discrete lifetimes of 2-40 s. These puncta are equally distributed over the cell surface of root epidermal cells and tip growing root hairs. In addition, the density of puncta does not decrease after growth termination of these cells, but decreases strongly when exocytosis is inhibited by treatment with brefeldin A.

Introduction

Exocytosis is a fundamental process for cells of all eukaryotic organisms. It is required for secretion of extracellular materials and for enlargement of the plasma membrane. In plant cells, exocytosis is also crucial for cell wall formation and cell elongation, which are coupled processes. Vesicle fusion for anisotropic plant cell elongation occurs in a non-random pattern, which implies that the sites of exocytosis have to be temporally and spatially controlled. This could occur through directed Golgi body transport by the actin cytoskeleton and targeting of Golgi vesicles to specific sites of the plasma membrane and/or by tethering and docking of the vesicles to a specific membrane domain before exocytosis. In yeast, the exocyst is involved in vesicle tethering prior to exocytotic vesicle membrane fusion with the plasma membrane. Since almost all plant cells expand in a polar fashion either by axial or by tip growth, a local tethering complex could be important for determination of the cell expansion orientation.

In budding yeast, bud growth requires polarized exocytosis. An octameric protein complex, termed the exocyst, has been identified that serves as a tethering factor for exocytotic vesicles specifically in the bud tip (TerBush et al., 1996). Polarized localization of the exocyst is essential for polarized secretion during bud formation (Hsu et al. 2004; Munson and Novick 2006; Zhang et al. 2008; Songer and Munson 2009).

The exocyst consists of SEC3, SEC5, SEC6, SEC8, SEC10, SEC15, EXO70 and EXO84 (Elias et al., 2003; Hsu et al., 1996; Hee et al., 1997, Zhang et al. 2010, Li et al., 2010). Budding yeast SEC3 is considered to be a landmark protein for polarized exocytosis, since it is localized to the plasma membrane where exocytosis will occur and involved in recruiting the other exocyst subunits that reside in the cytoplasm or are associated to vesicles to this location (Finger et al. 1998; Wiederkehr et al. 2003; Hutagalung et al., 2009). It is thought that the polarized localization of SEC3 is mediated by interactions with phosphatidylinositol 4,5-bisphosphate (PI(4,5)P2) in the inner leaflet of the plasma membrane (He et al. 2007; Liu et al. 2007; Zhang et al. 2008) and with Rho family GTPases (He and Guo, 2009). The actin cytoskeleton that is essential for the delivery of the vesicle associated subunits is not involved in the positioning of SEC3 (Finger et al. 1998; Wiederkehr et al. 2003; Hutagalung et al., 2009).

The plant exocyst has received relatively little attention, although it could serve as a key component for the regulation of polarized exocytosis during cell expansion. All exocyst subunits are conserved in plants and a plant specific amplification of EXO70 genes has occurred during evolution, resulting in 23 EXO70 genes in Arabidopsis and 39 in rice (Elias et al., 2003; Synek et al., 2006; Li et al., 2010). The expression patterns of these EXO70 genes are different but they are all expressed in cells that are actively dividing or expanding (Li et al., 2010), supporting the idea that the exocyst is involved in the regulation of polarized exocytosis in plant cells.

Mutations in plant exocyst subunits which are encoded by one or two genes (SEC5, SEC6, SEC8, SEC15) cause defects in pollen germination and tube growth (Cole et al., 2005; Synek et al., 2006), suggesting an important function of the exocyst during plant cell tip growth. Mutations in the exocyst subunits which are encoded by more than two copies of genes (EXO84 (3 genes) and EXO70 (23 genes)) cause mild defects (Synek et al., 2006; Samuel et al., 2009; Kulich et al., 2010; Pecenková et al., 2011). Plant homologues of SEC3 have only been studied in maize. A mutation in the SEC3 encoding gene *ROOTHAIRLESS1* results in the failure of proper root hair elongation (Wen et al., 2005). However, the expression patterns of maize SEC3 genes are not known, which makes it difficult to interpret this result. In Arabidopsis, SEC3 is encoded by 2 nearly identical genes in a tandem arrangement (Elias et al., 2003). This has hampered genetic analysis of SEC3 function in Arabidopsis. Interestingly, in Arabidopsis the ICR1 adaptor protein interacts with SEC3, which provides a putative link to activated ROP (Rho of plants) GTPases (Lavy et al., 2007). Since ROP GTPases serve as intracellular polarity markers (Yang, 2008), this link suggests that exocyst recruitment could be (partially) ROP mediated.

Hála et al. (2008) have shown by immunocytochemistry that SEC6, SEC8 and EXO70A1 are enriched in the apex of growing tobacco pollen tubes, which is consistent with a role in polarized exocytosis. In tobacco Bright Yellow 2 (BY-2) suspension cultured cells, transient expression of Arabidopsis SEC5A, SEC15A, SEC15B and EXO84B fused to GFP resulted in fluorescent, globular structures in the perinuclear cytosol (Chong et al., 2010), whereas immunofluorescence revealed that the intracellular localization of EXO70 proteins differs depending on the isoform; they either show a cytoplasmic organization or localize to smaller or larger compartments with different degrees of co-localization with snares specific for early endosomes, late endosomes and the trans Golgi network (Chong et al., 2009; Wang et al., 2010).

Distinct structures were also observed by Samuel et al. (2009) in stigma cells expressing RFP:EXO70A1. Upon opening of the flowers, the RFP:EXO70A1 fluorescence relocated to the cell cortex, suggesting that EXO70A1 localization depends on the developmental stage. During cytokinesis, the Arabidopsis exocyst subunits, SEC6, SEC8, SEC15B, EXO70A1 and EXO84B localize to the early cell plate, whereafter their localization on the cell plate disappears (Fendrych et al., 2010). After completion of cytokinesis, exocyst subunits reappear on the division wall for a short period after completion of cytokinesis (Fendrych et al., 2010).

Recent research has revealed that EXO70E2 localizes to discrete punctate structures at the plasma membrane and in the cytosol of Arabidopsis cells and tobacco BY-2 suspension cultured cells (Wang et al., 2010). The compartments at the plasma membrane are contained by two membranes, both of which are EXO70E2 decorated, and secretory. Upon secretion, the inner membrane is expelled into the apoplast. These organelles that do not co-localize with any known organelle have been named EXPO (exocyst positive organelles; Wang et al., 2010). For a better understanding of the localization of different exocyst subunits and their assembly into multi-component complexes additional work is needed.

Here we report the characterization of the two *SEC3* genes in Arabidopsis, *SEC3A* and *SEC3B*. Disruption of the *SEC3B* gene is gametophytically lethal, whereas disruption of the *SEC3A* gene is embryo lethal, with defects in the acquisition of embryo polarity. During cytokinesis, SEC3A-GFP localizes to the early cell plate and to the completed division wall, respectively, similarly to other exocyst subunits (Fendrych et al., 2010). In interphase cells, SEC3A-GFP localizes to the cytoplasm and to the plasma membrane, where it forms immobile, punctate structures with discrete lifetimes. In tip growing root hairs, the puncta localize over the whole cell surface and the amount of puncta does not decrease strongly in fully-grown cells. Inhibition of exocytosis does cause a strong reduction in the density of the puncta. Since the density of SEC3A-GFP puncta does not depend on (the location of) cell expansion, this indicates that SEC3A mediates a type of exocytosis not related to cell growth. Our data show that polar localization of SEC3A-GFP in the cell cortex only occurs during and just after cytokinesis and that SEC3A-GFP puncta are evenly spread throughout the cell cortex in interphase cells.

Results

Interactions between the subunits of the exocyst complex in Arabidopsis

To gain insight in the assembly and structure of the plant exocyst, we determined the interactions between different exocyst subunits using a matrix based yeast two-hybrid assay. Interactions between the exocyst subunits, SEC3A, SEC5A, SEC6, SEC8, SEC10, SEC15A, SEC15B, EXO70H7, EXO70A1, EXO84B and EXO84C, were determined. In the self-activation assessment of the baits, SEC3A, SEC10 and EXO84C showed very strong self-activation; therefore they could not be used as baits in the interaction test. 6 pairs of strong interactions were detected for which all three reporter genes were activated: SEC3A interacts with EXO70 A1 and SEC5A, SEC15B interacts with both EXO84B and EXO84C, EXO70A1 interacts with EXO84C, and EXO70H7 interacts with EXO84B (Table 1; Supplemental Figure 1). For two pairs only the LacZ reporter gene was activated: SEC5A with SEC6 and SEC5A with EXO84C, and hence, these putative weak interactions need to be confirmed by alternative methods. We decided to focus on SEC3, because of its prominent role in the yeast exocyst complex.

Table 1. Interactions between exocyst subunits in Arabidopsis as determined by yeast-two-hybrid assays.

Protein	Interacts with
SEC3A	EXO70A1
	SEC5A
SEC5A	EXO84C (LacZ only)
	SEC6 (LacZ only)
SEC15B	EXO84B
	EXO84C
EXO70H7	EXO84B
EXO70A1	EXO84C

Arabidopsis has two *SEC3* genes in a tandem organization with expression patterns that partially overlap

Arabidopsis processes two genes that encode SEC3, *SEC3A* (At1g47550) and *SEC3B* (At1g47560), which are tandemly duplicated and share 97% sequence identity on the protein level. The ATH1 whole-genome chip is not able to discriminate between *SEC3A* and *SEC3B* expression. However, ESTs and a search against the Arabidopsis MPSS database reveal that both genes are expressed (Chong et al., 2010). We determined the temporal and spatial expression patterns of *SEC3A* and *SEC3B* by expression of *SEC3A* genomic-β-glucuronidase (GUS) gene and pSEC3B-GUS fusions. Six independent transgenic plants expressing *SEC3A* genomic sequence fused to GUS were examined histologically for GUS activity. In light-grown seedlings, *SEC3A* was expressed in cotyledons and root but not in hypocotyls, and highly expressed in shoot apical meristems (Figure 1A). In roots, *SEC3A* was highly expressed in the root tip, the vasculature (Figure 1B) and in lateral root primordia (Figure 1C). Unlike in younger seedlings, *SEC3A* expression was observed in the hypocotyl of older seedlings (Figure 1D). In both expanding and expanded rosette leaves, SEC3A expression was detected (Figure 1E). In flowers, *SEC3A* expression was not detected in petals and sepals (Figure 1F), but strong *SEC3A* expression was detected in the stigma (Figure 3G), unfertilized ovules (Figure1G) and pollen (Figure 1H). In embryos, *SEC3A* expression was observed in the early heart stage (Figure 1I), the heart stage (Figure 1J) and the torpedo stage (Figure 1K). *SEC3B* expression was analyzed in six independent pSEC3B-GUS expressing plants. *SEC3B* expression is strong in the vasculature throughout the plant, with the exception of that in the stems and middle parts of the leaves (Supplemental figure 1). Weaker expression is observed in the cotyledons of embryos in the cotyledon stage, in young leaves, cotyledons and roots, stems and fruits (Supplemental figure 2). Thus, *SEC3A* and *SEC3B* expression partially overlap, where *SEC3B* expression is strongest in the vasculature and *SEC3A* expresses in various tissues of both seedlings and mature plants and preferentially in tissues containing dividing and expanding cells, such as shoot apical meristem, root tip, lateral root primordia and developing embryos.
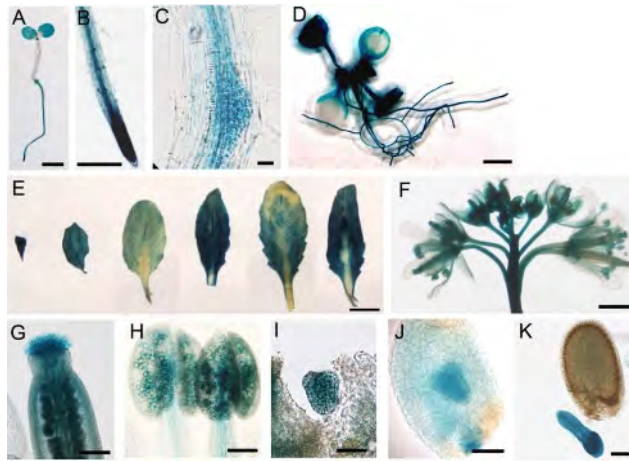
Figure 1. *SEC3A* genomic sequence:GUS expression pattern in seedlings and mature plants. GUS staining pattern of a one week old seedling (A), one week old root (B), a lateral root primordium (C), a two week old seedling (D), different rosette leaves of a one month old plant (E), immature and mature flowers (F), an unfertilized stigma (G), developing pollen (H) and embryos of different developing stages (early heart (I), heart (J), torpedo (K)). Bars = 5 mm (A), 1 mm (B), 100 μm (C), 1 mm (D), 5 mm (E), 500 μm (F), 100 μm (G – K).
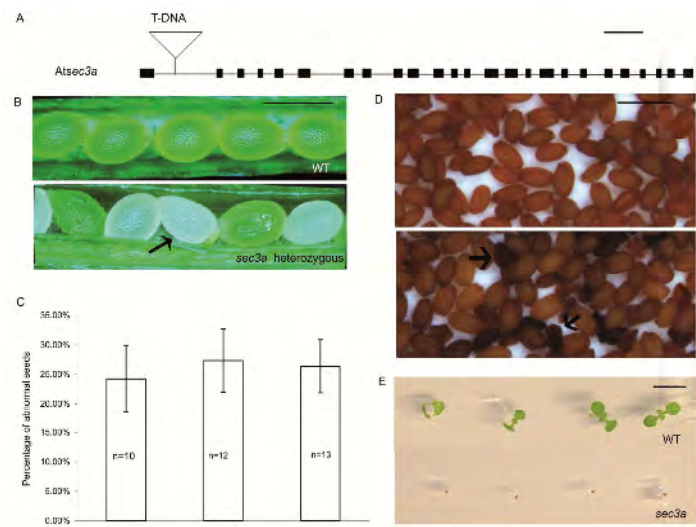

Figure 2. A T-DNA insertion in *SEC3A* causes embryo lethality. (A) Schematic representation of the *SEC3a* gene (At1g47550). The black boxes represent exons and the T-DNA insert is located in the first intron. (B) Immature wild type siliques show a full set of green seeds; immature *sec3a* heterozygous siliques show both green and white seeds. The arrow points to an abnormal seed. (C) In siliques of different plants that are heterozygous for *sec3a*, approximately 25% of the seeds is abnormal. Three independent heterozygous plants were picked and at least 10 siliques from each plant were examined, as indicated in the bars of (C). The error bars indicate standard deviations. (D) Mature seeds from wild type and *sec 3a* heterozygous siliques. *sec3a* heterozygous plants produce both seeds that appear normal and dark-brown winkled seeds (black arrows). (E) In contrast to normally appearing seeds (top row) from plants heterozygous for *sec3a*, dark-brown wrinkled seeds (bottom row) do not germinate. This picture shows 7 day old seedlings. Scale bars = 500 bp (A), 1 mm (B and D) and 5 mm (E).

Identification of an embryo lethal *sec3a* and a gametophytic lethal *sec3b* mutant

Using a PCR-based genotyping approach, we identified a SALK line (SALK_145185) harboring a T-DNA insertion in the first intron of the *SEC3A* (At1g47550) gene (Figure 2A) and a SALK line (SALK_015980) harbouring a T-DNA insertion in the first intron of SEC3B (At1g47560). We performed PCR amplification of the *SEC3A* and *SEC3B* wild type alleles with primers flanking the T-DNA insertions and amplification of the mutant *sec3a* and *sec3b* alleles with one primer flanking the T-DNA insertion and the T-DNA left-border primer LBa1. Only heterozygous and wild type plants were identified for both T-DNA insertion lines (Supplemental Figure 3). The *sec3a* allele segregated in a ratio of 1:2 in progeny of selfed heterozygous plants (30.0 % wild type: 70.0 % heterozygous; n=350 plants (Table 2)), whereas the *sec3b* allele segregated in a ratio of 1:1 (52.2 % wildtype: 47.8 % heterozygous; n= 134 plants). Since no homozygous plants were identified in both lines and the 1:2 segregation ratio of the *sec3a* allele is typical for embryo lethality, we tested immature siliques from heterozygous *sec3a* and *sec3b* plants for the presence of white or otherwise abnormal seeds. When the immature siliques from s*ec3b* heterozygous plants were dissected, no such seeds were observed. Taken together with the 1:1 segregation ratio, this is indicative of gametophytic lethality. In heterozygous *sec3a* plants green and white seeds within single siliques were observed. In contrast, only green seeds were present in the immature siliques from wild type plants (Figure 2B). White seeds indicate embryo lethality (Meinke and Sussex, 1979). We scored the number of white seeds from 10 siliques from three individual plants heterozygous for *sec3a*. In all these lines, about 25% of seeds were white, suggesting that the sec3a mutation is recessively embryo lethal (Figure 2C). The mature seeds from heterozygous and wild type plants were also compared, showing a mixture of dark-brown, small, wrinkled seeds and normal light brown seeds in heterozygous plants and only normal light brown seeds in the wild type (Figure 2D). We tested germination by placing wrinkled seeds and normal seeds on half MS plates to score the germination rate. The normal seeds all germinated but none of the wrinkled seeds had germinated after one week (n = 300; Figure 2E). To determine whether, besides embryo lethality, the *sec3a* mutation causes gametophytic defects, we analyzed the progeny of heterozygous *SEC3A/sec3a* lines and performed reciprocal crosses between *SEC3A/sec3a* and wild-type plants by applying pollen grains from the heterozygous plants onto the stigma of wild type plants, and vice versa. The genotype of progeny was determined by PCR. In the progeny of *SEC3A/sec3a*, the *sec3a* allele segregated as expected (Table 2). In the

progeny of the reciprocal crosses, the transmission of the *sec3a* allele was not affected when *SEC3A/sec3a* was used as either pollen donor or pollen receiver (Table 2), demonstrating that gametophytic transmission of the *sec3a* allele is normal. Thus, SEC3A and SEC3B appear both to be essential for different stages of plant development. We focussed on the *sec3a* mutant.

Table 2. Inheritance of the *sec3a* allele as determined by reciprocal crosses

Natural self *of* SEC3A heterozygous	Number of progeny	Progeny Genotype Wild type SEC3A/SEC3A	Heterozygous SEC3A/*sec3a*	Homozygous *sec3a/sec3a*	Expected ratio wt: heterozygous	P
	350	245	105	0	1:2	0.17*
Reciprocal crosses						
Pollen source: sec3a heterozygous	186	100	86	0	1:1	0.30*
Pollen source: wild-type	214	115	99	0	1:1	0.27*

*P values were determined using the X^2 test. P>0.05 is different from the expected ratio.

Embryo development in *sec3a* is arrested in globular stage

To examine if the white seeds in the progeny of plants heterozygous for *sec3a* were harboring aborted embryos, we investigated embryo development in these seeds by comparing embryo development in white and normal seeds from the same siliques of various developmental stages. From the 2-cell stage to the 32-cell stage, we could not discriminate mutant embryos from wild type ones. Unlike normally developing embryos that become heart shaped 4 days after fertilization (Figure 3A-3B), the mutant embryos failed to undergo this developmental step (Figure 3E-3F). Mutant embryos from siliques in which the wild type embryos had developed to the cotyledonary stage (Figure 3C) were still globular, although their size and the number of cells had increased beyond the normal size and number of cells of globular embryos (Figure 3G). Thus, although cell division is not inhibited, aberrant embryos fail to acquire a heart shape. To investigate the defects that could underlie this failur

we made sections through seeds with mutant embryos from siliques that contained bended cotyledon stage embryos to investigate cell patterning. In normal embryos of this age, a clear epidermis consisting of one cell layer is present (Figure 3D). The width of this layer and the number of radial cells in the layer are maintained by the direction of cell division: cells only divide anticlinally, in the plane of the layer. The sections through mutant embryos show that the outer cell layer displays divisions in the periclinal direction as well, indicating that the aberrant embryos have defects in determination of cell division plane, giving rise to aberrant patterning of cells and consequently failure to acquire tissue polarity (Figure 3H).
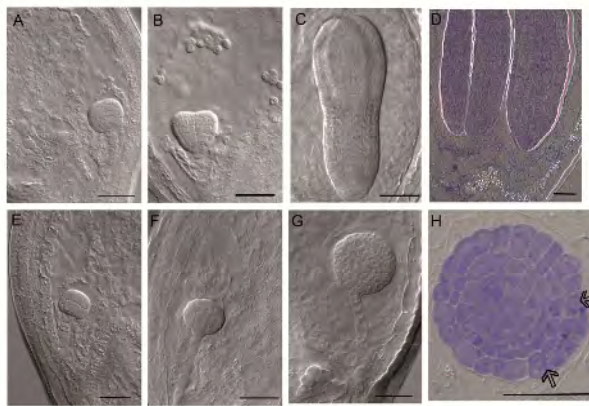

Figure 3. Embryo development is arrested during the globular stage in 25% of the seeds of plants heterozygous for *sec3a*. Wild-type (A - C) and mutant (E-G) embryos in seeds from the same silique (A and E; B and F and C and G) were compared at the different stages of embryo development. (D and H) Toluidine Blue staining of the wild type embryo at the cotyledon stage (D) and the mutant embryo (H) of the same age and from the same silique. Arrows point to epidermal cells with aberrant division planes. Bars = 50 μm.

The *sec3a* mutant phenotype is rescued by genetic complementation

To confirm whether the embryo lethal phenotype is solely caused by the T- DNA insertion within the *SEC3A* gene, genetic complementation was performed by introducing the full-length *SEC3A* genomic DNA driven by the endogenous *SEC3A* promoter (ProSEC3A:SEC3A) into plants heterozygous for *sec3a.* In addition, we introduced a similar construct with the GFP coding region fused to the 5' end of the full-length of the *SEC3A* genomic sequence (ProSEC3A:SEC3A-GFP). We scored for white seeds in two T1 lines carrying the ProSEC3A:SEC3A construct to assess the percentage of seeds in which embryo development was arrested. In contrast to uncomplemented T1 plants that carried approximately 25% white seeds, both lines had a strongly reduced number of abnormal (white) seeds (2.18% (n = 1,008 seeds from 14 siliques) and 1.55 % (n = 645 seeds from 10 siliques), respectively). Transgenic T1 plants heterozygous for the sec3a allele complemented with the ProSEC3A:SEC3A-GFP construct showed percentages of white seeds below 2% (n=7

independent transformants). The percentages of white seeds that we observed were lower than that expected in T1 plants carrying one complementation construct (6.25%). It is possible that the T1 plants carry more than one complementation construct. This is confirmed by plating out T2 seeds on selective medium for the complementation construct, which revealed that in all lines less than 3% of the total population, which if far less than the expected value of 13.3% percent (12.5% of the total population, taking into account that only 93.75% of the population is viable). All T1 seeds germinated normally and contained normally developed embryos. Therefore, the embryo lethal phenotype was genetically complemented by introduction of functional *SEC3A* gene constructs, demonstrating the mutant phenotype is caused by the *sec3a* T-DNA insertion allele. Since it is not possible to discriminate between plants homozygous or heterozygous for the T-DNA insertion by genotyping because of the complementation construct, we tested the progeny from plants carrying both the T-DNA insertion and the complementation construct for resistance against the complementation construct. We used seeds from populations of which less than 1% did not carry the complementation construct and presumed that these populations were homozygous for *sec3a*.

SEC3A tagged with GFP (SEC3A-GFP) is present in the cytosol and accumulates in puncta at the plasma membrane

To determine the subcellular localization of SEC3A, transgenic T2 plants carrying the SEC3A-GFP fusion construct, selected as described above, were used. Two cell types were chosen for microscopic analysis of the SEC3A-GFP localization: root hairs and root epidermal cells. Root hairs expand by tip growth; their expansion is extremely polarized and occurs exclusively at the tip. Root epidermal cell expansion is also polar but occurs over the whole cell facets parallel to the elongation direction of the root. We refer to this type of cell expansion as axial growth (also called intercalary or diffuse growth, review: Ketelaar and Emons, 2001). We studied SEC3A-GFP localization both in expanding and fully-grown cells.

In both cell types, we observed SEC3A-GFP fluorescence evenly distributed throughout the cytoplasm and brightly fluorescent cell compartments, which is clearly visible in Figure 4F. These compartments are reminiscent to the exocyst positive compartment EXPO in the cytoplasm, identified by Wang et al. (2010). At the plasma membrane of both cell types, SEC3A-GFP fluorescence had a punctate distribution (Figure 4A-4D). We did not observe strong differences in the density of the puncta in expanding and fully-grown cells: 0.58 ± 0.67 μm^{-2} in the tube of growing root hairs compared to 0.49 ± 0.48 μm^{-2} in the tube of fully-grown root hairs (p=0.30) and $0.50 \pm$

0.09 μm^{-2} in expanding root epidermal cells, compared to 0.42 ± 0.04 μm^{-2} in expanded root epidermal cells (p=0.15; Figure 4E). Since the tip of growing root hairs

harbors many vesicles and is the location of cell elongation, it was important to determine SEC3A puncta density at this location. Since it is technically challenging to measure the density of puncta in the surface of the dome of the root hair tip because of its curvature, we measured the fluorescence intensities of membrane regions in median confocal sections (Figure 4F). Cell expansion does not occur in the root hair tube and expansion rates differ in different regions of the dome. The side of the dome has the fastest expansion rate and the tip expansion rate is slower (Shaw et al., 2000). We measured fluorescence intensities in the plasma membrane region of the side of the dome and the tip of the dome and compared these intensities to the fluorescence intensity of the plasma membrane of the tube (Figure 4G). Surprisingly, we did not observe significant differences in fluorescence intensity between the different membrane areas of the expanding tip and the membrane area of the non-expanding root hair tube (P=0.29 between the tube of the side of the dome, and P=0.12 between the tube and the tip). Together, these observations show that SEC3A puncta at the plasma membrane do not preferentially accumulate in expanding areas of cells. Thus, the localization of SEC3A suggests that it is not specifically recruited to polar exocytosis events in interphase cells.

SEC3A-GFP forms discrete, immobile puncta with a lifetime of seconds at the plasma membrane
To determine the behavior over time of the SEC3A-GFP puncta at the plasma membrane, we photobleached the SEC3A-GFP that was already present and analyzed the recovery of fluorescence over time. We studied the behavior of individual SEC3A-GFP puncta at the plasma membrane of tubes of growing root hairs (Figure 5A), fully-grown root hairs (Figure 5B), the plasma membrane of the outer periclinal face of expanding root epidermal cells (Figure 5C; Supplemental Movie 1 on line) and that of fully grown root epidermal cells (Figure 5D; Supplemental Movie 2 on line). In both cell types and both in expanding and fully expanded cells, new fluorescent SEC3A-GFP puncta appeared at the plasma membrane after photobleaching. All SEC3A-GFP puncta were immobile and behaved similar in terms of the kinetics of fluorescence intensity. When puncta first appeared their fluorescence was low but detectable. Over time, their fluorescence intensity increased until it reached a maximum intensity,

whereafter the fluorescence intensity gradually decreased until it completely disappeared (Figure 5E). The characteristic behavior of SEC3A-GFP puncta is illustrated in Figure 5F, where the average fluorescence intensities of puncta in a fully expanded root epidermal cell are followed during their life time with the peak fluorescence intensity centered at time 0 (n=12).
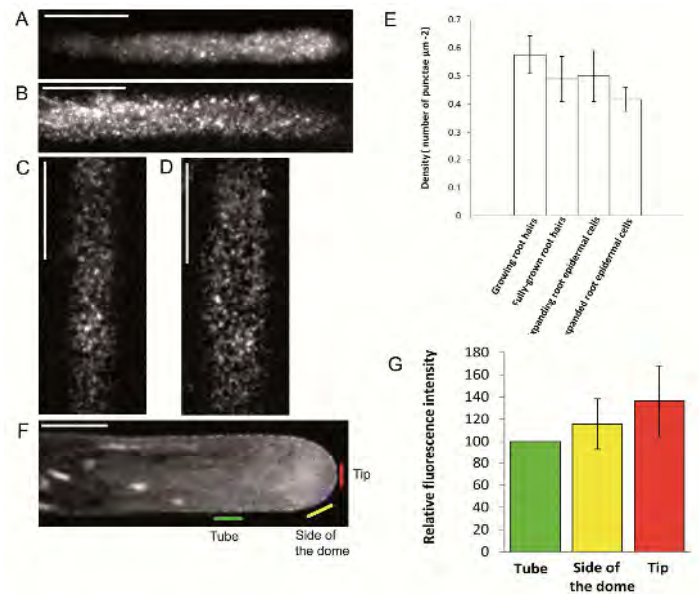

Figure 4. SEC3A-GFP fluorescence localizes as puncta at the plasma membrane, is evenly distributed throughout the cytosol and accumulates in cell compartments. (A – D) SEC3A-GFP is localized to the plasma membrane as discrete punctate in growing root hairs (A), in fully grown root hairs (B), in elongating root epidermal cells (C) and fully grown root epidermal cells (D). (E) The density of puncta in the cortex of growing and fully grown root hairs and root epidermal cells. The density in fully grown cells is significantly lower than that in growing cells of the same type. The error bars indicate standard deviations (n > 100 puncta per cell in 4 cells per sample). (F) An image of the median plane of a growing root hair shows that some of the SEC3A-GFP fluorescence is evenly distributed throughout the cytoplasm and that fluorescent puncta localize to the plasma membrane. The three areas marked by color lines represent different regions of the cell surface that were used for analysis in (G): the tube, the side of the apical dome and the extreme apex. (G) The fluorescence intensities of different regions of the plasma membrane. The GFP fluorescence intensity of the plasma membrane of the root hair tube was normalized to 100 in each cell to allow comparison of different cells. The fluorescence intensities of the extreme tip and the side of the domewere multiplied by the same factor that we used to set the fluorescence intensity of the root hair tube of different cells to 100. The error bars indicate standard deviations. Bars = 10 μm.

To check if there are differences in lifetime of the puncta between different cell types and/or between growing and fully-grown cells, we measured the lifetimes of the GFP-SEC3A-GFP punta in growing and fully-grown root epidermal cells and in the tube region of growing and fully-grown root hairs (Figure 5G). We collected image sequences with 2 seconds intervals between sequential images, and determined the amount of frames during which each punctum was present and used these values to calculate an average lifetime. Within individual cells, lifetimes were highly variable, ranging from 2 to 40 s. The average lifetime of SEC3A-GFP puncta was 6.3 ± 2.7 s in the tube region of growing root hairs (n=81 from 3 cells), 6.6 ± 3.4 s in the tube region of fully-grown root hairs (n=113 from 5 cells), 6.7 ± 3.6 s in expanding root epidermal cells (n=86 from 4 cells) and 12.6 ± 8.3 s in fully grown root epidermal cells (n=127 from 5 cells). The average SEC3A-GFP punctum life time in the growing root hairs was not different from that in fully-grown root hairs (p=0.49). The lifetime in expanded root epidermal cells was much longer (p=0.001) than that in expanding root epidermal cells, which is accounted for by a small population (10.24%) of puncta with long lifetimes (>24 s) in fully expanded root epidermal cells (Figure 5G).

SEC3A-GFP is not delivered to the plasma membrane by the Golgi system

To test whether SEC3A is delivered to the plasma membrane by the Golgi system we tested if it associates with exocytotic vesicles. We used the amphiphilic styryl dye FM4-64 to stain the vesicle pool in the apex of expanding root hairs. It is assumed that FM4-64 decorates membranes of endocytic vesicles rapidly and that also exocytotic vesicles are decorated rapidly (Griffing, 2008; Van Gisbergen et al., 2008). We did not see any SEC3A accumulation in the vesicle rich region in the apex of growing root hairs other than the fluorescence that is present throughout the cytoplasm (Figure 6). From this we conclude that SEC3A-GFP is cytoplasmic and does not localize to FM4-64 labeled vesicles. Together with the absence of a strong correlation with cell expansion this suggests that SEC3A recruitment to the plasma membrane is not mediated by the Golgi system. To further investigate whether SEC3A recruitment to the plasma membrane depends on exocytosis, we applied brefeldin A (BFA) to growing root hairs and measured the density and life time of SEC3A-GFP puncta at the plasma membrane. BFA is a macrocyclic lactone of fungal origin. It is an effective inhibitor of Golgi-based secretion in plants (reviewed in: Robinson et al., 2008). We applied a concentration range of BFA to growing root hairs. The lowest concentration BFA that caused complete root hair growth inhibition after two hours was 5 μg/ml. Occasionally swollen root hair tips were observed, but root hairs were still alive and cytoplasmic
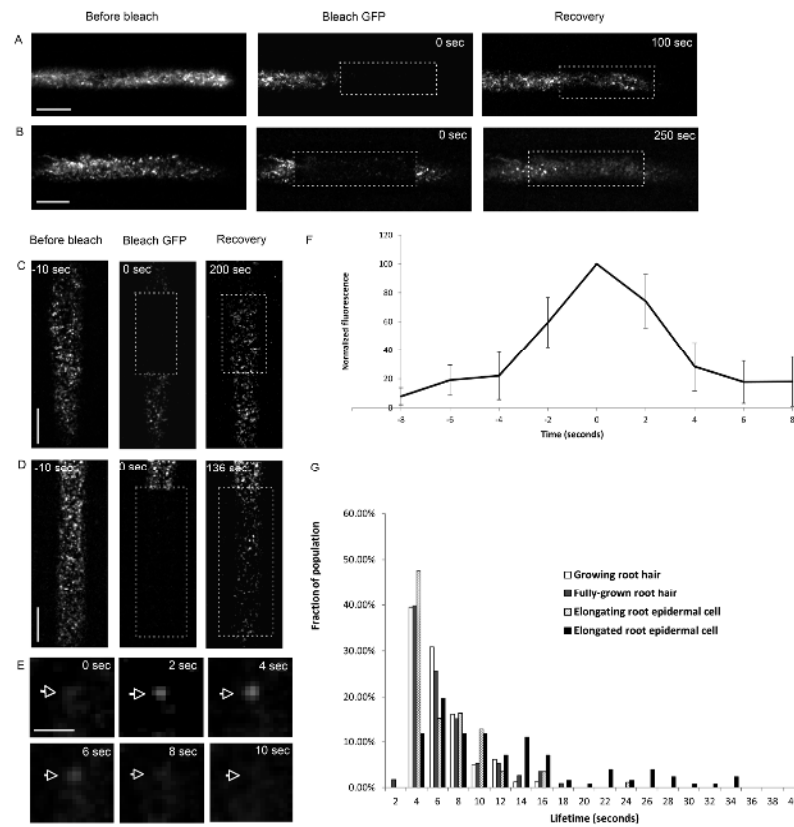
Figure 5. SEC3A-GFP forms discrete, immobile puncta with discrete lifetimes. (A – D) Time course of photobleaching and recovery of SEC3A-GFP at the plasma membrane of a growing root hair tube (A), a fully-grown root hair tube (B), an expanding root epidermal cell (C; Supplemental Movie 1 on line) and a fully expanded root epidermal cell (D; Supplemental Movie 2 on line). The three consecutive images show SEC3A-GFP before photobleaching, immediately after photobleaching and the recovery of SEC3A-GFP puncta over time. Dashed boxes indicate the bleached areas. (E) An individual SEC3A-GFP punctum that appears and, approximately 10 seconds later, disappears. (F) The average normalized fluorescence intensity of puncta over time (n = 12) from one fully expanded root epidermal cell. The highest fluorescence was centered at time 0. Bars show standard deviations. (G) A comparison of the lifetimes of SEC3A-GFP puncta in growing root hairs, fully-grown root hairs, expanding root epidermal cells and expanded root epidermal cells. Bars = 10 μm (A – D), 1 μm (E)

streaming continued. The inhibition of root hair growth showed that treatment with 5 μg ml^{-1} BFA successfully inhibits Golgi-based secretion in root hairs. Under these conditions, SEC3A-GFP still localized as puncta to the plasma membrane throughout the root hair tube. However, the density of the SEC3A-GFP puncta had reduced dramatically after two hours of treatment compared with that in untreated cells (0.23 ± 0.05 μm^{-2} from 4 cells compared to 0.58 ± 0.67 μm^{-2} before treatment; p<0.001;

Figure 7A). After 4 hours of BFA treatment, the density decreased even further (0.09 ±
0.04 μm^{-2}; from 4 cells; Figure 7A). The SEC3A-GFP puncta still showed their
characteristic increase and decrease in fluorescence intensity during their life time,
but the average life time was increased when compared to control cells (10.0 ± 4.3 s,
n=51 from 4 cells in BFA treated cells (2 hours) to 6.3 ± 2.7 s in control cells; p<0.001;
Figure 7B). The lifetime of SEC3A-GFP puncta remained constant after 4 hours of
treatment (10.1 ± 5.1 s after 4 hours, n=48 from 4 cells; p=0.93; Figure 7B). Since the
density of SEC3A-GFP puncta decreases and the lifetime increases during treatment
with BFA, disruption of exocytotic vesicle production causes a decrease in recruitment
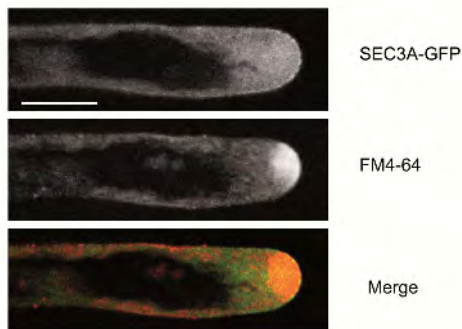of SEC3A-GFP puncta to the plasma membrane.

Figure 6. SEC3A-GFP does not decorate the pool of vesicles in the apex of growing root hairs. A median section of a growing root hair expressing SEC3A-GFP, counterstained with the membrane marker FM4-64, shows that there is no increased SEC3A-GFP signal present in the apical region where vesicles accumulate. Bar = 10 μm.
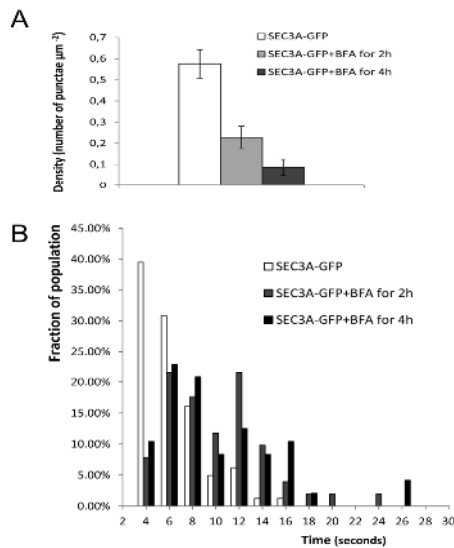
Figure 7. Density and lifetime of SEC3A-GFP puncta at the plasma membrane of tubes of growing root hairs are affected by the secretory trafficking inhibitor Brefeldin A. (A) The density of SEC3A-GFP puncta at the plasma membrane in growing root hairs treated with 5 μg/ml brefeldin A. The error bars indicate standard deviations. (B) The life times of SEC3A-GFP puncta at the plasma membrane in growing root hairs treated with 5 μg/ml brefeldin A.

SEC3A-GFP puncta do not co-localize with cortical microtubules and the insertion of cellulose synthase complexes into the plasma membrane

Since insertion of CESA complexes into the plasma membrane, which is likely to be an exocytotic event, occurs predominantly along cortical microtubules, we tested whether SEC3A-GFP puncta co-localized with these cortical microtubules. We crossed a mCherry-TUA5 expressing line (Gutierrez et al., 2009) with SEC3A-GFP expressing lines. The optical coverage of cortical microtubules in the analysed cells was 30.3 ± 0.9 % (n= 3 cells; Figure 8A). If the SEC3A-GFP puncta appear at random locations of the cell cortex, the expected percentage of puncta colocalizing with cortical microtubules is approximately 30%. 38 out of 125 SEC3A-GFP puncta showed colocalization with CMTs, which is 28.9% (Figure 8A; Supplemental Movie 3 on line). This is not significantly different from the expected percentage (t-test, P=0.59). To test co-localization of SEC3A-GFP with CESA complexes directly, we crossed a tdTomato-CESA6 expressing line (Gutierrez et al., 2009) into a SEC3A-GFP expressing line and searched for co-localization of SEC3A-GFP with the insertion of cellulose synthase complexes. This was done by photobleaching existing tdTomato-CESA6 in the plasma membrane. We performed a co-localization analysis of newly inserted tdTomato-CESA6 with SEC3A-GFP puncta during the insertion process (both the erratic movement and static phase as described by Gutierrez et al., 2009) and found that only 2 % of the cellulose synthase complex insertion events correlated with the presence of a SEC3A punctum at the same location (n = 100 insertion events in 5 independent cells; Figure 8B; Supplemental Movie 4 on line). Thus, it is unlikely that SEC3A puncta are involved in exocytosis for the insertion of cellulose synthase complexes into the plasma membrane.

SEC3A-GFP transiently localizes to the early cell plate, is absent during cell plate extension and re-appears at the division wall

In mitotic cells, the exocyst subunits, SEC6, SEC8, SEC15B, EXO70A1 and EXO84B are localized to the initiating cell plate, disappear during cell plate extension and reappear on the division wall for some time after completion of cytokinesis (Fendrych et al., 2010). Our analysis of *SEC3A* gene expression with GUS staining also shows that the *SEC3A* gene is highly expressed in the area of the root tip where cells divide. To determine if SEC3A, similar to other exocyst subunits, localizes to the developing cell plate and division wall, we studied the localization of SEC3A-GFP in the course of cell plate formation in dividing cells of the Arabidopsis root meristem. In the meristematic cells in both the epidermal and cortical cell layer, SEC3A-GFP localized to distinct structures with high fluorescence intensity in some cells (Figure 9A). To gain insight

into the SEC3A-GFP localization, we counterstained with FM4-64, which labels developing cell plates (Donukshe et al., 2006) and followed the SEC3A localization in cells of the root meristem over time. An accumulation of SEC3A-GFP fluorescence was associated with the appearance of the cell plate. During the centrifugal expansion of the cell plate to the parental cell walls, the SEC3A-GFP fluorescence disappeared (Figure 9B). SEC3A-GFP accumulation during early cell plate formation lasted 173 ± 15 sec (n=5 cells). When cell plate formation had completed, SEC3A-GFP fluorescence started to accumulate at the division wall. The fluorescence intensity of SEC3A-GFP increased, remained unchanged for some time, and then gradually decreased to the level of the other cell faces (Figure 9C). The average residence time of SEC3A-GFP at the division wall was 27 ± 5 min (n=15 cells from 3 independent root meristems). Thus, SEC3A localization during cytokinesis is similar to the localization of other exocyst subunits.
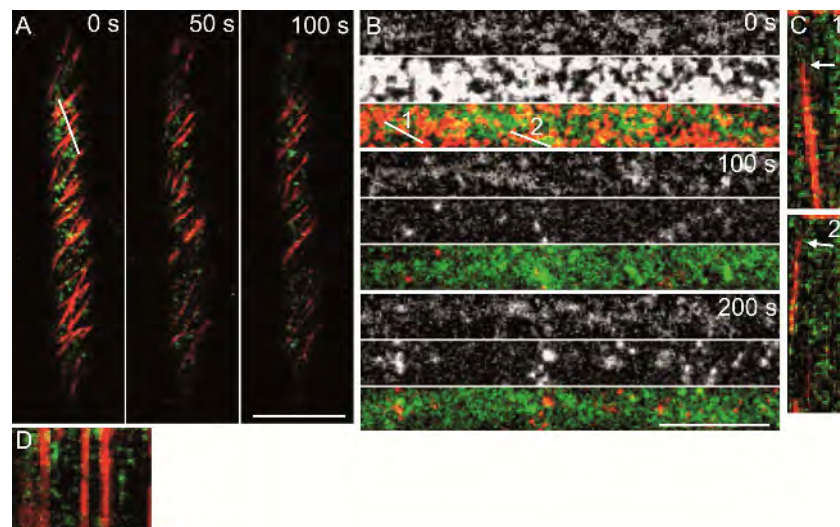

Figure 8. SEC3A-GFP puncta do not preferentially colocalize with CMTs and do not co-localize with CESA complex insertion events. Time series of a line expressing mCherry-TUA5 (red) and SEC3A-GFP (green (A); Supplemental Movie 3 on line) and a time series of a line expressing tdTomato-CESA6 (middle panels and red in merged images) and SEC3A-GFP (upper panels and green in merged images (B); Supplemental Movie 4 on line). To clearly mark CESA complex insertion events, the CESA channel has been photobleached after the first frame. C shows two kymographs of CESA complex insertion into the plasma membrane and their subsequent movement over time. The arrows mark the insertion events that do not co-localize with a SEC3A-GFP punctum. D shows a kymograph of SEC3A puncta (green) and cortical microtubules (red) where no preferential co-localization is observed. Kymograph locations have been marked in a and b by white lines. Bar= 10 μm (A), and 5 μm (B)
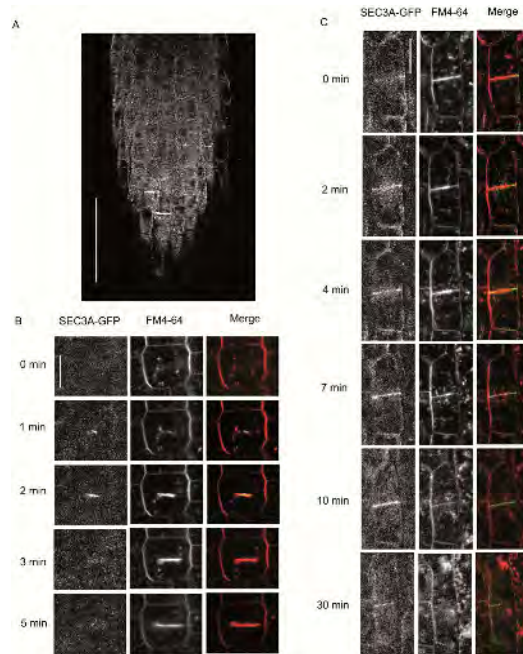
Figure 9. SEC3A-GFP localizes to early cell plates, is absent during later stages of cell plate development and reappears on the division wall after cytokinesis has completed. (A) SEC3A-GFP localizes to distinct cross walls in the root meristem. (B) SEC3A-GFP decorates the cell plate during its early stages and disappears during later stages of cell plate expansion in a root cortical cell. Cell membranes are counterstained with FM4-64. (C) After completion of cytokinesis, SEC3A-GFP accumulates at the division wall. Bars = 50 μm (A) and 10 μm (B and C).

Discussion

Our results help decipher the role of the exocyst in general and particularly SEC3 in plant development. In interphase cells, SEC3A-GFP has a cytoplasmic localization and accumulates as immobile puncta at the plasma membrane with average life times of 6.3 to 12.6 seconds depending on the cell type. Although SEC3 may be involved in exocytosis, it is not involved in the insertion of cellulose synthases into the plasma membrane and the density of SECA-GFP puncta does not depend on (polar) cell growth in interphase cells. The localization of SEC3A-GFP during cytokinesis and the failure of *sec3a* mutants to progress beyond the globular stage of embryo development suggest that SEC3A is involved in the correct positioning of cell plates.

Interactions between different Arabidopsis exocyst subunits have been identified using different techniques. Hála et al. (2008) used chromatographic fractionation and yeast-two hybrid assays, whereas Pecenková et al. (2011) used yeast-two hybrid assays and FRET (Fluorescence Resonance Energy Transfer) analysis between several subunits (Pecenková et al., 2011). Together, these results strongly suggest that

exocyst composition and probably also function is conserved in plants. While co-fractionation shows that different exocyst subunits are in the same complex in plants (SEC3, SEC5, SEC6, SEC8, SEC10, SEC15 and EXO70A1; Hála et al., 2008), the pair-wise interactions found by the yeast two-hybrid assay give additional insight in exocyst assembly. We have identified additional interactions between different exocyst subunits: SEC3A interacted with SEC5A, SEC15B interacted with both EXO84B and EXO84C, EXO70A1 interacted with EXO84C, and EXO70H7 interacts with EXO84B. In addition we determined two weak interactions in the yeast-two hybrid assay: SEC5A with SEC6 and SEC5A with EXO84C. Knowledge about interactions within the exocyst could aid the deciphering of exocyst structure.

SEC3A in cytokinesis

Although *sec3a* and *sec3b* null mutants are both lethal, the moment of lethality is different. Whereas the *sec3b* null mutant is gametophytically lethal, the *sec3a* null mutant is embryonically lethal, which differs from defects in other exocyst subunit mutants that have been described (Cole et al., 2005; Synek et al., 2006; Samuel et al., 2009; Kulich et al., 2010; Pecenková et al., 2011). The successful transmission of the *sec3a* allele from the male and female gametophytes to the progeny allows us to study exocyst functioning in somatic development, which is not possible in exocyst mutants that are gametophytically lethal. The failure of the *sec3a* mutant embryo to develop from globular to heart shape, together with the inability to correctly position cell divisions in the layer that gives rise to the epidermis shows that embryo polarization is not established properly in the *sec3a* mutant. The localization of exocyst subunits on the cell plate (Fendrych et al., 2010; our results) together with incorrectly oriented cell divisions in *sec3a* embryos suggests that the exocyst is involved in determining the orientation of cell divisions, or in transducing signals that are involved in determining the orientation of division planes. Since SEC3A interacts with ICR1 (interactor of constitutive active ROP1) which could transduce ROP mediated signalling to the exocyst (Lavy et al., 2007; Bloch et al., 2008), ROP signalling may be involved in this process. The work of Humphries et al. (2011) showing that ROPs indeed play a key role in polarization of plant cell divisions strengthens the idea that the exocyst could be a ROP effector in this process.

Similar to the other exocyst subunits, SEC6, SEC8, SEC15B, EXO70A1 and EXO84B (Fendrych et al., 2010), SEC3A localizes to the initiating cell plate, where after it

dissociates from the expanding cell plate, re-appears on the newly formed cell wall for approximately 30 minutes, where after it is evenly distributed over all plasma membranes. However, compared to SEC6-GFP, GFP-SEC8, GFP-SEC15B, GFP-EXO70A1 and EXO84B-GFP, which locate to the initiation site of the cell plate for 30 to 60 seconds (Fendrych et al., 2010), SEC3A-GFP has a longer average residence time of 173 seconds during the onset of cytokinesis. In contrast, the average residence time of SEC3A-GFP at the newly formed wall was 25 minutes. This residence time was much shorter than that of EXO84B-GFP which was approximately one hour (Fendrych et al., 2010). The co-localization of different exocyst subunits at the cell plate suggests that these exocyst subunits function as a complex during cell plate formation. The difference in the residence times between SEC3A and other subunits suggests that the exocyst assembly could be a time-course based process. Surprisingly, we find a much longer accumulation time of SEC3A-GFP than that has been found for other exocyst subunits during the onset of cytokinesis (Fendrych et al., 2010), whereas its accumulation is much shorter than other exocyst subunits on the division wall. To gain more insight in exocyst localization and recruitment during cytokinesis, for example whether it localizes in punctate structures on the cell plate, simultaneous live cell labelling of different exocyst subunits would be indispensible. Unfortunately, within Arabidopsis organs, microscopy resolution is not sufficient to determine the exact localization of exocyst subunits on the cell plate.

Localization and behaviour of SEC3A-GFP puncta at the plasma membrane of interphase cells

SEC3A is cytoplasmic and localizes transiently to the plasma membrane in puncta with an average life time varying from 6.3 to 12.6 seconds. There is no difference in density of puncta between the growing root hair tip, the non-growing tube and the fully-grown hair, and no difference between expanding and fully-grown root epidermal cells. Thus, it is unlikely that SEC3A has a role in exocytosis of cell wall matrix polysaccharides, unless the SEC3A-GFP puncta serve as an anchoring location for the remainder of the exocyst. In this case, although evenly spaced, SEC3A-GFP puncta in the plasma membrane may only mediate exocytotic events when interaction with the exocyst subunits on the exocytotic vesicle occurs. SEC3A could be compared to a door handle, always present, which requires an actor to open the door. This differs from the situation in budding yeast. In budding yeast, SEC3 localizes to plasma membrane areas where polarized exocytosis occurs; presumptive bud sites, the tips of budding cells and the mother-daughter cell neck during cytokinesis, where it plays a

role in tethering secretory vesicles (Finger et al., 1998). Also in growing tobacco pollen tubes, Hála et al. (2008) showed accumulation of SEC6, SEC8 and EXO70A1 in the apical region where expansion occurs. Unlike the polar localization of SEC3 in yeast and the polar localization of exocyst subunits in tip-growing pollen tubes, SEC3A-GFP does not show polarized localization on the plasma membrane of polarly expanding plant cells.

EXO70E2 localizes to discrete punctate structures that are present both in association with the plasma membrane and in the cytosol. This is different from the localization of SEC3A-GFP, that does not localize to punctate structures in the cytoplasm. The EXO70E2 containing compartments in the cytoplasm were termed EXPO, as they did not co-localize with any conventional organelle (Wang et al., 2010). Unlike EXO70E2, SEC3A-GFP only forms discrete puncta at the plasma membrane, and not within the cytosol. This may suggest that either SEC3A recruits EXPOs during their fusion with the plasma membrane, or that the SEC3A and EXO70E2 puncta are separate structures. The first hypothesis is consistent with the observations in budding yeast where SEC3A functions as a landmark protein at the plasma membrane, where most other exocyst subunits (SEC5, SEC6, SEC8, SEC10, SEC15 and EXO84) are recruited via attachment to exocytotic vesicles (Zhang et al., 2008; Hutagalung et al; 2009). Budding yeast EXO70 localizes to the plasma membrane, but unlike SEC3, its localization is dependent on the actin cytoskeleton (Hutagalung et al., 2009). This is consistent with the localization of EXO70E2 to both EXPOs and plasma membrane puncta in plant cells.

Plasma membrane localized SEC3A-GFP puncta have discrete lifetimes. The fluorescence intensity during the lifetime of a punctum can be divided into 3 phases: firstly, it gradually increases, it then remains constant for a short time span and finally it decreases gradually. This is consistent with a recruitment of multiple SEC3A proteins over time from the cytosol, followed by a gradual dissociation in the last phase. The gradual migration of SEC3A-GFP to the plasma membrane appears in the confocal slice and causes a local increase in fluorescence intensity. The yeast exocyst is thought to consist of single, or at most few proteins per subunit (Munson and Novick, 2006). As the puncta in the plasma membrane of interphase cells are unlikely to represent single SEC3A-GFP proteins, our results show that the plant exocyst either consists of multiple SEC3A proteins, or that multiple exocyst mediated events occur in one punctum. The decrease in density of SEC3A-GFP puncta during BFA treatment

suggests that the presence of SEC3A at the plasma membrane is dependent on the presence of Golgi derived vesicles or vesicle associated factors, for example other exocyst subunits.

As discussed above, the similar, uniform density and similar lifetimes of SEC3A-GFP puncta at the plasma membrane suggest that SEC3A mediates an exocytotic event that is not related to (polarized) cell expansion. The only type of exocytosis that occurs over the cell surface that currently can be detected using fluorescence microscopy is that of cellulose synthases (CESA) into the plasma membrane (Gutierrez et al., 2009; Crowell et al., 2009). We do not find co-localization between SEC3A and CESA insertion into the plasma membrane. Therefore, SEC3A does not appear to be involved in the insertion of CESA, but it could mediate exocytosis of cell wall matrix via Golgi vesicles. However, we have not been able to show this directly and cannot exclude that SEC3A mediates exocytotic events not related to cell wall formation, for example insertion of trans-membrane receptors or ion channels into the plasma membrane. Pecenková et al. (2011) have shown the involvement of Exo70B2 and Exo70H1 in plant defence against pathogens. Insertion of receptors into the plasma membrane by an exocytotic mechanism during pathogen defence could be mediated by the SEC3A-GFP puncta.

Methods

Plant material, plant transformation and growth

All Arabidopsis lines used had a Col-0 background. Plants were grown in a growth room at 22 °C with a 16h light and 8 h darkness photoperiod. Arabidopsis transformation was performed by floral dipping as described by Clough and Bent (1998). Seeds were surface-sterilized as described by Ketelaar et al. (2004) followed by stratification at 4°C for 2 days. Seeds were grown on plates containing half strength Murashige and Skoog salts (Duchefa, Haarlem, The Netherlands) and 0.7% Phyto agar (Duchefa), pH 5.7 or in biofoil slides as described by Ketelaar et al. (2004) for fluorescence microscopy, with the exception that we used 0.16% (w/v) Hoagland's basal salt mixture (Sigma-Aldrich, Zwijndrecht, The Netherlands), 0.0096%(w/v) myo-Inositol (Merck), 0.00168%(w/v) Thiamine-HCl (Calbiochem – Merck, Darmstadt, Germany), supplemented with 1% sucrose (Duchefa), and 0.7% Phyto agar (Duchefa), pH 5.7.

Yeast Two-hybrid assay

The cDNAs of Arabidopsis *SEC3A, SEC5A, SEC6, SEC8, SEC10, SEC15A, SEC15B, EXO70A1, EXO70H5, EXO70H7, EXO84B* and *EXO84C* were amplified by PCR (The primer sequences are given in Supplemental Table 1) and cloned into the pCR8/GW/TOPO vector (Invitrogen). The coding sequence of each protein in the entry clone was confirmed by sequencing and transferred into the GATEWAY destination

vectors pDEST32 (pBDGAL4, bait) and pDEST22 (pADGAL4, prey; Invitrogen). Due to technical problems, SEC15A, EXO70H5 and EXO84B could not be cloned into the pDEST32 vector and SEC10 could not be cloned into pDEST22 vector. All the constructed bait vectors were transformed into the yeast strain PJ69-4α (MATa; James et al., 1996) and transformants were selected on SD plates lacking Leu. All the constructed prey vectors were transformed into yeast strain PJ69-4a (MATα; James et al., 1996) and the transformants were selected on SD plates lacking Trp. Subsequently, all the baits were tested for self-activation of the yeast reporter genes and the basal expression level of the HIS3 reporter gene was determined by titrating HIS activity with 3-Amino-1,2,4-Triazole (3AT). Addition of 10mM 3-AT inhibited the growth of yeast in the absence of HIS, except for SEC3A, SEC10 and EXO84C. Diploid yeast containing both bait and prey were generated by mating the two yeast strains on SD plates followed by selection on SD plates lacking Leu and Trp. Next, the diploid yeast strains were transferred to SD plates lacking Leu, Trp and Ade, and SD plates lacking Leu, Trp and HIS supplemented with 10mM 3AT, respectively. The β-galactosidase assay was performed as described by Duttweiler (1996).

Identification of the *sec3a* and *sec3b* mutants

The T-DNA insertion lines SALK_145185 and SALK_015980 were obtained from NASC (European Arabidopsis Stock Centre, http://arabidopsis.info/) and verified by PCR-based genotyping. Total genomic DNA was extracted as described by Edwards et al. (1991). The wild-type alleles were amplified using gene specific primers (Supplemental table I) and the insert alleles were amplified using a gene specific primer and the T-DNA left border primer LBa1 5'TGGTTCACGTAGTGGGCCATCG- 3'. Examples of genotyping PCR results for both T-DNA insertion lines are given in Supplemental figure 3.

Phenotypic analysis

Seed development was analyzed by dissecting siliques of self-pollinated plants and scoring the number of normal and abnormal seeds present in each silique. Three independent plants were examined and at least 10 siliques were scored per plant.

To determine the terminal phenotype of *sec3a* embryos, seeds were excised from siliques from heterozygous plants and cleared in Hoyer's solution as described (Liu and Meinke, 1998). Then the seeds were mounted and observed for defects in embryogenesis under an Eclipse 80i microscope (Nikon) equipped with Nomarski optics.

β-glucuronidase (GUS) assay

A 7,589-bp genomic DNA fragment containing 967-bp of sequence upstream from the start codon and the full-length genomic sequence of *SEC3A* was amplified by PCR using the primers 5'-CATGGAAGCCAGAAGTCCTCTCATTTC -3' and 5'-AAAGCCGGGACTTAGCCATCC-3'. The amplified fragment was cloned into the pDONR207 vector (Invitrogen) followed by recombination into the Gateway binary vector pMDC162 (Curtis et al., 2003) and transformed into Arabidopsis by the floral dip method (Clough and Bent, 1998). GUS staining was performed as described by Fiers et al. (2004). Staining patterns were observed and documented using a stereomicroscope.

Embryo sectioning and staining

Siliques were harvested from immature heterozygous plants, and the seeds with the wild type embryos at the torpedo stage were dissected from siliques under a binocular microscope. Seeds were fixed overnight in 4% paraformaldehyde and 0.25% glutaraldehyde in 50mM sodium phosphate buffer, pH 7.2, rinsed for three times in the same buffer, and dehydrated in graded ethanol series (10%, 30%, 50%, 70%, 90%, 100%) and embedded into Technovit 7100 (Heraeus Kulzer GmbH, Wehrheim, Germany) according to the manufacturer's instructions. 3 μm thick sections were cut with a rotation microtome (HM 340, Microm GmbH, Walldorf, Germany). Sections were stained in fresh 0.05% toluidine blue and observed under a light microscope.

Genetic complementation

A 7989-bp fragment encompassing the SEC3A genomic DNA, including 967-bp upstream sequence and 397-bp downstream sequence was amplified by PCR using the

primers 5'-GGGGACAAGTTTGTACAAAAAAGCAGGCTCACTCGGAGTTAATATGTATGCGC
-3' and 5'-GGGGACCACTTTGTACAAGAAAGCTGGGT5AAAGCCGGGACTTAGCCATCC-3'.

The amplified fragment was recombined into the vector pDONR207 (Invitrogen),
followed by recombination into the Gateway binary vector pMDC99 (Curtis et al.,
2003). The transformed plants harboring the SEC3A gene were selected on 20 µg ml^{-1}
hygromycin-containing plates. The insert genotyping PCR (see above) was used to
identify transformants that were heterozygous for the *sec3a* allele. The heterozygous
transformants were selfed and investigated for the seed development phenotype.

Construction of GFP fusion gene construct
The entry clone was generated as described previously (see GUS fusion protein). The
entry clone was recombined into the Gateway binary vector pMDC107 (Curtis et al.,
2003). The selection and complementation analysis of transformants was conducted
as described above (genetic complementation).

Microscopy
SEC3A-GFP fluorescence was imaged using a Nikon Eclipse Ti inverted microscope
connected to a Roper Scientific spinning disk system, consisting of a CSU-X1 spinning
disk head (Yokogawa), QuantEM:512SC CCD camera (Roper Scientific) and a 1.2×
magnifying lens between the spinning disk head and the camera. The GFP was excited
using a 491nm laser line.

Photobleaching was performed using the FRAP/PA system (Roper Scientific) fed into
the spinning disk microscope. The 491 nm laser line was used at 100% intensity (10
ms per scan point of 4 pixels in diameter) to photobleach GFP.

Image analysis
All imaging processing was performed using Image J software
(http://rsb.info.nih.gov/ij/). Figures were composed in Photoshop CS2 (Adobe). For
density measurements of SEC3A-GFP puncta, images frames 5 random time points in
single time series were used where after the densities within one time series were
averaged. For measuring lifetimes of SEC3A-GFP puncta, time-lapse sequences of the
plasma membrane after photobleaching were used in which individual SEC3A-GFP
puncta were more clearly visible. In these sequences, the behavior of puncta was
identical to that in unbleached samples.

FM4-64 staining and drug treatments

FM4-64 and Brefeldin A stock solutions were prepared in DMSO. The stock solutions were diluted at least 1000 fold in liquid Hoaglands medium. Medium containing 17 μM FM4-64 was pipetted on the surface of the biofoil slides containing the seeds and allowed to diffuse downward towards the root hairs. Drug treatments were performed by submerging biofoil slides into drug containing medium for 20 min.

Accession numbers

Arabidopsis Genome Initiative numbers for the genes used in this study are At1g47550 (*SEC3A*), At1g76850 (*SEC5A*), At1g71820 (*SEC6*), At3g10380 (*SEC8*), At5g12370 (*SEC10*), At3g56640 (*SEC15A*), At4g02350 (*SEC15B*), At2g28640 (*EXO70H5*), At5g59730 (*EXO70H7*), At5g03540 (*EXO70A1*), At5g49830 (*EXO84B*) and At1g10180 (*EXO84C*).

Acknowledgements

References

- Bloch, D., Hazak, O., Lavy, M., and Yalovsky, S. (2008). A novel ROP/RAC GTPase effector integrates plant cell form and pattern formation. Plant Signal Behav 3, 41-43.
- Chong, Y.T., Gidda, S.K., Sanford, C., Parkinson, J., Mullen, R.T., and Goring, D.R. (2010). Characterization of the Arabidopsis thaliana exocyst complex gene families by phylogenetic, expression profiling, and subcellular localization studies. New Phytol 185, 401-419.
- Clough, S.J., and Bent, A.F. (1998). Floral dip: a simplified method for Agrobacterium-mediated transformation of Arabidopsis thaliana. Plant J 16, 735-743.
- Cole, R.A., Synek, L., Zárský, V., and Fowler, J.E. (2005). SEC8, a subunit of the putative Arabidopsis exocyst complex, facilitates pollen germination and competitive pollen tube growth. Plant Physiol 138, 2005-2018.
- Crowell, E.F., Bischoff, V., Desprez, T., Rolland, A., Stierhof, Y.D., Schumacher, K., Gonneau, M., Hofte, H., and Vernhettes, S. (2009). Pausing of Golgi bodies on microtubules regulates secretion of cellulose synthase complexes in Arabidopsis. Plant Cell 21, 1141-1154.
- Curtis, M.D., and Grossniklaus, U. (2003). A gateway cloning vector set for high-throughput functional analysis of genes in planta. Plant Physiol 133, 462-469.
- Dhonukshe, P., Baluška, F., Schlicht, M., Hlavacka, A., Šamaj, J.,Friml, J., Gadella, T.W.J. (2006) Endocytosis of cell surface material mediates cell plate formation during plant cytokinesis. Developmental Cell, Volume 10, Issue 1, 137-150.
- Duttweiler, H.M. (1996). A highly sensitive and non-lethal beta-galactosidase plate assay for yeast. Trends Genet 12, 340-341.
- Edwards, K., Johnstone, C., and Thompson, C. (1991). A simple and rapid method for the
- reparation of plant genomic DNA for PCR analysis. Nucleic Acids Res 19, 1349.
- Eliás, M., Drdová, E., Ziak, D., Bavlnka, B., Hála, M., Cvrcková, F., Soukupová, H., and Zárský, V. (2003). The exocyst complex in plants. Cell Biol Int 27, 199-201.
- Emons, A.M.C., and Ketelaar, T. (2001). The cytoskeleton in plant cell growth: lessons from root hairs. New Phytologist 152, 409-418.
- Fendrych, M., Synek, L., Pecenková, T., Toupalová, H.,Cole, R., Drdová, E., Nebesarová, J., Sedinová, M., Hála, M., Fowler, J.E., and Zárský, V. (2010). The Arabidopsis exocyst complex is involved in cytokinesis and cell plate maturation. Plant Cell 22, 3053-3065.
- Fiers, M., Hause, G., Boutilier, K., Casamitjana-Martinez, E., Weijers, D., Offringa, R., van der Geest, L., van Lookeren Campagne, M., and Liu, C.M. (2004). Mis-expression of the CLV3/ESR-like gene CLE19 in Arabidopsis leads to a consumption of root meristem. Gene 327, 37-49.
- Finger, F.P., Hughes, T.E., and Novick, P. (1998). Sec3p is a spatial landmark for polarized secretion in budding yeast. Cell 92, 559-571.
- Griffing, L.R. (2008). FRET analysis of transmembrane flipping of FM4-64 in plant cells: is FM4-64 a robust marker for endocytosis? J Microsc 231, 291-298.
- Gutierrez, R., Lindeboom, J.J., Paredez, A.R., Emons, A.M., and Ehrhardt, D.W. (2009). Arabidopsis cortical microtubules position cellulose synthase delivery to the plasma membrane and interact with cellulose synthase trafficking compartments. Nat Cell Biol 11, 797-806.
- Hála, M., Cole, R., Synek, L., Drdová, E., Pecenková, T., Nordheim, A., Lamkemeyer, T., Madlung, J., Hochholdinger, F., Fowler, J.E., and Zárský, V. (2008). An exocyst complex functions
- in plant cell growth in Arabidopsis and tobacco. Plant Cell 20, 1330-1345.
- He, B., and Guo, W. (2009). The exocyst complex in polarized exocytosis. Curr Opin Cell Biol 21, 537-542.
- He, B., Xi, F., Zhang, X., Zhang, J., and Guo, W. (2007). Exo70 interacts with phospholipids and mediates the targeting of the exocyst to the plasma membrane. EMBO J 26, 4053-4065.
- Hsu, S.C., TerBush, D., Abraham, M., and Guo, W. (2004). The exocyst complex in polarized exocytosis. Int Rev Cytol 233, 243-265.
- Hsu, S.C., Ting, A.E., Hazuka, C.D., Davanger, S., Kenny, J.W., Kee, Y., and Scheller, R.H. (1996). The mammalian brain rsec6/8 complex. Neuron 17, 1209-1219.
- Hutagalung, A.H., Coleman, J., Pypaert, M., and Novick, P.J. (2009). An internal domain of Exo70p is required for actin-independent localization and mediates assembly of specific exocyst components. Mol Biol Cell 20, 153-163.
- James, P., Halladay, J., and Craig, E.A. (1996). Genomic libraries and a host strain designed for highly efficient two-hybrid selection in yeast. Genetics 144, 1425-1436.
- Kee, Y., Yoo, J.S., Hazuka, C.D., Peterson, K.E., Hsu, S.C., and Scheller, R.H. (1997). Subunit structure of the mammalian exocyst complex. Proc Natl Acad Sci U S A 94, 14438-14443.

- Ketelaar, T., Anthony, R.G., and Hussey, P.J. (2004). Green fluorescent protein-mTalin causes defects in actin organization and cell expansion in Arabidopsis and inhibits actin depolymerizing factor's actin depolymerizing activity in vitro. Plant Physiol 136, 3990-3998.
- Kulich, I., Cole, R., Drdová, E., Cvrcková, F., Soukup, A., Fowler, J., and Zárský, V. (2010). Arabidopsis exocyst subunits SEC8 and EXO70A1 and exocyst interactor ROH1 are involved in the localized deposition of seed coat pectin. New Phytol 188, 615-625.
- Lavy, M., Bloch, D., Hazak, O., Gutman, I., Poraty, L., Sorek, N., Sternberg, H., and Yalovsky, S. (2007). A Novel ROP/RAC effector links cell polarity, root-meristem maintenance, and vesicle trafficking. Curr Biol 17, 947-952.
- Li, S., van Os, G.M., Ren, S., Yu, D., Ketelaar, T., Emons, A.M., and Liu, C.M. (2010). Expression and functional analyses of EXO70 genes in Arabidopsis implicate their roles in regulating cell type-specific exocytosis. Plant Physiol 154, 1819-1830.
- Lindeboom, J., Mulder, B.M., Vos, J.W., Ketelaar, T., and Emons, A.M. (2008). Cellulose microfibril deposition: coordinated activity at the plant plasma membrane. J Microsc 231, 192-200.
- Liu, C.M., and Meinke, D.W. (1998). The titan mutants of Arabidopsis are disrupted in mitosis and cell cycle control during seed development. Plant J 16, 21-31.
- Liu, J., Zuo, X., Yue, P., and Guo, W. (2007). Phosphatidylinositol 4,5-bisphosphate mediates the targeting of the exocyst to the plasma membrane for exocytosis in mammalian cells. Mol Biol Cell 18, 4483-4492.
- Meinke, D.W., and Sussex, I.M. (1979). Embryo-lethal mutants of Arabidopsis thaliana. A model system for genetic analysis of plant embryo development. Dev Biol 72, 50-61.
- Munson, M., and Novick, P. (2006). The exocyst defrocked, a framework of rods revealed. Nat Struct Mol Biol 13, 577-581.
- Pecenková, T., Hála, M., Kulich, I., Kocourková, D., Drdová, E., Fendrych, M., Toupalová, H., and Zárský, V. (2011). The role for the exocyst complex subunits Exo70B2 and Exo70H1 in the plant-pathogen interaction. J Exp Bot 62, 2107-2116.
- Robinson, D.G., Langhans, M., Saint-Jore-Dupas, C., and Hawes, C. (2008). BFA effects are tissue and not just plant specific. Trends Plant Sci 13, 405-408.
- Samuel, M.A., Chong, Y.T., Haasen, K.E., Aldea-Brydges, M.G., Stone, S.L., and Goring, D.R. (2009). Cellular pathways regulating responses to compatible and self-incompatible pollen in Brassica and Arabidopsis stigmas intersect at Exo70A1, a putative component of the exocyst complex. Plant Cell 21, 2655-2671.
- Shaw, S.L., Dumais, J., and Long, S.R. (2000). Cell surface expansion in polarly growing root hairs of Medicago truncatula. Plant Physiol 124, 959-970.
- Songer, J.A., and Munson, M. (2009). Sec6p anchors the assembled exocyst complex at sites of secretion. Mol Biol Cell 20, 973-982.
- Synek, L., Schlager, N., Eliás, M., Quentin, M., Hauser, M.T., and Zárský, V. (2006). AtEXO70A1, a member of a family of putative exocyst subunits specifically expanded in land plants, is important for polar growth and plant development. Plant J 48, 54-72.
- TerBush, D.R., Maurice, T., Roth, D., and Novick, P. (1996). The Exocyst is a multiprotein complex required for exocytosis in Saccharomyces cerevisiae. EMBO J 15, 6483-6494.
- van Gisbergen, P.A., Esseling-Ozdoba, A., and Vos, J.W. (2008). Microinjecting FM4-64 validates it as a marker of the endocytic pathway in plants. J Microsc 231, 284-290.
- Wang, J., Ding, Y., Hillmer, S., Miao, Y., Lo, S.W., Wang, X., Robinson, D.G., and Jiang, L. (2010). EXPO, an exocyst-positive organelle distinct from multivesicular endosomes and autophagosomes, mediates cytosol to cell wall exocytosis in Arabidopsis and tobacco cells. Plant Cell 22, 4009-4030.
- Wen, T.J., Hochholdinger, F., Sauer, M., Bruce, W., and Schnable, P.S. (2005). The roothairless1 gene of maize encodes a homolog of sec3, which is involved in polar exocytosis. Plant Physiol 138, 1637-1643.
- Wiederkehr, A., Du, Y., Pypaert, M., Ferro-Novick, S., and Novick, P. (2003). Sec3p is needed for the spatial regulation of secretion and for the inheritance of the cortical endoplasmic reticulum. Mol Biol Cell 14, 4770-4782.
- Yang, Z. (2008). Cell polarity signaling in Arabidopsis. Annu Rev Cell Dev Biol 24, 551-575.
- Zhang, X., Orlando, K., He, B., Xi, F., Zhang, J., Zajac, A., and Guo, W. (2008). Membrane association and functional regulation of Sec3 by phospholipids and Cdc42. J Cell Biol 180, 145-158.
- Zhang, Y., Liu, C.M., Emons, A.M., and Ketelaar, T. (2010). The plant exocyst. J Integr Plant Biol 52, 138-146.

Supplemental data

Supplemental figure 1. **Pairwise interactions between exocyst subunits detected by yeast-two-hybrid assays.**

(A) Yeast growth on a SD-Leu-Trp-Ade plate. (B) shows yeast growth on a SD-Leu-Trp-His+3AT (20mM) plate and (C) shows an X-Gal assay.

Supplemental figure 2. Expression pattern of SEC3B in the cotelydon stage embryo (A), silique (B), rosette leaf (C), seedling (D), flower, (E) and stem (F).

Supplemental figure 3. Genotyping of the SALK_145185 (*SEC3A*) and SALK_015980 (*SEC3B*) T-DNA insertion lines reveals plants that are either wild type or heterozygous for both the *sec3a* and *sec3b* allele, but no plants that are homozygous mutant. PCR amplification of the wild-type allele is show in the top rows and that of the inserts in the bottom rows. Lines with only

Supplemental table 1. Primer sequences.

Protein	Gene	CDS (bp)	Forward Primer	Reverse Primer
SEC3A	At1g47550	2664	5'-ATGGCGAAATCAAGCGCCGAC-3'	5'-TTACATGGAAGCCAGAAGTCCTCTCATTTC-3'
SEC3B	At1g47560	2664	5'-ATGAAAACTTCAACCCACCGC-3'	5'-CTTAGAACTAGCCAATCAACGCG-3'
SEC5A	At1g76850	3273	5'-ATGTCGAGCGATAGCAATGATCTTGAC-3'	5'-TTATCTTCGTCTGGGTCGGGC-3'
SEC6	At1g71820	2259	5'-ATGATGGTCGAAGATCTTGGTGTGG-3'	5'-TTAAGTGAGTTTTCGCCACATAGATCCTTTG-3'
SEC8	At3g10380	3162	5'-ATGGGGATTTTCAATGGTTTGCC-3'	5'-TTAATGAGAAAGAATTTCCAAAAGGCGG-3'
SEC10	At5g12370	2786	5'-ATGACAGAAGGAATCAGAGCAAGAGGAC-3'	5'-TCAGCTCAAGCTTGGCCACAAG-3'
SEC15A	At3g56640	2370	5'-ATGGAGGCCAAACCAAAAAGGAG-3'	5'-TCAGTTAAATTCCTTGAGTCTCTTCTTGAGC-3'
SEC15B	At4g02350	2316	5'-ATGCAATCGTCGAAAGGAC-3'	5'-TCAGCTCACATCTTTCAATCTCTTTATCAACG-3'
EXO70H5	At2g28640	1818	5'-ATGATGCTACTATTTAAACCGTCTTTAACTCTAGGAAGAAG-3'	5'-TCAACGTCCTGATTCTGAATCTTTAAGTGAAC-3'
EXO70H7	At5g59730	1905	5'-ATGGGGAAGCATTTATTCCGATCATC	5'- TCAATGACTACTACGTCCGCCACG-3'
EXO70A1	At5g03540	1917	5'-ATGGCTGTTGATAGCAGAATGGATCTG-3'	5'-TTACCGGCGTGGTTCATTCATAGAC-3'
EXO84B	At5g49830	2310	5'-ATGGAGAGCAGCGAGGAAGACG-3'	3'-TCAAGACTCAGAATCGGTGAAAGATGG-3'
EXO84C	At1g10180	2259	5'-ATGGCGGCGAAGACGGC-3'	5'- TCAATAGCTGCCATGAGATCTCGC-3'

Supplemental Movie 1. SEC3A-GFP localization in puncta on the plasma membrane of an elongating root epidermal cell before and after photobleaching.

Supplemental Movie 2. SEC3A-GFP localization in puncta on the plasma membrane of a fully grown root epidermal cell before and after photobleaching.

Supplemental Movie 3. Co-localization of cortical microtubules and SEC3A-GFP puncta.

Supplemental Movie 4. Co-localization of SEC3A-GFP and tdTomatoCESA6.

Chapter 3

Microtubules focus the movement direction of CESA complexes in Arabidopsis root hairs

Ying Zhang [1], Kris van 't Klooster [1],

Anne Mie C. Emons [1,2], Tijs Ketelaar [1]

[1] Laboratory of Cell Biology, Wageningen University, Building 107, Radix W1, Drovendaalsesteeg 1, 6708 PB Wageningen, The Netherlands

[2] Department of Biomolecular Systems, FOM Institute for Atomic and Molecular Physics, Science Park 104, 1098 XG, Amsterdam, The Netherlands

Abstract

In Arabidopsis hypocotyl cells, cortical microtubules serve as a scaffold for the insertion of most cellulose synthase complexes (CESA complexes) into the plasma membrane and guide their movement during cellulose microfibril production, thus determining the orientation of microfibril deposition. In the absence of cortical microtubules, the population of CESA complexes still moves in a uniform direction in these cells, but the angle of movement is different. Since ageing root hairs have gradually decreasing densities of cortical microtubules in the root hair tubes, they are ideal to study the correlation between CMT density and CESA complex insertion and movement direction.

We show that CESA complex insertion into the plasma membrane occurs in both the tip and the tube of root hairs, in growing hairs most abundantly at the side of the hemisphere, where hair tips expand most. CESA complex insertion rates in root hair tubes correlate with CESA complex densities, which allowed us to determine an average CESA complex lifetime of 12.8 ± 1.3 min. The movement of CESA complexes in the plasma membrane of root hair tubes is bidirectional in a net-axial orientation (0.0 ± 13.9° from the cell's long axis) in growing and in a net-Z-helical orientation (-13.2 ± 15.4° from the cell's long axis) in fully-grown hairs. Cortical microtubule (CMT) orientation is nearly axial in both growing (3.1 ± 19.7°) and fully-grown (-1.5 ± 14.6°) cells. We identified 2 populations of CESA complexes, those tracking CMTs and those that do not. The movement direction of complexes that track CMTs is 5.7 ± 9.6° compared to -18.4 ± 20.9° for complexes in between CMTs. After CMT depolymerization, the average direction of CESA complex movement did not change, and the variation in movement direction was similar to that of CESA complexes not tracking CMTs in untreated root hair tubes (-16.7 ± 21.0° in the absence of CMT compared to -18.4 ± 20.9° for CESA complexes not tracking CMTs). Thus, CESA complexes in growing Arabidopsis root hairs that are guided by CMTs move in a more axial angle and have a more uniform movement direction than those that are not. The more uniform and axial movement direction, together with the preferential insertion on CMTs could contribute to straight root hair growth.

Key words:

Cellulose synthase complex, cellulose microfibril, cortical microtubule, cytoskeleton, root hair, tip growing cell, growing and fully-grown cells

Introduction

Root hairs are tip-growing cells. During cell elongation only the tip expands. At the tip, cell wall matrix is deposited against the existing cell wall by exocytosis: Golgi vesicle membranes fuse with the plasma membrane and deliver their polysaccharide/glycoprotein content to the existing cell wall (Reviewed in Miller et al. 1997, Sandhu et al., 2009). The actin cytoskeleton is required for the delivery of Golgi bodies with their vesicles (Miller et al. 1999, de Ruijter et al. 2000, Ketelaar et al. 2003). Cellulose microfibrils are observed in both the tip and the tube of both growing and fully-grown root hairs (Akkerman et al., 2012). Rosettes, the cellulose synthase (CESA) complexes that harbor the gucosyltranferases (Kimura et al 1999) are present in root hair membranes (Emons, 1985).

Fluorescently tagged CESA complexes can be observed by live cell imaging in cells of growing Arabidopsis hypocotyl cells (Paredez et al., 2006), which are axially growing cells, i.e. elongating over their whole longitudinal surface, while the transverse wall faces do not extend. The nascent cellulose microfibrils in the longitudinal cell faces are transverse to the cell's elongation direction (Green 1962; Hamant et al., 2010), as are the cortical microtubules (CMTs). In elongating Arabidopsis hypocotyl cells the CMTs are not required for an ordered pattern of movement of the CESA complexes (Paredez et al., 2006; see also Emons et al., 2007), but are required for maintaining their movement direction transverse to the elongation direction of the cell (Paredez et al., 2006). Although CMTs are not required for the insertion of CESA complexes into the plasma membrane of hypocotyl epidermis cells, in the presence of CMTs this insertion occurs predominantly along them (Gutierrez et al. 2009). Since ageing root hairs have gradually decreasing densities of CMTs in the root hair tubes (Emons and Traas, 1986, Van Bruaene et al., 2004), they are ideal to study the correlation between CMT density and CESA complex insertion and movement direction.

Since all root hair expansion occurs in the tip, the hair tube is a non-expanding cell part. The root hair part comparable to the elongating longitudinal cell face of axially growing cells is the tip, where the fastest elongation occurs at the sides of the hemisphere (Shaw et al. 2000). In elongating root hairs, both CMTs and endoplasmic microtubules come up to the cell apex, but do not appear to loop through it (Arabidopsis van Bruaene et al., 2004, *Medicago truncatula*: Timmers et al., 2007).
All studied growing root hairs have randomly oriented cellulose microfibrils at the tip,

including Arabidopsis (Akkerman et al., 2012). This layer of cellulose microfibrils remains present after growth termination and covers the whole outer surface of the hair (Emons and Wolters-Arts, 1983; Emons, 1989; Arabidopsis: Akkerman et al., 2012). Inside this outer cell wall layer with a random texture a "secondary wall", in the definition of cell wall deposited after cell elongation, is deposited in the no longer expanding root hair tube, which, depending on the species has an axially, helically or helicoidally, but never a transversely oriented texture of cellulose microfibrils (Emons and van Maaren 1987), and is steeply helical in Arabidopsis (Akkerman et al., 2012).

Here we show that CESA complexes are inserted into the plasma membrane of both the tube and the tip of growing and fully-grown root hairs. CESA complex insertion is at least two-fold higher at the side of the hemisphere, where most expansion occurs, than in the tube of growing root hairs. CESA complexes move bidirectionally in a net-axial tonet- Z-helical pattern in the tube's plasma membrane depending on the root hair developmental stage at similar velocities (284 ± 53 nm.min^{-1}) as those reported in hypocotyl cells. Insertion of CESA complexes occurs preferentially on CMTs (growing hairs 64.7 ± 11.3 %, fully-grown hairs 62.0 ± 10.2 %). In fully-grown root hairs, 48.8 ± 6.7 % of the CESA complexes tracks CMTs, the remainder moves in between CMTs. Although CESA complexes that move on CMTs move in a different angle than those in between CMTs ($5.7 \pm 9.6°$ on CMTs compared to $-18.4 \pm 20.9°$ in between CMTs), depolymerzation does hardly change the orientation of CESA complex movement ($-16.7 \pm 21.0°$ compared to $-13.2 \pm 15.4°$ in untreated cells), but increases the standard deviation of the movement direction. This standard deviation is comparable to that of the CESA complexes that move in between CMTs. We conclude that CESA complexes deposit cellulose microfibrils in a default direction, but guidance by CMTs focusses cellulose microfibril deposition direction into a tighter helix.

Results

CESA complexes are inserted into the plasma membrane of the whole root hair, in growing hairs preferentially at the side of the hemisphere
To determine where CESA complexes are inserted into the plasma membrane of growing and fully-grown root hair, we followed GFP-CESA3 recovery in the plasma membrane after photobleaching in three different regions of root hairs: the extreme tip, the side of the hemisphere and the tube (Figure 1A). In all areas CESA complex insertion occurred. Cell expansion occurs only in the tip region, the hemisphere or dome of growing root hairs (Shaw et al., 2000). In fully-grown root hairs, cell

expansion has ceased and therefore all three different regions do not expand. The relative intensity of CESA fluorescence was measured in the plasma membrane in three regions every 2 seconds for 10 minutes during recovery after photobleaching. In growing root hairs, the side of the hemisphere shows the highest GFP-CESA3 recovery rate and the tube shows the slowest GFP-CESA3 recovery rate (Figure 1B). In fully-grown root hairs, the GFP-CESA3 recovery rate is uniform in the three different regions (Figure 1C). Thus, the faster recovery of GFP-CESA3 on the side of the hemisphere is specific for growing root hairs, which indicates that the CESA complex insertion rate is highest in the plasma membrane of the side of the hemisphere where cell expansion occurs most (Shaw et al., 2000) and more cell wall material needs to be deposited. Since this area of the hair dome expands, the number of CESA complexes is continuously diluted in this area; thus, compared to the insertion rate in the root hair tube the insertion rate in this expanding area is likely to be higher than the increase we measure.

Preferential CESA complex insertion occurs on CMTs independent of the CESA complex density

The recovery after photobleaching of CESA complex fluorescence in the plasma membrane of the tube in growing and fully-grown root hairs (Figure 1B and C), indicates that CESA complexes are inserted in regions where cell expansion does not occur. To determine more precisely where insertion occurs and whether the insertion rate correlates with CMT density in the tube of growing and fully-grown root hairs, we photobleached GFP-CESA3 and then visualized the GFP-CESA3 fluorescence recovery in plant lines co-expressing GFP-CESA3 and the microtubule marker mCherry-MAP4-MBD (Gutierrez et al., 2009). During photobleaching of GFP-CESA3 with the 491 nm laser line, mCherry-MAP4-MBD was also locally bleached but CMT fluorescence recovered very rapidly (generally within 1 min of photobleaching); thus, photobleaching of CMTs did not interfere with the analysis of CESA complex insertion coincident with CMTs. CESA complex insertion events were determined as described by Gutierrez et al. (2009).

In the plasma membrane of tubes of both growing and fully-grown root hairs, CESA complexes were inserted into the plasma membrane (Figure 2A). We measured density of CMTs as the percentage of the cell surface area covered by CMT fluorescence, the optical coverage. After growth termination, the density of CMTs decreases in ageing cells; from an average optical coverage in growing root hair tubes of 41.6 ± 3.8 % to an average optical coverage in fully-grown root hair tubes of 20.8 ±

4.6 %, which is significantly lower (P<0.001; Figure 2B). Interestingly the amount of insertion events on CMTs did not decrease significantly (P=0.63) in fully-grown cells: in growing root hairs, 64.7 ± 11.3 % of the insertions events occurred on CMTs, and in fully-grown root hairs, 62.0 ± 10.2 %. These values do not differ significantly (Figure 2B). Thus, when microtubule abundance is lower, there is a stronger preference for insertion on CMTs when one takes the decreased optical coverage into account.
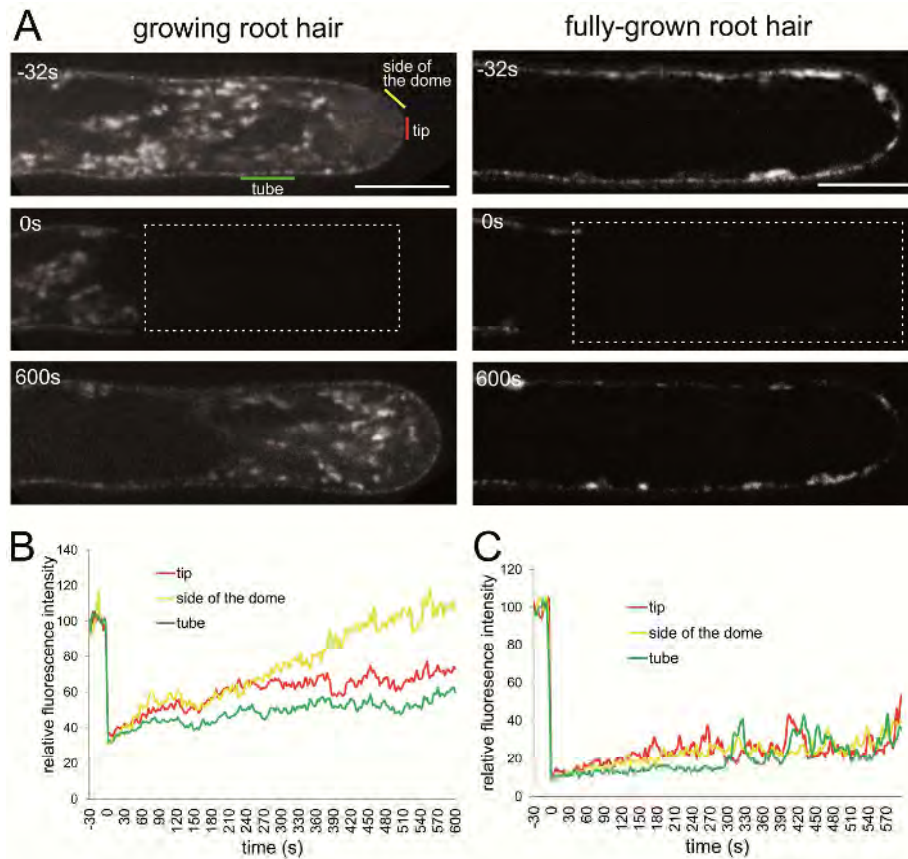

Figure 1. CESA complexes are inserted into the plasma membrane of the tip and tube region of growing and fully-grown root hairs. Fluorescence recovery of GFP-CESA3 is highest at the side of the hemisphere of growing hairs.
(A) The three subsequent images show GFP-CESA3 before photobleaching, immediately after photobleaching and the recovery after 10 min in the median plane of a growing and a fully-grown root hair. The different areas, the tip, the side of the hemisphere and the tube are indicated in gray lines. Bars=10 μm.
(B) and (C) Relative fluorescence intensity in time, showing fluorescence recovery of GFP-CESA3 in the three different areas in the plasma membrane in a growing root hair (B) and a fully-grown root hair (C). The normalized fluorescence intensities from three different cells were averaged.
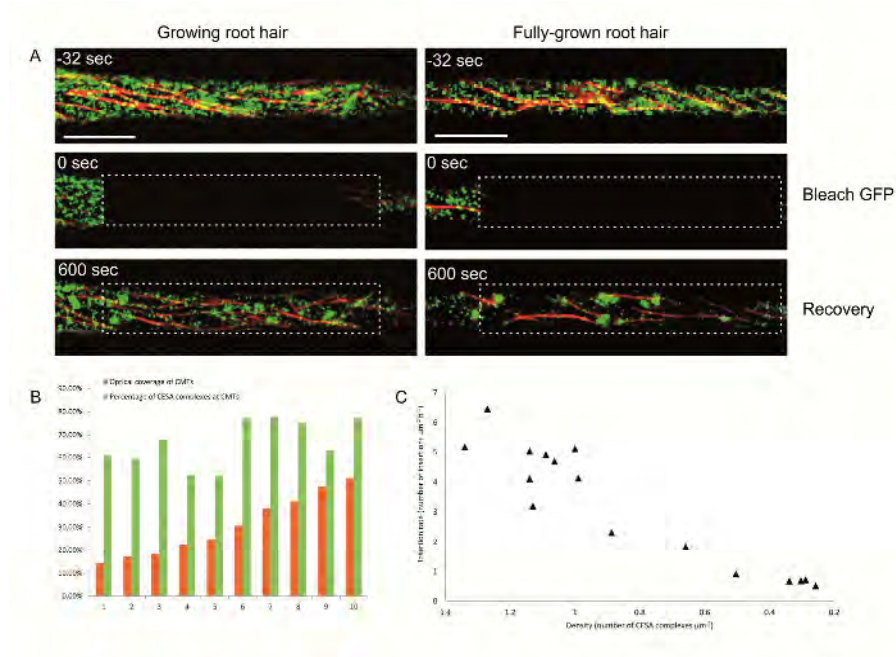
Figure 2. CESA complexes are inserted into the plasma membrane of the tube region of growing and fully-grown root hairs, preferentially at sites coincident with cortical microtubules.
(A) The three constitutive images show GFP-CESA3 before photobleaching, immediately after photobleaching and 10 min after photobleaching in the tube region of growing and fully-grown root hairs. CMT are labeled by mCherry-MAP4-MBD. The CMT are also bleached but their fluorescence recovers within one minute. The dashed boxes indicate the bleached areas. Bars=10μm.
(B) Percentage of CESA complex insertions on CMT in ten different cells with different optical coverage of CMT shows that with a low density of CMTs relatively more insertions occur on the CMT.
(C) CESA complex insertion rates in cells with different CESA complex densities show that insertion rates decrease with CESA complex density.

The average CESA complex lifetime in Arabidopsis root hairs is 12.8 ± 1.4 min.
If CESA complex density correlates with its insertion rate, and densities and insertion rates are known, one can calculate the average CESA complex lifetime. Since CESA complex density was uniform throughout the root hair tube (Figure2A), any tube region can be used for density analysis. To determine the correlation between CESA complex density and insertion rate, we measured CESA complex insertion rate in root hairs with different CESA complex densities. The CESA complex insertion rate indeed correlated with CESA complex density; it decreases linearly when CESA complex density decreases (Figure 2C)

If decreased CESA complex density is caused by a decreased CESA complex insertion rate, the CESA complexes must have a constant average lifetime. We used the CESA complex density and insertion rate in different root hairs to calculate the average lifetime of the whole population of CESA complexes in the photobleached region (Figure 3). For each cell area, the lifetime of CESA complexes is CESA density divided by CESA insertion rate. As expected, the calculated lifetimes do not differ significantly in the root hairs with different CESA complex densities, which allowed us to pool the data and calculate an average lifetime of 12.8 ± 1.3 min. After depolymerization of CMTs with oryzalin, the CESA complex density still correlated with the insertion rate, but the average lifetime of CESA complexes significantly increased to 22.3 ± 3.6 min (Kolmogorov-Smirnov test, P = 0.000).
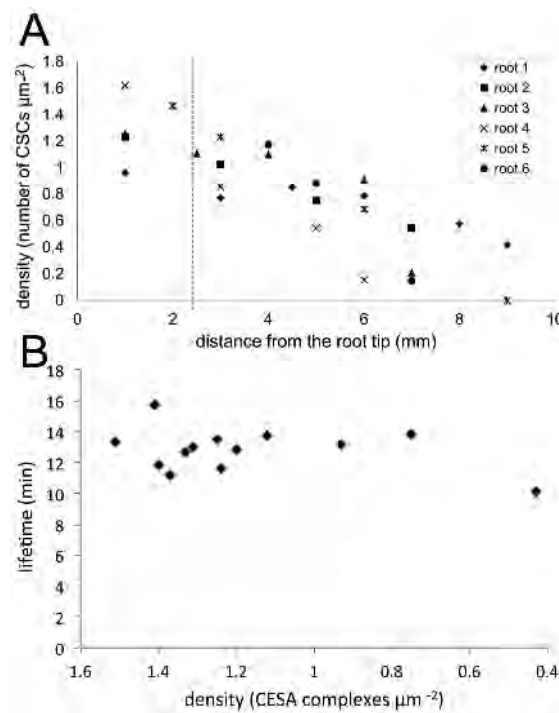

Figure 3. CESA complex density decreases when root hairs age and correlates with insertion rate.
(A) CESA complex density in root hairs on the different locations of the root. On the left side of the dashed line, densities are taken from growing root hairs. On the right side of the dashed line, densities are taken from fully-grown root hairs. With increasing distance of the root hair from the root tip, CESA complex gradually decreases.
(B) Average CESA complex lifetime in root hairs with different densities shows that the lifetime is constant, namely 12.8 ± 1.4 min.

CESA complexes preferentially localize coincident with CMTs

CESA complexes track CMTs in elongating hypocotyl cells (Paredez et al., 2006) and CESA complex insertion preferentially occurs coincident with CMTs, independent of the CMT density. To determine whether in root hairs of various developmental stages all CESA complexes or only part of CESA complexes preferentially track CMTs while depositing cellulose microfibrils, we measured coincident localization with CMTs at 5 random time points (Figure 4A and B) and compared the average value with the optical coverage of CMTs. In both growing and fully-grown root hairs with different CESA complex and CMT densities, the percentage of CESA complexes coincident with CMTs in root hair tubes is significantly higher (P<0.01 in both growing (71.7 ± 3.8 %) and fully-grown (48.8 ± 6.7 %) root hairs) than the optical coverage of CMTs (growing root hairs: 41.6 ± 3.8 %, and fully-grown root hairs: 20.8 ± 4.6 %). The percentage CESA complexes coincident with CMTs is significantly lower in fully-grown cells (P<0.001). However, when optical coverage of CMTs is taken into account by dividing the fraction of CESA complexes on CMT by the optical coverage of CMTs, a significantly higher preference for co-localization of CESA complexes with CMTs is observed at low CMT density than at high CMT density (P<0.01; Figure 4C).
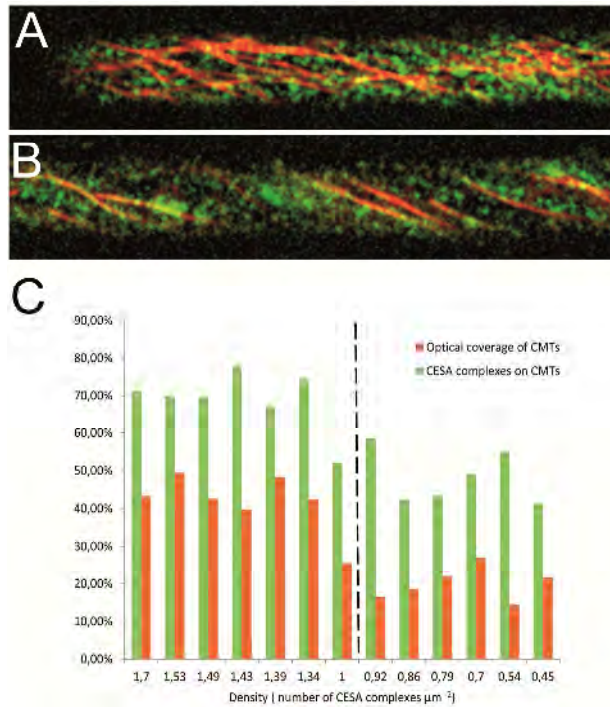

Figure 4 Co-localization of CESA complexes and CMT in the plasma membrane in the tube region of growing and fully-grown root hairs.
(A)and (B) Visualization of CESA complexes by labeling CESA complexes with GFP-CESA3 and CMT with mCherry-MAP4-MBD in the plasma membrane in the root hair tube of a growing (A) and fully-grown (B) root hair. Bar= 10µm.
(C) Plot of the portion of CESA complexes coincident with CMT and optical coverage of CMT in different root hairs with different densities. The left part of the dashed line represents the tube of growing root hairs and the right part the tube of fully-grown root hairs. In each root hair, the percentage of CESA complexes is much higher that the optical coverage of CMT.

CESA complexes exhibit bidirectional Z-helical movement, in fully-grown root hairs with a larger angle from the long axis of the hair than in growing ones

In elongating hypocotyl cells, CESA complexes move bidirectionally with an average velocity of 330 ± 65 nm.min^{-1} (Paredez et al., 2006). To determine if the velocity of CESA complexes is uniform throughout the root hair tube and if the velocity is dependent on CESA complex density and/or developmental stage of the hair, we measured CESA complex velocity in the different locations of root hair tubes in both growing and fully-grown root hairs. The velocity of CESA complex movement is independent of location in the tube (Supplemental figure 1), and the velocities in growing (277.7 ± 51.2 nm.min^{-1}) and fully-grown (304.6 ± 58.7 nm.min^{-1}) root hairs are not significantly different (t-test; p=0.24) and average 284 ± 53 nm min^{-1}. The CESA complex movement is bidirectional (Figure 5A). To determine the CESA complex movement angle, we followed individual CESA complexes in growing and fully-grown root hairs (figure 5B). Since the distribution of angles is not Gaussian, we used non-parametric tests and used median values rather than averages. The median angle of CESA complex movement is 0.0° ± 13.9° (average absolute deviation; n=219) from the cell's long axis in growing root hairs, and -13.0° ± 14.7° (n=396) in fully-grown root hairs (figure 5C and D. The difference in the median angle between growing and fully-grown root hairs is small, but highly significant (P=0.000; Kolmogorov-Smirnov test). When looking from the base of the hair to the tip the movement orientation points downwards in a Z-helix. Thus, on average, CESA complexes move in a net-axial pattern in growing root hairs and a net-Z-elical pattern in fully-grown root hairs.

Since CESA complexes preferentially follow CMTs, we asked to what extent the difference of the net-axial movement pattern in growing and the net-helical movement pattern in fully-grown root hairs is caused by different orientations of CMTs. By measuring CMT direction (figure 5D) we found that the median angle of CMT direction is 3.1° ±19.7°(n=168) in growing root hairs and -1.5° ± 14.6° (n=205) in fully-grown root hairs. Although the average CESA complex movement direction and average CMT direction are significantly different in growing root hairs (P < 0.01), the difference is small. In fully-grown root hairs, however, the direction of CMTs is almost axial whereas the average direction of CESA complex movement is helical and significantly different from the CMT angle (P<0.0001). The deviation between the CMT angle and CESA complex movement direction is due to the fact that in growing hairs a large proportion of the CESA complexes track CMTs by which CMTs keep the CESA complex movement direction axial. In fully-grown hairs over half of the CESA complexes do not follow CMTs.
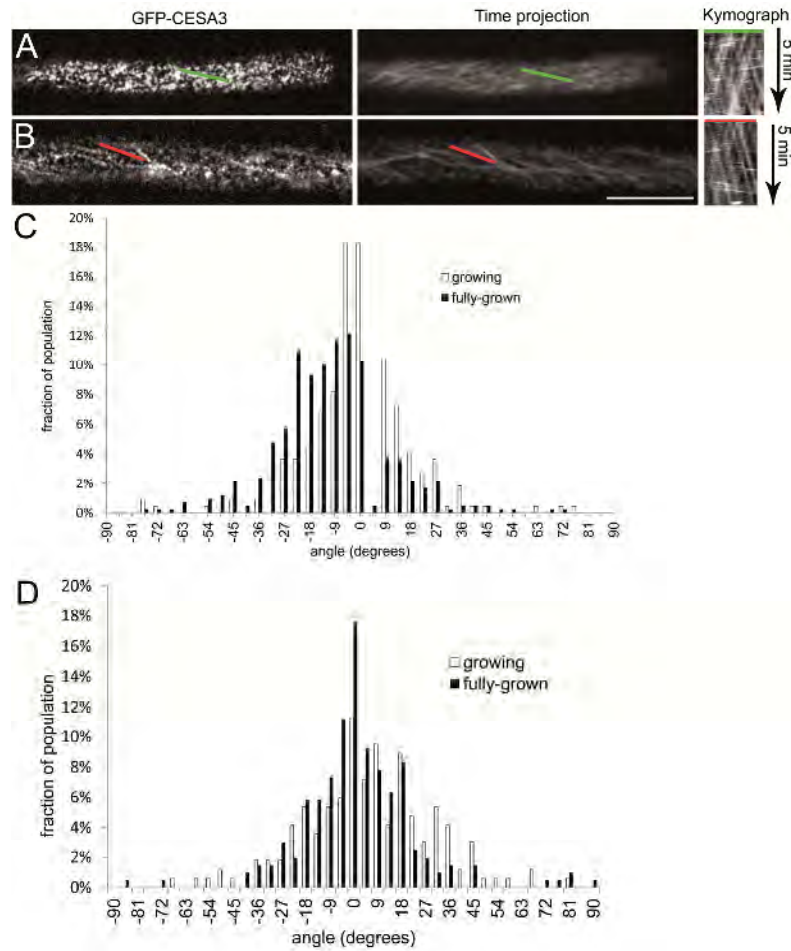
Figure 5. CESA complexes move bidirectionally in an axially in the plasma membrane in the tube of growing root hairs and helically in fully-grown root hairs.

(A and B) Visualization of CESA complexes with GFP-CESA3 in growing (A) and fully–grown (B) root hairs. Time projections made from a 5 min. time lapse movie show the trajectories of CESA complex movement. Kymographs show the bidirectional movement of CESA complexes along the trajectory indicated by the colored lines.

(C) Distribution of angles of CESA complex movement in growing and fully-grown root hairs. 219 CESA complexes from 6 growing root hairs and 419 CESA complexes from 14 fully-grown root hairs were measured. The CESA complex movement shows a net-axial pattern in the growing hairs and a net-helical pattern in the fully-grown hairs.

(D) Distribution of CMT direction in growing and fully-grown root hairs. CMT from 5 growing root hairs and 7 fully-grown root hairs were measured. CMT in both growing and fully-grown hairs are net-axially aligned. Thus, CMT orientation cannot account for the helical pattern of CESA complex movement in the fully-grown hairs.

The overall CESA complex movement direction does not depend on CESA complex density in the presence as well as absence of CMTs

CESA complex density decreases with root hair age (Figure 3A). To determine if CESA complex density affects the direction of CESA complex movement, we measured the movement direction of CESA complexes. To exclude the influence of CMTs on the movement direction of CESA complexes, we also determined the CESA complex movement direction after CMT depolymerization by oryzalin treatment. Since growing root hairs become wavy after CMT depolymerization (Ketelaar et al., 2003); we only used fully-grown root hairs for this experiment. CMTs in root hairs have completely depolymerized within 15 minutes (Figure 6A), but we allowed 6 h to ascertain that CESA complexes had sufficient time to adapt to the absence of CMTs (Figure 6B). Unlike in hypocotyl cells, CMT depolymerization in root hair cells is rapid and no transient CMT reorganization occurs; CMTs just shorten and disappear. When the CESA complex density changes, the average direction of CESA complex movement is not affected, both in the presence and absence of CMTs (Figure 6B). Therefore, CESA complex density is not a factor that is involved in determining the direction of CESA complex movement, within the range of CESA complex densities in these cells.
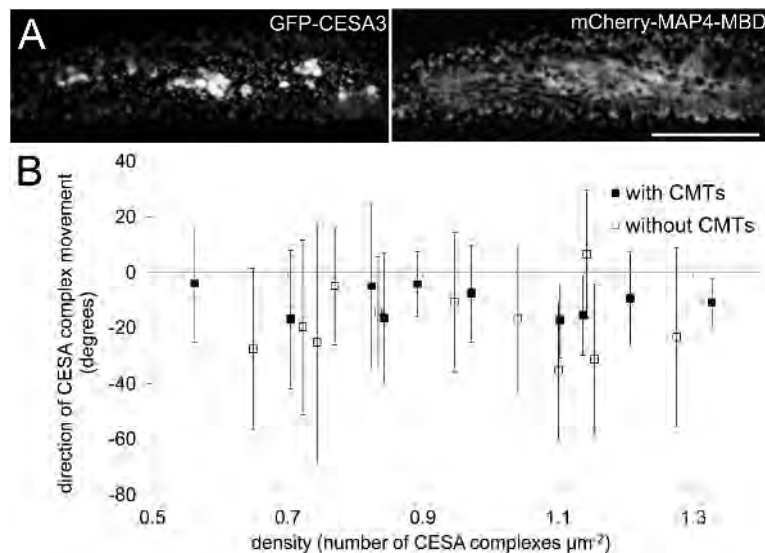

Figure 6. Direction of CESA complex movement in fully-grown root hairs with different densities in the presence and absence of CMT

(A) After 2h of oryzalin treatment, CESA complexes were present in the plasma membrane of the root hair tube, and CMT had been depolymerized.

(B) The direction of CESA complex movement is not dependent on the CESA complex density in the presence and absence of CMT (the movement directions of 30 CESA complexes per cell were measured). Error bars indicate standard deviations.

In the absence of CMTs the movement direction of CESA complexes is as the direction of those that are between CMTs in untreated cells

The direction of CESA complex movement is not dependent on CESA complex density regardless of whether the CMTs are present or not (Figure 5B), but what is the general relation between CESA complex movement direction and CMT orientation? To answer this question, we measured the direction of CESA complex movement in untreated and oryzalin-treated cells. We used fully-grown root hairs to do the measurements. For untreated cells, we discriminated two populations of CESA complexes: those tracking CMTs (48.8 ± 6.7 %) and those not tracking CMTs (51.7 ± 7.2 %). Firstly, we compared the direction of CESA complex movement in the presence and absence of CMTs (Figure 7A). The median angle of CESA complex movement is -13.2° ± 15.4° (absolute average standard deviation; n = 449) in the presence of CMTs and -16.7° ± 21.0° (n = 356) in the absence of CMTs. This difference is small but highly significant (P < 0.001). Next, we compared the movement direction of CESA complexes tracking CMTs with those not tracking CMTs (Figure 7B). The median angle is 5.7° ± 9.6° (n = 85) for CESA complexes tracking CMTs and -18.4° ±20.9° (n = 122) for those not tracking CMTs. The movement orientation of CESA complexes tracking CMTs is significantly different from those that do not track CMTs (P<0.001). Besides this difference the standard deviation of the movement direction of CESA complexes not tracking CMTs is much higher than that of CESA complexes that track CMTs. For this reason, CESA complexes that track CMTs deposit a more focused array of cellulose microfibrils. Then, we compared the direction of CESA complex movement in the absence of CMTs with that of CESA complexes in between CMTs (Figure 7C). The median angle is -16.7° ± 21.0° (n = 356) for CESA complexes in the absence of CMTs and -18.4° ±20.9° (n = 122) for CESA complexes not tracking CMTs. Thus, the direction of CESA complex movement in the absence of CMTs does not differ significantly from that of CESA complexes in between CMTs when CMTs are present (P=0.757). These results suggest that CMTs not only affect the median angle of CESA complex movement direction, they significantly reduce the variation in movement direction: CMTs focus CESA complex movement direction.

The CESA complexes for secondary cell wall formation are present in the root hair plasma membrane but do not move

We show that CESA complexes for primary cell wall formation (labeled by GFP-CESA3) move in the tube of growing cells where cell expansion does not occur and in fully-grown cells, which may indicate that the CESA complexes for primary cell wall formation are sufficient for producing cellulose to build up the cell wall of the root

hair tube. To exclude that the diminishing density of primary CESA complexes in ageing root hairs is caused by replacement by secondary CESA complexes, known to
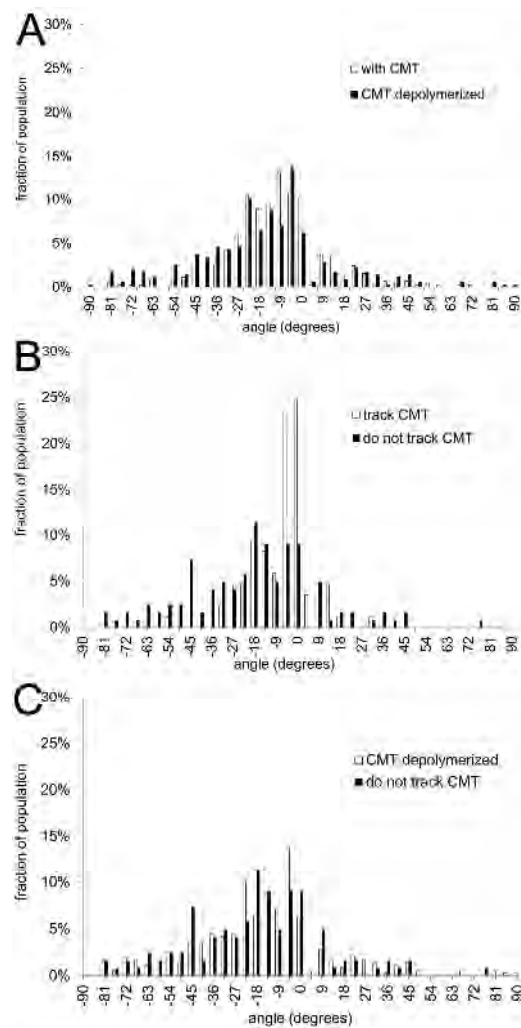
Figure 7. CESA complex movement in the presence and absence of CMT.
(A) The directions of CESA complex movements in untreated and in cells treated for 6-hours with oryzalin.
(B) Plot of the movement directions of two CESA complex populations in the same cells (CESA complexes tracking CMT and CESA complexes not tracking CMT).
(C) The movement directions of CESA complexes not tracking CMT in untreated cells resemble those of CESA complexes in the absence of CMT.

be mainly active in xylem cells, we detected secondary CESA complexes in root hairs by expressing GFP-CESA4. Expression of the GFP-CESA4 fusion construct under its endogenous promoter complemented the c*esa4* mutant (SALK_084627 (Alonso et al., 2003)) phenotype and allowed for localization studies of GFP-CESA4. To determine whether the GFP-CESA4 fusion protein localized as expected, we observed the GFP-CESA4 fluorescence in differentiating xylem cells of the root. GFP-IRX3 (CESA7) one of the subunits of CESA complexes for secondary cell wall formation) showed fluorescent Golgi bodies that moved rapidly in the longitudinal axis of developing banded xylem cells (Gardiner et al., 2003; Wightman et al., 2009). We observed similar fluorescently tagged structures in our GFP-CESA4 line (Figure 8A), which moved with velocities resembling those of cytoplasmic streaming in the differentiating xylem cells (Supplemental movie). Next, we visualized GFP-CESA4 in the cortical plane of root hair tubes. In both growing and fully-grown root hairs, GFP-CESA4 localizes to small particles and larger structures (Figure 8B and C). Most of the small particles wiggled, but did not move over long distances. The larger structures, probably Golgi bodies, displayed rapid directional motion (supplemental movie). Since CESA complexes for secondary cell wall formation do not move in the plasma membrane of root hairs, it is very unlikely that they produce cellulose microfibrils. In ageing fully-grown root hairs, neither GFP-CESA4 fluorescence nor GFP-CESA3 fluorescence was observed, and old root hair cell walls do not become thicker in aging cells (Akkerman et al. 2012)
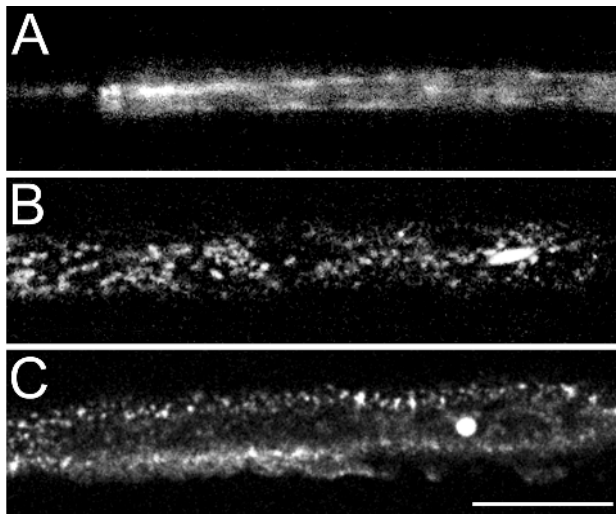

Figure 8. Localization of GFP-CESA4 in xylem vessels and root hair tubes.
(A) GFP-CESA4 forms brightly fluorescent regions in xylem.
(B) GFP-CESA4 is present as particles and patches in the cortical plane in the tube of growing root hairs.
(C) GFP-CESA4 is present in the cortical plane of the tube of fully-grown root hairs, similar to (B). Bar: 10 µm.

An overview of the obtained values is given in Table 1

Table 1. Measured values of different CESA complex and CMT properties in growing and fully-grown root hair tubes.

	Growing root hairs	Fully-grown root hairs
CESA complex velocity (nm.min^{-1})	277.7 ± 51.2	304.6 ± 58.7
CESA complex lifetime (min)	12.8 ± 1.3	22.3 ± 3.6
CESA complex insertions coincident with CMTs (%)	64.7 ± 11.3	62.2 ± 10.2
Optical coverage of CMTs (%)	41.6 ± 3.8	20.8 ± 4.6
CMT orientation (°)	3.1 ± 19.7	-1.5 ± 14.6
CESA complexes tracking CMTs (%)	71.7 ± 3.8	48.8 ± 6.7
CESA complexes in between CMTs (%)	nd	51.7 ± 7.2
Average CESA complex movement direction (°)	0.0 ± 13.9	-13.2 ± 15.4
Average movement direction of CESA complexes tracking CMTs (°)	nd	5.7 ± 9.6
Average movement direction of CESA complexes in between CMTs (°)	nd	-18.4 ± 20.9
Average movement direction of CESA complexes in the absence of CMTs (°)	nd	-16.7 ± 21.0

Discussion

Our data identify a function of CMTs in the insertion location, insertion rate or lifetime, movement directionality and focussing of the movement direction of CESA complexes in root hair cells. Although CMTs are involved in all these processes, remarkably little defects in cellulose deposition occur in the absence of microtubules; it appear that CMTs are involved in fine-tuning CESA complex orientation and decreasing the variation in orientation. Besides this, the lifetime of CESA complexes is increased in the absence of CMTs. Our data do not show whether this is a direct effect of CMT depolymerisation or if the increased lifetime is caused by a compensation mechanism for a reduction in CESA complex insertion. Since the lower CMT density in ageing root hairs correlates with a decreased CESA complex insertion rate, but does not affect CESA complex lifetime, unless when CMTs are fully depolymerized, CMTs can be identified as a facilitator of CESA complex insertion; not only in terms of location, but also in terms of total amount of insertion events. This line of reasoning suggests that the increased lifetime of CESA complexes in the absence of CMTs is a secondary effect which compensates the decrease in CESA complex insertion rate and suggests a feedback mechanism between CESA complex insertion and lifetime.

Cellulose microfibrils in growing and fully-grown Arabidopsis root hair cells are produced by primary cell wall CESA complexes

Unlike in elongating diffuse, axially growing cells where the whole longitudinal walls elongate, root hair growth only occurs at the tip. Thus, the cell wall of the tip of root hairs directly compares to the longitudinal cell walls of axially growing cells in which cellulose microfibrils are organized transversely to the cell elongation direction. Thus, in the hemispherically expanding root hair tip, which expands in all directions, a cellulose microfibril organization in all directions, i.e. a random cell wall texture should be present, which is indeed the case (Arabidopsis: Akkerman et al., 2012).

It is well established that specific CESA proteins are involved in primary cell wall deposition (CESA1, 2, 3, 5, 6 and 9; Persson et al., 2007; Desprez et al., 2007) and others in the deposition of local cell wall thickenings of tracheary element cells of the xylem (CESA4, 7 and 8 (Taylor et al., 2003)), called primary and secondary CESA respectively. Almost all plant cells deposit a secondary cell wall, an even, smooth, wall produced by definition after cell elongation has ceased. Little is known of the composition of the CESA complexes that contribute to the formation of these cell walls. Although publically available gene expression data show that the secondary CESAs are expressed in root hairs (http://bar.utoronto.ca) and the secondary CESA complex subunit CESA4 is present in compartments in the cytoplasm and the plasma membrane of the fully-grown hairs where cellulose is still being deposited (our data), their lack of movement shows that they do not contribute to cellulose deposition. Thus, only primary CESA complexes contribute to cell wall formation in Arabidopsis root hairs.

CESA3 insertion takes place into the plasma membrane of the whole root hair tip and tube, and the mean CESA complex lifetime is 12 min

Golgi vesicles accumulate in the tip of growing root hairs (Miller et al. 1997 and references herein; Ketelaar et al., 2007. At those tips exocytosis is thought to occur by which the plasma membrane elongates, plasma membrane proteins, including the cellulose synthases, are inserted into the plasma membrane, and cell wall matrix is deposited as the content of the Golgi vesicles. For protonemata of the moss *Funaria hygrometrica* it has been shown that particle rosettes, the name of the CESA complexes before it had been shown that they contain the glucosyltransferases for cellulose production (Kimura et al. 1999), are present at the tip of these tip-growing cells; their density decreases gradually towards the base of the cell (Rudolp, 1987; Rudolph and Schnepf, 1988). In root hairs of the fern *Equisetum hyemale*, rosettes

were shown to occur in the whole plasma membrane of the growing hair tube (Emons 1985). We have found that in Arabidopsis root hairs CESA complexes occur, move and are inserted in the plasma membrane of both tip and tube of both elongating and elongated hairs. We show that insertion of CESA complexes gradually decreases in ageing root hairs until insertion of CESA complexes dwindles, at the same time cell wall thickness increase stops (Akkerman et al. 2012).

Park et al. (2011) could not detect fluorescently tagged primary CESA complexes in tips of growing Arabidopsis root hairs. Since cellulose microfibrils are present in the tip of growing root hairs (Akkerman et al., 2011; Park et al., 2011), Park et al. (2011) proposed that a possible candidate for the production of the cellulose microfibrils in Arabidopsis root hair tips is the CESA-like protein CSLD3, which localizes to the plasma membrane in tips of growing root hairs, is essential for cell wall integrity of the expanding tips, and has (1,4)-β glucan synthase activity (Park et al. 2011). Our work does not exclude a role for CSLD3 in cellulose microfibril production in root hair tips, but shows that primary CESA complexes are present as well. Moreover, their insertion into the plasma membrane is even at highest rate in the flanks of the hemisphere tip.

The fact that CESA complexes are inserted not only at the hair's tip where exocytotic vesicles accumulate but also in the hair tube has consequences for our ideas about the machinery of CESA complex insertion. The amount of vesicles and the amount of exocytosis in the tips of growing root hairs is much higher than in the root hair tube (Ketelaar et al., 2007); still the amount of CESA insertions in the tip of growing root hairs is only two-fold, or perhaps somewhat more, higher than the amount of insertions in the tube. This suggests that most of the vesicles that accumulate in the tip do not contain CESA complexes in their membrane, unlike those in the root hair tube. This is consistent with the relatively low GFP-CESA3 fluorescence that we observe in the vesicle rich apex in growing root hairs. Thus, our data suggest that either there are vesicles in Arabidopsis root hairs destined for cell growth that probably contain cell wall matrix materials and that there is a separate mechanism or vesicle type that mediates CESA complex insertion into the plasma membrane. Since exocytosis, if occurring along the whole plasma membrane of the tube, is spread out, an accumulation of CESA containing vesicles along the tube membrane is not required. Such dispersed vesicles could well have been overlooked in electron microscopy studies. Although we do not understand the precise insertion mechanism of CESA complexes to the plasma membrane, the Golgi bodies that provide the CESA

complexes line up along the tube's plasma membrane (Gutierrez et al., 2009; Akkerman et al., 2011) including in electron microscopy studies (Lindeboom et al., 2007; Miller et al., 1997; Emons, 1987).

The relation between density of CESA complexes and their insertion rate in root hairs of all developmental stages allowed us to estimate the average lifetime of CESA complexes, i.e. the residence time of a CESA complex moving inside the plasma membrane. This approach does not reveal the variation in the life times of CESA complexes, but the mean lifetime of individual CESA complexes in the whole population. Since this lifetime is 12.8 minutes, and the average CESA velocity 284 μm.min^{-1}, the mean cellulose microfibril length a CESA complex produces is 3.2 μm in untreated Arabidopsis root hairs and 6.3 μm in oryzalin treated root hairs. In FESEM images of cellulose microfibrils of these and other cells (Akkerman et al., 2012), hardly any ends of cellulose microfibrils have been observed, suggesting that microfibrils are longer than the lifetime of a CESA complex, but cellulose microfibril length has not and cannot be measured in such preparations.

Cortical microtubules focus CESA-complex insertion and movement
In tip growing pollen tubes, Cai et al. (2011) used immunocytochemistry to show that CESA complexes occur on as well as between CMTs. Using live cell imaging we find that in tubes of fully-grown root hairs a considerable amount of CESA complexes is positioned between CMTs, up to 51.7 %, while in the root epidermal cells we measured 10% (Zhang et al., submitted), which latter percentage could be accounted for by the occurrence of microtubule dynamic instability. The CESA complexes between the CMTs in fully-grown root hairs move in a different, more helical angle then those on CMTs, but also with a larger variance. In the absence of CMTs, all CESA complexes in root hair tubes follow the same helical pattern as the CESA complexes that move between CMTs in untreated cells. Is there another, morphogenetic function for microtubules, by fine tuning CESA insertion and movement in root hair tubes? In the absence of CMTs, root hair tip growth continues with the same velocity, the diameter of the growing tip is not affected, but root hairs become wavy (Bibikova et al., 1999; Ketelaar et al., 2002; Van Bruaene et al., 2004) and in *Medicago truncatula* root hair elongation is slower (Sieberer et al., 2002). It has been shown before that actin filaments determine whether or not root hairs elongate (Miller et al., 1999; Ketelaar et al., 2002, 2003) and that CMTs somehow guide the growth machinery in root hairs (Ketelaar et al., 2003; Bibikova et al., 1999). Our present work sheds some light on this mechanism. Fluorescence recovery after photobleaching of GFP:CESA3 is

highest at the rim of the hemisphere (Figure 1) where most expansion occurs (Shaw et al., 2000). CMTs come up to this area and a bit further into the tip, but do not seem to loop through it (Van Bruaene et al., 2004). Their density is high in the subapex of elongating hairs, by which they can focus, constrict, CESA insertion and movement in this area where CMTs are likely to focus the direction of cell growth. This may be part of the mechanism leading to root hairs with fixed diameter.

Material and Methods

Plant material

All the *Arabidopsis* lines had a Col-0 background. *Arabidopsis thaliana* plants expressing pCESA3: GFP-CESA3 were used for imaging of CESA complexes. The pCESA3:GFP-CESA3 seeds were provided by S. Vernhettes (Insitut National de la Recherche Agronomicque, Versailles, France; Desprez et al., 2007). For simultaneous imaging of microtubules and CSCs, microtubules were visualized in the above line by expression of 35s:mCherry-MAP4-MBD as described by Gutierrez et al. (2009).

Seeds were surfaced sterilized by soaking for 1 min in 70% ethanol and then for 4 min in 5-10% bleach (Sodium hypochlorite) with 0.05% Triton-X 100, followed by 4 rinses in sterile distilled water. Seeds were maintained in a small volume of water and stratified at 4°C for 2 days.

Seedlings were grown for root hair imaging as described by Ketelaar et al. (2004), with the exception that we used Hoaglands medium , containing 0.16%(w/v) Hoaglands' basal salt mixture (Sigma-Aldrich), 0.0096%(w/v) myo-Inositol (Merck), 0.00168%(w/v) Thiamine-HCl (Calbiochem)(pH 5.7) supplemented with 1% sucrose (Duchefa), and 0.7% Phyto agar (Duchefa). The seedlings were grown at 22°C with for 4 days under long day conditions (16 h light, 8 h darkness).

Drug treatment

Oryzalin stock solution was prepared in DMSO. The stock solution was freshly diluted to 2µM in liquid Hoaglands medium before use. Oryzalin treatment was performed by submerging biofoil slides into drug containing medium for 20 min and then taken out and kept in petri dish for 6 hours.

Confocal microscopy

The seedlings were mounted to the Eclipse Ti inverted microscope (Nikon) equipped with a 100/1.4 NA oil immersion objective. Spinning disk confocal imaging of seedlings expressing GFP-CESA3 and mCherry-MAP4-MBD was conducted using a Roper Scientific spinning disk system, consisting of a CSU-X1 spinning disk head (Yokogawa), QuantEM: 512SC CCD camera (Roper Scientific) and a 1.2× magnifying lens between the spinning disk head and the camera. A multi-channel AOTF device (AA Opto-Electronic Company) was applied for excitation switching and shuttering, and band pass filters (530/50 nm for GFP, and 640/50 nm for mCherry; Chroma Technology). GFP and mCherry were excited by 491nm and 561nm laser lines, respectively. Exposure times of 600 -2000 ms for GFP and 300 ms for mCherry were used.

Photobleaching was carried out by FRAP/PA system (Roper Scientific) incorporated into the spinning disk microscope described above. The focal plane was scanned by the focused laser light by a pair of galvometer-driven mirrors inside the FRAP/PA unit. A 491 nm laser (5 ms per scan point of 4 pixels in diameter) with 87% laser power was used to photobleach GFP.

The time interval for all the time-laps series was 2 seconds.

Image processing

All imaging processing was performed using Image J software (http://rsb.info.nih.gov/ij/) and plugins. Firstly, noise was reduced by running the WalkingAverage plugin (three-frame window), whereafter the background signal was removed by the "Subtract Background" command (rolling ball radius of 20-30 pixels) in Image J.

Quantification of CSC velocity and density

Seedlings expressing GFP-CESA3 were used for imaging. 10 min of time-laps movies were used for measuring CESA complexes velocity and density in root hairs. The locations where the velocity and density was measured in the root hair tube regions were calculated the distance from the root hair tips and the velocity and density in different locations were compared statistically. A segmented line following CSC trajectories in the root hair tube was drawn along the time-lapse movies in Image J and the kymographs were created by MultipeKymograph plugin. Velocities of CSCs were determined using the "read velocity by tsp" plugin. The density of CSCs in the

plasma membrane was determined by counting the number of fluorescent particles in the focal plane of the plasma membrane that were migrating at constant velocities between 250 -500 nm.min-1 the root hair tube.

Quantification of CESA complex insertion rate and percentage of insertions on CMTs

The seedlings expressing GFP-CESA3 and mCherry-MP4-MBD were used for the insertion event analysis of CESA complexes and the relation with CMTs. At a random location of root hair tube region, GFP-CESA3 fluorescence was bleached with 481 nm laser line and fluorescence recovery of GFP-CESA was visualized for 10 min after photobleaching. The insertion events were determined according to the three criteria described as Gutierrez et al. (2009). The quantification of CESA complex insertions on

CMTs and the calculation of optical coverage of CMTs were performed as described by Gutierrez et al. (2009). In our analysis, the insertion rate and the insertions on CMTs were analyzed in different root hairs with different densities and the 1 min of time-laps movies before photobleaching was used to determine the density. 311 insertion events in 6 growing root hairs and 201 insertion events in fully-grown root hairs were analyzed. The insertion rate in absence of CMTs was performed by depolymerizing CMTs with 1µm of oryzalin for 6 hours and then the GFP-CESA3 fluorescence photobleaching and recovery was visualized as described above.

Colocalization analysis of CESA complexes and CMTs

The seedlings expressing GFP-CESA3 and mCherry-MP4-MBD were used for the co-localization analysis of CESA complexes and CMTs. For each root hair with different density, 5 random frames from a 5-min of time lapse movie were selected to mark the centroids of CESA complexes in a random large area (> 6 um^2). The centroids of CESA complexes were mapped onto the binary image of CMTs to determine the colocalization.

Quantification of the direction of CESA complex movement and CMT

The seedlings expressing GFP-CESA3 and mCherry-MP4-MBD were used and 10 min of time lapse movies were made to follow CESA complexes and CMTs. The orientation (from -180 degrees to 180 degrees) of CESA complex movement was determined by drawing a line along the movement trajectory and the angle of the line was calculated with Image J. The angles were converted to the range of -90 degrees to 90 degrees.

The directions of CMT were determined by making a time-projection of the time lapse movie and then drawing a line along the CMT. The angles (from -90 degrees to 90 degrees) were calculated with Image J. The histograms of movement angles were made with bin sized of 4.5 degrees.

Acknowledgements

References

- Akkerman, M., Franssen-Verheijen, M.A., Immerzeel, P., Hollander, L.D., Schel, J.H., and Emons, A.M. (2012). Texture of cellulose microfibrils of root hair cell walls of *Arabidopsis thaliana, Medicago truncatula*, and *Vicia sativa*. J Microsc. 247, 60-67.

- Bibikova, T.N., Blancaflor, E.B., and Gilroy, S. (1999). Microtubules regulate tip growth and orientation in root hairs of *Arabidopsis thaliana*. Plant J. 17, 657-665.

- Cai, G., Faleri, C., Del Casino, C., Emons, A.M., and Cresti, M. (2011). Distribution of callose synthase, cellulose synthase, and sucrose synthase in tobacco pollen tube is controlled in dissimilar ways by actin filaments and microtubules. Plant Physiol. 155, 1169-1190.

- Desprez, T., Juraniec, M., Crowell, E.F., Jouy, H., Pochylova, Z., Parcy, F., Höfte, H., Gonneau, M., and Vernhettes, S. (2007). Organization of cellulose synthase complexes involved in primary cell wall synthesis in *Arabidopsis thaliana*. Proc Natl Acad Sci U S A. 104, 15572-15577.

- De Ruijter, N.C.A., Bisseling, T., and Emons, A.M.C. (1999). *Rhizobium* nod factors induce an increase in sub-apical fine bundles of actin filaments in *Vicia sativa* root hairs within minutes. Mol. Plant-Microbe Interact. 12, 829–832.

- De Ruijter N.C. and Malhó R. (2000). Plant fungal tip growth: where do we go from here? Trends Plant Sci. 5:453-454.

- Emons, A.M.C. (1985). Plasma-membrane rosettes in root hairs of *Equisetum hyemale*. Planta 163, 350-359.

- Emons, A.M.C. (1989). Helicoidal microfibril deposition in a tip-growing cell and microtubule alignment during tip morphogenesis: a dry-cleaving and freeze –substitution study. *Can. J. Bot.* 67, 2401-2408.

- Emons, A. M. C. and Wolters-Arts, A. M. C. (1983). Cortical microtubules and microfibril deposition in the cell wall of root hairs of *Equisetum hyemale*. Protoplasma 117, 68-81.

- Emons, A. M. C. and Traas, J. A. (1986). Coated pits and coated vesicles on the plasma membrane of plant cells. Eur. J. Cell Biol. 41, 57-64.

- Emons, A.M.C. and Van Maaren, N. (1987). Helicoidal cell wall texture in root hairs. Planta 170, 145-151.

- Emons, A.M., Höfte, H., and Mulder, B.M. (2007). Microtubules and cellulose microfibrils: how intimate is their relationship? Trends Plant Sci. 12, 279-281.

- Gardiner J.C., Taylor N.G., Turner S.R. (2003). Control of cellulose synthase complex localization in developing xylem. Plant Cell. 15:1740-1748.

- Green, P.B. (1962). Mechanism for plant cellular morphogenesis. Science 138, 1404-1405.

- Gutierrez, R., Lindeboom, J.J., Paredez, A.R., Emons, A.M., and Ehrhardt, D.W. (2009). Arabidopsis cortical microtubules position cellulose synthase delivery to the plasma membrane and interact with cellulose synthase trafficking compartments. Nat. Cell Biol. 11, 797-806.

- Hamant, O., Traas, J., and Boudaoud, A. (2010). Regulation of shape and patterning in plant development. Curr Opin Genet Dev. 20, 454-459.

- Ketelaar T., Allwood E.G., Hussey P.J.(2007) Actin organization and root hair development are disrupted by ethanol-induced overexpression of Arabidopsis actin interacting protein 1 (AIP1). New Phytol. 174:57-62.

- Ketelaar, T., de Ruijter, N.C.A. and Emons, A.M.C. (2003). Unstable F-actin specifies the area and microtubule direction of cell expansion in Arabidopsis root hairs. Plant Cell 15, 285-292.

- Ketelaar T, Faivre-Moskalenko C, Esseling JJ, de Ruijter NC, Grierson CS, Dogterom M, Emons AM. (2002). Positioning of nuclei in Arabidopsis root hairs: an actin-regulated process of tip growth.Plant Cell. 14:2941-2955.

- Kimura, S., Laosinchai, W., Itoh, T., Cui, X., Linder, C.R., and Brown, R.M. Jr. (1999). Immunogold labeling of rosette terminal cellulose-synthesizing complexes in the vascular plant *Vigna angularis*. Plant Cell 11, 2075-2086.

- Lindeboom J., Mulder B.M., Vos J.W., Ketelaar T., Emons A.M. (2008) Cellulose microfibril deposition: coordinated activity at the plant plasma membrane. J. Microsc. 231, 192–200.

- Miller, D.D., De Ruijter, N.C.A., and Emons, A.M.C. (1997). From signal to form: aspects of the cytoskeleton-plasma membrane-cell wall continuum in root hair tips. J. Exp. Botany 48, 1881-1896.
- Miller, D.D., De Ruijter, N.C.A., Bisseling, T. and Emons, A.M.C. (1999). The role of actin in root hair morphogenesis: Studies with lipochito-oligosaccharide as a growth stimulator and cytochalasin as an actin perturbing drug. Plant J. 17, 141-154.
- Paradez, A.R., Somerville, C.R., and Ehrhardt, D.W. (2006). Visualization of cellulose synthase demonstrates functional association with microtubules. Science 312, 1491-1495.
- Park S., Szumlanski A.L., Gu F., Guo F., Nielsen E. (2011). A role for CSLD3 during cell-wall synthesis in apical plasma membranes of tip-growing root-hair cells. Nat Cell Biol. 13:973-980.
- Persson, S., Paredez, A., Carroll, A., Palsdottir, H., Doblin, M., Poindexter, P., Khitrov, N., Auer, M., and Somerville, C.R. (2007).Genetic evidence for three unique components in primary cell- wall cellulose synthase complexes in Arabidopsis. Proc Natl Acad Sci U S A. 104, 15566-15571.
- Rudolph, U. (1987). Occurrence of rosettes in the ER membrane of young *Funaria hygrometrica* protonemata. Naturwiss 74, 439.
- Rudolph, U., and Schnepf, E. (1988). Investigations of the turnover of the putative cellulose-synthesizing particle rosettes within the plasma membrane of *Funaria hygrometrica* protonema cells. 1. Effects of monensin and cytochalasin B. Protoplasma 143, 63–73.
- Sandhu, A.P., Randhawa, G.S., and Dhugga, K.S. (2009). Plant cell wall matrix polysaccharide biosynthesis. Mol Plant 2, 840-850.
- Shaw, S.L., Dumais, J. and Long, S.R. (2000). Cell surface expansion in polarly growing root hairs of *Medicago truncatula*. Plant Physiol. 124, 959-970.
- Sieberer, B.J., Timmers, A.C., Lhuissier, F.G., and Emons, A.M. (2002). Endoplasmic microtubules configure the subapical cytoplasm and are required for fast growth of *Medicago truncatula* root hairs. Plant Physiol. 130, 977-988.
- Taylor, N.G., Howells, R.M., Huttly, A.K., Vickers, K., and Turner, S.R. (2003). Interactions among three distinct CesA proteins essential for cellulose synthesis. Proc Natl Acad Sci USA 100, 1450–1455.
- Timmers, A.C.J., Vallotton, P., Heym, C., and Menzel, D. (2007). Microtubule dynamics in root hairs of *Medicago truncatula*. European Journal of Cell Biology 86, 69-83.
- Van Bruaene, N., Joss, G., and Van Oostveldt, P. (2004). Reorganization and in vivo dynamics of microtubules during Arabidopsis root hair development. Plant Physiol. 136, 3905-3919.
- Wightman, R., Marshall, R., and Turner, S.R. (2009). A cellulose synthase-containing compartment moves rapidly beneath sites of secondary wall synthesis. Plant Cell Physiol. 50, 584-594.

Chapter 4

Cellulose synthase complex, cortical microtubule, and cellulose microfibril alignment in *Arabidopsis* root epidermal cells

Ying Zhang[1], Miriam Akkerman[1], Tiny Franssen-Verheijen, Anne Mie C. Emons, Tijs Ketelaar

Laboratory of Cell Biology, Department of Plant Sciences, Wageningen University, Droevendaalsesteeg 1, 6708 PB Wageningen, The Netherlands

[1]These authors contributed equally to this work

Abstract

Cellulose microfibrils (CMFs) are the main load bearing structures of plant cell walls. They are produced by cellulose synthase (CESA) complexes that move through the plasma membrane. In axially growing hypocotyl cells CMF alignment is determined by microtubules guiding the CESA complexes (Paredez et al. 2006). In these cells, spacing of cortical microtubules (CMTs) is wider than that of the CMFs, which are deposited as a uniform layer (Crowell et al. 2011). To understand how CESA complexes that are guided by CMTs can produce a uniform layer of CMFs, we studied the orientation, density, alignment and movement of CMTs and CESA complexes using immunocytochemistry and live cell imaging of root epidermal cells. Furthermore we studied the orientation and density of CMFs in the innermost cell wall layer of these cells with Field Emission Scanning Electron Microscopy (FESEM). The CMTs, the rows of CESA complexes and the innermost CMFs lay in the same orientation, approximately transverse to the elongation axis in both the inner and outer periclinal cell face in the elongation zone and root hair zone. CESA complexes predominantly move in rows along CMTs in both directions. While the density of CMTs and CESA rows corresponds, the density of CMFs in the innermost cell wall layer is much higher and CMFs form an even layer. After analysis of timelapse movies of CMTs we conclude that CMTs reposition over time, so that CESA complexes produce an even cell wall layer.

Introduction

Plant cells are surrounded by cell walls, which expand during cell elongation. The load bearing polymers in these cell walls are crystalline cellulose microfibrils (CMFs). It is generally thought that in axially (also called diffuse or intercalary) growing cells, the orientation of these CMFs determines the cell elongation direction, which is perpendicular to the orientation of the CMFs (Green 1962; Baskin 2005).

CMFs are produced by cellulose synthase (CESA) complexes in the plasma membrane, which at electron microscopy resolution can be seen as hexametric rosettes (Kimura et al., 1999; Mueller and Brown; 1980 Emons, 1985). Live cell imaging of these CESA complexes tagged with fluorescent proteins has shown their movement within the plane of the plasma membrane in Arabidopsis hypocotyl cells (Paredez et al. 2006; Debolt et al. 2007; Persson et al. 2007; Desprez et al. 2007; Gu et al. 2010, Crowell et al. 2009, 2011; Gutierrez et al. 2009; Chan et al. 2010, 2011), guided by the cortical microtubules (CMTs) (Paredez et al. 2006, Fujita et al. 2011, Bringmann et al. 2012), which in addition function in localizing the insertion of CESA complexes into the plasma membrane. However, in the absence of the CMTs CESA complexes still move in an ordered, though different, pattern through the plasma membrane (Paredez et al. 2006; see also Emons et al. 2007).

In axially growing root cells studied by means of immuno-cytochemistry and transmission electron microscopy, respectively, alignment of CMTs and CMFs is in the same overall direction, transverse to the elongation axis of the cell (reviewed in Baskin, 2001). Later studies, using live cell imaging of both CMTs and CESA complexes, have increased our understanding of the process of CMF alignment (Paredez et al., 2006; Debolt et al., 2007; Persson et al., 2007; Crowell et al., 2009, 2011; Gutierrez et al., 2009; Chan et al., 2010, 2011). In elongating etiolated Arabidopsis hypocotyl cells different orientations of both CMTs and CMFs are found in the outer epidermal cell surface (Chan et al., 2010), but at the wall of the inner epidermal cell surface both polymers remain transverse (Crowell et al., 2011, Chan et al 2011) during the whole cell elongation phase, implicating that a transverse CMF orientation in the inner periclinal wall could be sufficient and required for cell elongation in these cells (Crowell et al. 2011).

Since we were not able to study CESA movement in the inner cell face of root epidermal cells using live cell probes, CESA complex localization was in addition studied using immuno-cytochemistry on sections, which also allowed studying CESA localization in deeper cell layers. Moreover, an antibody raised against a conserved domain of CESA proteins labels all CESA complexes, which is not necessarily the case for the live cell imaging probes. We used an anti-CESA antibody, raised against the conserved cytoplasmic loop of the CESA catalytic subunit for visualization of the CESA complexes (Gillmor et al., 2002; Cai et al., 2011). Analysis of samples that were labelled with this antibody revealed lines of dots in the cell cortex, presumably the plasma membrane. In epidermal cells of the root elongation zone and root hair zone the orientation of the lines was transverse to the long axis of the cell at both the inner and outer periclinal cell face. This CESA complex patterning, and density, appeared to be similar to that in GFP:CESA3 expressing root epidermal cells, in which CESA complexes move in rows along CMTs. Using Field Emission Scanning Electron Microscopy (FESEM), we found that spacing between CMFs in the lastly deposited layer of the cell wall is uniform over the cell surface, as already shown earlier (Sugimoto et al 2000; Baskin et al. 2004) and the distance between neighbouring CMFs is much smaller than that between CMTs at the other side of the plasma membrane. How can such a uniform distribution of CMFs in the cell wall be obtained? We analyzed two hypotheses: CESA complexes in between the CMTs contribute considerably to CMF layer formation and/or CMTs reposition continuously. Our data favour the second alternative.

Results

Immunolabeling with an antibody against CESAs reveals that CESA complexes are present in rows of dots at the plasma membrane of Arabidopsis root epidermal and cortical cells
We used the CESA antibody characterized by Gillmor et al. (2002) and Cai et al. (2011) to label 4-5 µm thick sections of butylmethylmetacrylate (BMM; Baskin et al., 1992) embedded, cryo-fixed Arabidopsis roots. The antibody was raised against the conserved cytoplasmic loop of the CESA catalytic subunit and cross-reacts specifically with an intrinsic Arabidopsis plasma membrane protein of 120 kD (Gillmor et al., 2002; Cai et al., 2011).

To test the specificity of the CESA labelling, we checked whether CESA complexes

could be detected in the plasma membrane underlying developing secondary cell wall thickenings in differentiating xylem cells. Many rosettes, which represent the CESA complexes (Kimura et al. 1999) are present at these locations (Herth, 1985; Gardiner et al., 2003). Supplemental Figure 1 shows that our immunolabeling procedure recognizes these accumulations of CESA complexes in developing tracheary elements of the xylem. After confirmation of the antibody specificity in our samples, we proceeded to study the CESA complex localization at the outer and inner faces of root epidermal cells and root cortical cells. Figure 1 shows typical examples of sections containing large stretches of the plasma membrane underlying the outer and inner periclinal cell faces of root epidermal cells. The antibody against CESA localizes to dots patterned in more or less transversely oriented rows in the cell cortex of the inner and outer periclinal cell faces of epidermal cells in the root elongation zone and the root hair zone (Figure 1A: cells in the root elongation zone and Figure 1B: cells in the root hair zone). We have two reasons to presume that these dots are in the plasma membrane: biochemistry shows an accumulation of the antigen that is being recognized by the antibody in the plasma membrane fraction (Cai et al. 2011), and GFP-tagged CESA complexes localize to the plasma membrane with a similar pattern, where they move with the velocity of approx. 300 nm min^{-1} known from CESA complexes producing CMFs (Paredez et al. 2006), see below.
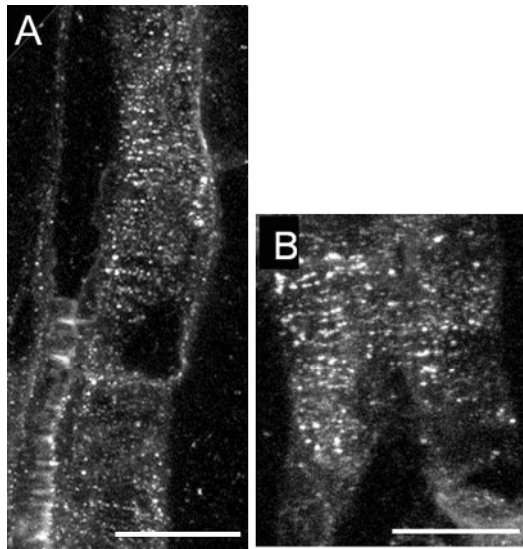

Figure 1. Immunolabeling with a CESA antibody on BMM sections of cryo-fixed Arabidopsis roots reveals rows of dots that are oriented transversely to the long cell axis in epidermal cells of A the root elongation zone and B of the root hair zone. Bar: 10 μm.

The CESA rows were oriented transversely to the elongation axis of the root and helically in older cells located further away from the root tip. We measured the density of CESA dots in the rows and the density of rows in both the inner and outer periclinal cell face of cells in the elongation zone and cells in the root hair zone, where cell elongation ceases (Beemster and Baskin 1998). The density of rows was measured along a line perpendicular to the rows. Table 1 gives an overview of the measurements. The density of rows of CESA complexes in cells in the elongation zone is slightly higher than this density in the root hair zone. For the inner and outer periclinal cell faces we found similar values. The density of dots in a row in cells in the elongation zone and cells in the root hair zone is similar both in inner and outer periclinal cell face.

The immunocytochemistry data were compared with live cell imaging data of CESA complexes in GFP:CESA3 (Gutierrez et al., 2009) expressing root epidermal cells. Figure 2 shows micrographs taken from time series (Supplemental Movies 1 and 2) of Arabidopsis root epidermal cells from the root elongation zone (figure 2A-C) and root hair zone (figure 2D-F). Although the overall image is the same as for the immunolabeled cells, particles are less distinct and, therefore, numbers of particles were more difficult to count. In addition, only the outer periclinal cell face could be studied. Over time, CESA complexes in a row move, one after the other, with velocities of 283 ± 56 nm min^{-1} in cells of the root elongation zone and 301 ± 60 nm min^{-1} in the root hair zone (supplemental movies 1 and 2), Kymographs show that the movement is bidirectional (Figure 3). Similar to the immunolabeled samples, we measured the angles of the CESA rows to the long axis of the root, and the density of the rows. These data are given in table I. Although the rows of CESA complexes are oriented transversely to the long axis of the cells in both immunolabeled and GFP:CESA3 expressing samples of elongating cells, there is more variation in the angles of rows in the cells expressing GFP:CESA3 (table I). For all measurements, at least 5 cells were measured.

CESA complexes follow CMTs in growing and fully-grown root epidermal cells
To relate the orientation and density of the rows of CESA complexes to the orientation and density of the CMTs, we immuno-labelled the CMTs using the same fixation and labelling procedures as used for CESA detection. In addition CMTs were visualized by live cell imaging using 35S::mCherry:MAP4-MBD (Figure 2C), which we used reviously (Gutierrez et al., 2009); Both methods gave similar results, but in immunolabeled samples it was possible to observe the CMTs of the inner cell faces of

Table I. Values measured in root epidermal cells using different techniques

| Outer periclinal cell face Elongation zone	Immuno	Live imaging GFP:CESA3	FESEM
Density of rows CESA complexes*	1.79 ± 1.15	0.93 ± 0.03	n/a
Orientation of rows CESA complexes**	0.3 ± 5.6˚	3.1 ± 19.9˚	n/a
Dots per micrometer in a row	1.80 ± 0.56	1.94 ± 0.30	n/a
Angles of cellulose microfibrils**	n/a	n/a	1.4 ± 3.0˚
Density cellulose microfibrils (CMF µm^{-1})	n/a	n/a	44.8 ± 5.7
Density of CMT (bundles) (CMT µm^{-1})	1.41 ± 0.17		
Outer periclinal cell face Root hair zone	Immuno	Live imaging GFP:CESA3	FESEM
Density of rows CESA complexes*	1.08 ± 0.23	0.75 ± 0.11	n/a
Orientation of rows CESA complexes**	10.7 ± 6.9˚	10.6 ± 32.0˚	n/a
Dots per micrometer in a row	1.54 ± 0.45	1.60 ±0.21	n/a
Angles of cellulose microfibrils**	n/a	n/a	10.1 ± 10.1˚
Density cellulose microfibrils (CMF µm^{-1})	n/a	n/a	48.2 ± 7.7
Density of CMT (bundles) (CMT µm^{-1})	1.08 ± 0.23		
Inner periclinal cell face Elongation zone	Immuno	Live imaging GFP:CESA3	FESEM
Density of rows CESA complexes*	1.59 ± 0.93	n/a	n/a
Orientation of rows CESA complexes**	2.1 ± 3.0˚	n/a	n/a
Dots per micrometer in a row	1.85 ± 0.24	n/a	n/a
Angles of cellulose microfibrils**	n/a	n/a	0.3 ± 7.2˚
Density cellulose microfibrils (CMF µm^{-1})	n/a	n/a	48.9 ± 8.2
Inner periclinal cell face Root hair zone	Immuno	Live imaging GFP:CESA3	FESEM
Density of rows CESA complexes*	0.97 ± 0.36	n/a	n/a
Orientation of rows CESA complexes**	7.2 ± 5.1˚	n/a	n/a
Dots per micrometer in a row	1.44 ± 0.50	n/a	n/a
Angles of cellulose microfibrils**	n/a	n/a	7.2 ± 10.0˚
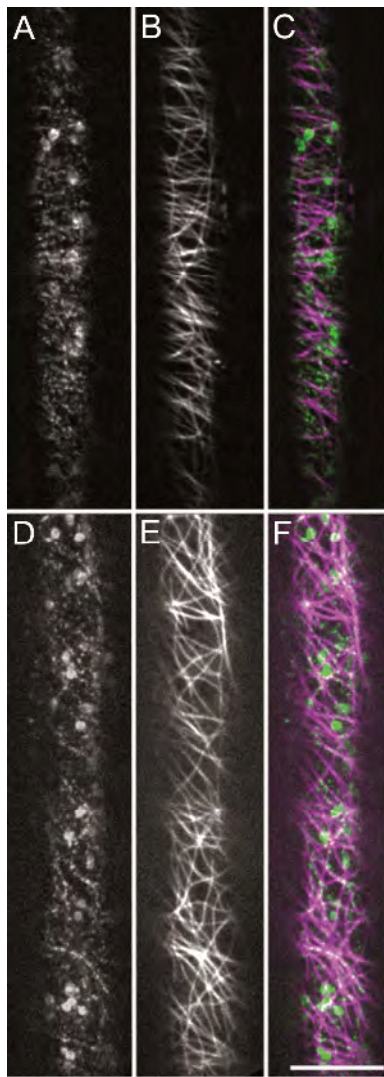
Figure 2. Micrographs of cells expressing the CESA complex marker GFP:CESA3 (A and D) and the microtubule marker mCherry:MBD (B and E). A-C show images from an epidermal cell in the root elongation zone. Most CMTs and rows of CESA complexes are oriented transversely to the growth axis of the cell. D-F show images from an epidermal cell in the root hair zone. In this cell the net orientation of CMTs and rows of CESA complexes is also transverse to the growth axis, but more variation in angle can be observed. C and F show overlays of GFP:CESA3 (green) and mCherry:MBD (red). The large lumps in the GFP:CESA3 images are Golgi bodies containing GFP:CESA3. Image sequences over time of these cells can be seen in supplemental movie 1 (cell from the elongation zone) and 2 (cell from the root hair zone). Bars: 10 μm.

Figure 3. Kymograph of CESA complexes in fully grown cells showing bidirectional motility of CESA complexes over a single CMT.
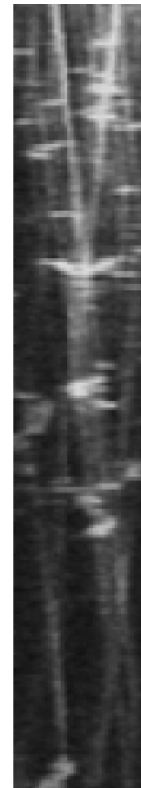
epidermal cells and sub-epidermal tissues as well (see supplement). Of the total amount of CESA complexes in the plasma membrane of GFP:CESA3 expressing cells, 93.7 ± 1.5 % of them tracked the CMTs in root epidermal cells in the elongation zone (n= 442 CESA complexes in 4 cells) and 95.8 ± 2.0 % in root epidermal cells in the root hair zone (n= 1050 CESA complexes in 8 cells).

In the root elongation zone (bundles of) CMTs and rows of CESA complexes were all transversely orientated to the root axis, both in the inner and outer cell face (sections). The density of the CMT (bundles) was similar to that of the CESA complex rows (1.41 ± 0.17 μm-1) measured in the sections of cells of the root elongation zone (n=102 CMTs in 6 cells) and 1.08 ± 0.23 μm-1 in cells of the root hair zone (n=98 CMTs in 5 cells).

FESEM-imaged microfibril orientation and density in root epidermal cells
CESA complexes produce CMFs. We visualized CMFs using Field Emission Scanning Electron Microscopy (FESEM) of cell walls from which the cell wall matrix material had been removed. Figure 4 shows overviews of roots (Figure 4A-B) with details of the most recently deposited CMFs of the inner and outer periclinal walls of an epidermal cell in the root elongation zone (Figure 4C-D). The CMF orientation in different wall facets of these cells was uniform. In epidermal cells of the root hair zone (Figure 5) we also found transversely oriented CMFs in the most recently deposited layers of inner (Figure 5C) and outer walls (Figure 5D). FESEM images of CMFs of plant cell wall show fibrilar structures of up to 10 nm in diameter. This is including the Platinum/Carbon deposit. In preparations of KMnO4 stained thin sections of material in which the cell wall matrix is removed almost completely (van der Wel et al., 1996) the diameter of single CMFs is approx. 3 nm (Emons, 1988), comparable to what is found by X-ray analysis (Kennedy et al., 2007). Comparison of thin sections and surface preparations indicate that the CMFs in such FESEM preparations do not coalesce, and are single CMFs (see for instance Akkerman et al., 2012 and references therein for Arabidopsis root hairs). Measurements of CMF densities and angles reveals an evenly spread layer of CMFs with densities of CMFs varying between 42.0 and 48.9 CMF μm-1 (table I; n > 200 CMFs in at least 5 independent cells per given value) and CMF angles to the long axis of the root were similar to those of CMTs and rows of CESA complexes (table I). Although the distances between FESEM-imaged microfibrils may not be very accurate, and it cannot be observed which CMFs are produced at a particular moment in time, it is clear that an even layer is produced

Figure 4. The orientation of the most recently deposited CMFs in the inner (C) and outer (D) periclinal wall of an epidermal cell in the root elongation zone. A and B show the exact locations of C and D. Bar: 500 nm.
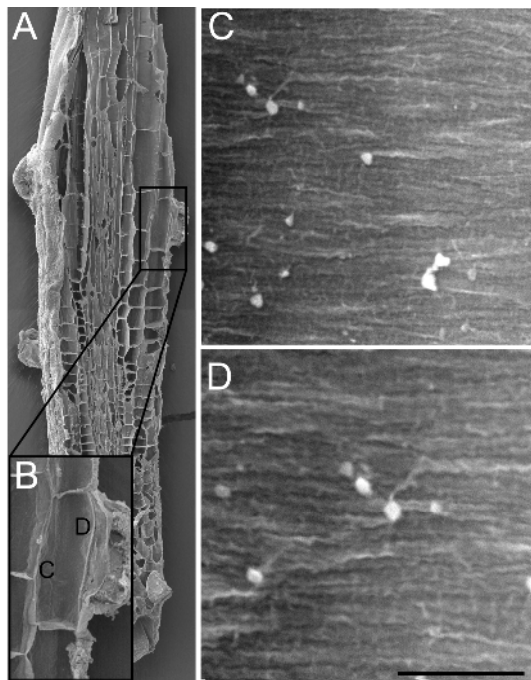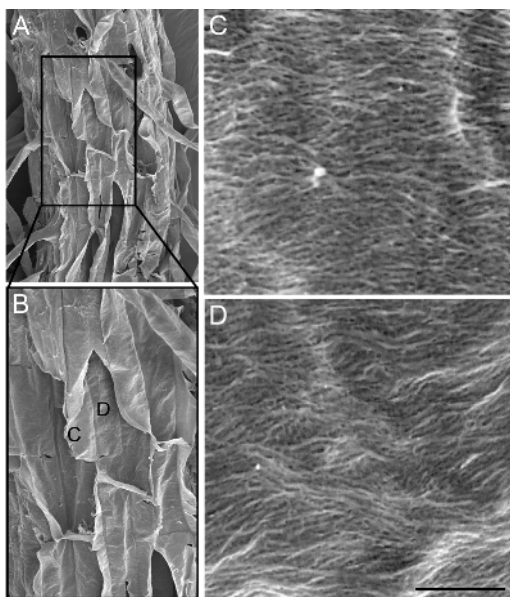

Figure 5. The orientation of the most recently deposited CMFs in the inner (C) and outer (D) periclinal wall of an epidermal cell in the root hair zone. A and B give the exact locations of C and D. Bar: 500 nm.

CMTs reposition continuously

There is a discrepancy between the more or less uniform distribution of CMFs in the most recently deposited layer of the cell wall and the rows of CESA complexes in the plasma membrane that produce CMFs. To solve the paradox that CESA complexes move in rows along CMTs while producing an evenly spread layer of CMFs, we tested whether CMT positions change over time by recording long-term movies of the CMTs. Since cell elongation would interfere with determination of CMT positions over time, for these experiments we used cells in the zone where root elongation was terminating and collected an image every 10 minutes (Figure 6). CMTs in these cells are still transversely oriented. When a time projection is made of 3 subsequent images, the percentage of the cell cortex that is covered by the CMTs was much higher than in individual images, showing that the CMTs indeed reposition continuously.
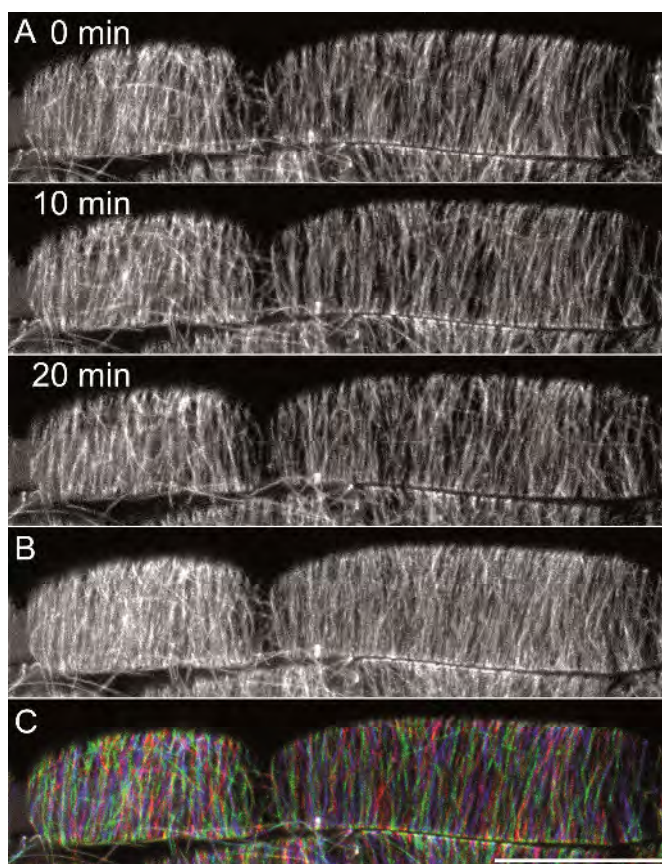

Figure 6. CMT organization changes over time to cover a larger part of the cell cortex. A shows three frames of a time series with 10 minutes intervals. B shows a black and white overlay of the three images shown in A and C shows a pseudocoloured overlay of the images shown in A, where 0 min is red, 10 minutes is green and 20 minutes is blue. Bar: 10 μm.

Discussion

We studied the relation between CMTs, CESA complexes and CMFs in root epidermal cells of Arabidopsis using live imaging of CESA complexes and CMTs with spinning disc microscopy, immunofluorescence labeling of CESA complexes and CMTs, and FESEM of CMFs.

In the plasma membrane of Arabidopsis root epidermal cells, CESA complexes are present as dots positioned in rows, where they move with an average velocity of approximately 300 nm min^{-1}. This is in accordance with the results on CESA complex movement as observed in hypocotyl cells of Arabidopsis (Paredez et al. 2006; Debolt et al. 2007; Persson et al. 2007; Desprez et al. 2007; Crowell et al. 2009; Gutierrez et al. 2009; Chan et al. 2010). This velocity was observed throughout the elongation and root hair zone of the root, from early stages of cell elongation, just after cell division, up to the root hair zone with fully-grown cells and also those higher up in the root having obliquely oriented CMFs (data not shown). Lower or higher velocities of CESA complexes might be measured depending on the temperature (Fujita et al. 2011).

The orientation of CMTs, CESA complex movement, and CMFs in elongating root epidermal cells up to the root hair zone is transverse to the elongation axis of the root. In older cells located further away from the root tip the orientation is helical. Orientations are similar in the inner and outer face of the root epidermal cell. This is different from the situation in elongating hypocotyl cells in which only in the inner cell face the orientation remains transverse during the whole elongation period (Chan et al., 2011; Crowell et al., 2011; Fujita et al., 2011). A difference in cell morphology is, however, that hypocotyl cells are more rounded at the outside than root epidermal cells.

Differences in the density of CESA rows and the variation in CESA row angles are observed using different visualization methods
Most results that were obtained using the different techniques are in accordance with each other. However some results are different when we compare the outcomes of the analyses of images obtained with different techniques.

The density of clear rows of CESA complexes in epidermal cells of the root elongation zone is almost twice as low in GFP:CESA3 lines compared to the immunocytochemistry results (0.93 ± 0.03 μm compared to 1.79 ± 1.15 μm). Since CESA complexes move along CMTs, this could be caused by the constant reorganization of CMTs and stabilization during fixation. We can also not exclude that the antibody labels more CESA complexes than the live probe so that more CESA complexes are detected. However the density of dots in a row does not differ between the different methods so this explanation is not very likely.

Although the average orientation of the rows of CESA complexes is similar in immunolabeled and live samples, the standard deviation is much higher in live samples. The variation in angle of CESA rows in the immunolabeled cells is similar to that of CMFs but much smaller than that of CESA rows in GFP:CESA3 expressing cells. One should realize that the CMFs that we see at the inside of the cell wall represent the tracks of CESA complexes during a certain period of time. An explanation for the difference in angle variation of CESA rows between the two different techniques could be that due to the laser light some CMTs might react by reorientation during live imaging. Also during fixation changes may occur in the CMT array and probably in the CESA complex rows that follow these CMTs.

CESA complexes run in rows but produce an even layer of CMFs because the CMTs that they follow reposition continuously

Analysis of the densities of CMTs, CMFs and CESA complex rows shows a similarity between the densities of CMTs and rows of CESA complexes that follow the CMTs, but a discrepancy between these two densities and that of the CMFs. Whereas the density of CMFs varies from 42.0 to 48.9 per μm, the maximal average density of CESA rows that we found was 1.79 per μm. This is understood when we realize that these CMFs have been made in a certain time period. How can CESA complexes that move in rows produce a layer of uniformly distributed and oriented CMFs as seen in the CMF preparations obtained with FESEM, and do not produce local wall thickenings of several CMFs on top of each other? Firstly, the limited resolution of the light microscope requires attention: a CMT is 25 nm across, a dimension like that of a CESA complex. In the light microscope these objects are imaged at a size consistent with the relevant airy disc, typically about 10 times larger. This indicates that the precise location of a CMF that is deposited by a CESA complex that co-localizes with a CMT cannot be resolved. If CESA complexes do not move over CMTs, but move up to several hundred nanometers away from CMTs, this could explain part, but not all of the even

distribution of CMFs, since the distance between CMTs is much larger than the resolution limit. Secondly, the majority of CESA complexes moves along CMTs, just like in etiolated hypocotyl cells (Paredez et al. 2006). We show that in the root epidermal cells over 90% of CESA complexes move, bidirectionnally, along CMTs. Since less than 10% of the CESA complexes produces a CMF between the CMTs, these cannot produce all the CMFs located between the CMTs. We hypothesized that the CMTs shift their orientation constantly. We were not able to measure this in elongating cells, since the constant elongation of these cells under the microscope is a complicating factor. Therefore we used cells from the root hair zone in which elongation just ceased but CMFs are still transverse to the elongation direction. We show that the CMTs constantly reorganise (Figure 6). Thus, CMT reorganization over time produces a uniform layer of CMFs, instead of producing a cell wall with local accumulations of CMFs on top of each other. The mechanism for the reorganization is probably the dynamic instability of the CMT ends in combination with the action of several known microtubule binding proteins (MAPs) as shown in a theoretical model that explains alignment of CMTs (see Tindemans et al, 2010). Among many regulatory MAPs the microtubule severing protein katanin plays an important role in microtubule dynamics (Uyttewaal et al 2012, Bichet et al., 2001; Burk et al., 2001; Burk and Ye, 2002; Nakamura et al., 2010; Stoppin-Mellet et al., 2006; Wasteneys and Ambrose, 2009). Furthermore the dynamic instability might also be regulated by a kinesin. Kinesins of the KinI/Kinesin-13 family are thought to have a regulatory role in the depolymerization at both ends of microtubules in *Drosophila* (Wu et al. 2006) and kinesin 13A has been localized to Golgi associated vesicles in Arabidopsis root cap peripheral cells using immunogold labeling for transmission electron microcopy (Wei et al. 2009).

Given the circumference of root epidermal cells, the movement velocity of CESA complexes, the density of CESA complexes in a row and the CMT reorganization velocity, our results on shifting CMTs explain how a uniform layer of CMFs can be formed.

Materials and methods

Plant growth
Surface sterilized Arabidopsis Col-0 seeds were germinated on vertically positioned agar plates containing half strength MS medium and 1.2% phyto-agar (Duchefa, Haarlem, The Netherlands) at 25°C with a 16/8 hr photoperiod at 150 µmol m^{-2} s^{-1}.

Rapid freeze fixation, sectioning and immunolabeling
3-day old seedlings were plunged into liquid propane, followed by freeze-substitution in methanol + 0.5% - 1% water free glutaraldehyde (GA) over a period of 4 days during which the temperature was gradually raised from -90°C to 0°C. The freeze substitution medium was gradually exchanged to 100% ethanol on ice, followed by a graded series of ethanol: butyl-methyl-metacrylate (BMM) (Baskin et al. 1992) followed by a 1 day wash in 100% BMM. BMM containing samples were polymerized at -20°C by exposure to UV light.
4-5 µm thick sections were produced using a Reichert Ultracut microtome. Sections were placed on a droplet of water on an object slide, stretched by exposure to chloroform vapour and baked onto the slides at a heating plate of 56°C for 30 minutes. Samples were labeled as described previously (Ketelaar et al., 2003).

Imaging and analysis of immunolabeled samples
Z-series were acquired of the immunolabeled sections using the standard FITC settings of a Zeiss LSM510 Pascal confocal laser scanning microscope. Image processing using Image J was performed as follows. Background signal was removed using the Substract Background command (100 pixels ball size) and maximum intensity z-projections were made of the z-series. Figures were made in Adobe Photoshop CS2.

Live cell imaging
Roots were grown in Biofoil sandwiches as described by Ketelaar et al., 2004. 4-5 days old seedlings were used. Imaging was performed on a spinning disk confocal microscope (Roper) using the settings as described by Gutierrez et al. (2009). Collected time series were processed by applying the Walking Average plugin and Image J rolling average algorithm and the Substract Background command (ball size 100 pixels).

FESEM analysis of cellulose microfibril texture

Plants were fixed with 3% glutaraldehyde in 0.1 M phosphate buffer (pH 7.2) for 3 hours at room temperature, followed by 3 washes in demi water of 10 minutes each. Plants were infiltrated with 20% sucrose for 1 hour, where after roots were dissected, placed on a rivet stud with Tissue Tek (Sakura Finetek Europe B.V., Alphen aan de Rijn, The Netherlands) and frozen in liquid nitrogen. To allow observation of the cell walls, the outer part of the roots was removed by longitudinal sectioning using cryo utramicrotomy. The remaining parts of the roots were thawed and washed in demi water 3 times for 10 minutes, where after cell contents were extracted during a 20 minutes treatment with 0.1% sodium hypochlorite. After extraction, samples were washed in demi water (3 times 10 minutes) and dehydrated through a graded ethanol series. Ethanol infiltrated samples were critical point dried with carbon dioxide, attached to a SEM sample holder using carbon adhesive tabs (EMS, Washington, USA) and sputter coated with 5 nm platinum in a dedicated preparation chamber (CT 1500 HF, Oxford Instruments, Oxford, UK). The roots were analyzed with a field emission scanning electron microscope (JEOL 6300 F, Tokyo, Japan) at ambient temperature at a working distance of 8 mm with SE detection at 3,5 – 5 kV. Images were digitally recorded using an Orion 6 camera (ELI, Charleroi, Belgium) and were resized and contrast stretched using Adobe Photoshop CS2.

Financial support

Acknowledgements

References

- Baskin TI, Busby CH, Fowke LC, Sammut M, Gubler F (1992) Improvements in immunostaining samples embedded in methacrylate: localization of microtubules and other antigens throughout developing organis in plants of diverse taxa. Planta 187: 405-413

- Baskin TI (2001) On the alignment of cellulose microfibrils by cortical microtubules: a review and a model. Protoplasma 215: 150-171

- Baskin TI (2005) Anisotropic Expansion of the Plant CellWall. Annu. Rev. Cell. Dev. Biol. 21:203-222

- Baskin TI, Beemster GT, Judy-March JE, Marga F (2004) Disorganization of cortical microtubules stimulates tangential expansion and reduces the uniformity of cellulose microfibril alignment among cells in the root of Arabidopsis. Plant Physiol. 135: 2279-2290

- Beemster GT, Baskin TI (1998) Analysis of cell division and elongation underlying the developmental acceleration of root growth in *Arabidopsis thaliana*. Plant Physiol. 116: 1515-1526

- Bichet A, Desnos T, Turner S, Grandjean O, Höfte H (2001) BOTERO1 is required for normal orientation of cortical microtubules and anisotropic cell expansion in Arabidopsis. Plant J. 25: 137-148

- Bringmann M, Li E, Sampathkumar A, Kocabek T, Hauser MT, Persson S (2012)POM-POM2/cellulose synthase interacting1 is essential for the functional association of cellulose synthase and microtubules in Arabidopsis. Plant Cell. 24: 163-177

- Burk DH, Liu B, Zhong R, Morrison WH, Ye ZH (2001) A katanin-like protein regulates normal cell wall biosynthesis and cell elongation. Plant Cell. 13: 807-827Burk DH, Ye ZH (2002)

- Burk DH, Ye ZH (2002) Alteration of oriented deposition of cellulose microfibrils by mutation of a katanin-like microtubule-severing protein. Plant Cell.;14 :2145-2160

- Cai G, Faleri C, Del Casino C, Emons AM, Cresti M (2011) Distribution of callose synthase, cellulose synthase, and sucrose synthase in tobacco pollen tube is controlled in dissimilar ways by actin filaments and microtubules. Plant Physiol. 155: 1169-1190

- Chan J, Calder G, Fox S, Lloyd C (2007) Cortical microtubule arrays undergo rotary movements in Arabidopsis hypocotyl epidermal cells. Nat. Cell Biol. 9: 171-175

- Chan J, Crowell E, Eder M, Calder G, Bunnewell S, Findlay K, Vernhettes S, Höfte H, Lloyd C (2010) The rotation of cellulose synthase trajectories is microtubule dependent and influences the texture of epidermal cell walls in Arabidopsis hypocotyls. J Cell Sci. 123: 3490-3495

- Chan J, Eder M, Crowell EF, Hampson J, Calder G, Lloyd C (2011) Microtubules and CESA tracks at the inner epidermal wall align independently of those on the outer wall of light-grown Arabidopsis hypocotyls. J. Cell Sci. 124: 1088-1094

- Crowell EF, Bischoff V, Desprez T, Rolland A, Stierhof YD, Schumacher K, Gonneau M, Höfte H, Vernhettes S (2009). Pausing of Golgi bodies on microtubules regulates secretion of cellulose synthase complexes in Arabidopsis. Plant Cell 21: 1141-1154

- Crowell EF, Timpano H, Desprez T, Franssen-Verheijen T, Emons AM, Höfte H, Vernhettes S (2011) Differential regulation of cellulose orientation at the inner and outer face of epidermal cells in the Arabidopsis hypocotyl. Plant Cell, in press.

- DeBolt S, Gutierrez R, Ehrhardt DW, Melo CV, Ross L, Cutler SR, Somerville C, Bonetta D (2007). Morlin, an inhibitor of cortical microtubule dynamics and cellulose synthase movement. Proc. Natl. Acad. Sci. USA 104: 5854-5859

- Desprez T, Juraniec M, Crowell EF, Jouy H, Pochylova Z, Parcy F, Höfte H, Gonneau M, Vernhettes S (2007) Organization of cellulose synthase complexes involved in primary cell wall synthesis in *Arabidopsis thaliana*. Proc. Natl. Acad. Sci. USA 104: 15572-15577

- Emons AMC (1985). Plasma-membrane rosettes in root hairs of *Equisetum hyemale*. Planta 163: 350-359

- Emons AMC (1988) Methods for visualizing cell wall texture. Acta botanica Neerlandica 37 :31-38

- Emons AM, Höfte H, Mulder BM (2007) Microtubules and cellulose microfibrils: how intimate is their relationship? Trends Plant Sci. 12: 279-281

- Fujita M, Himmelspach R, Hocart CH, Williamson RE, Mansfield SD, Wasteneys GO (2011) Cortical microtubules optimize cell-wall crystallinity to drive unidirectional growth in Arabidopsis. Plant J. 66: 915-928
- Gardiner JC, Taylor NG, Turner SR (2003) Control of cellulose synthase complex localization in developing xylem. Plant Cell 15: 1740-1748
- Gillmor CS, Poindexter P, Lorieau J, Palcic MM, Somerville C (2002) α-Glucosidase I is required for cellulose biosynthesis and morphogenesis in Arabidopsis. J. Cell Biol. 156: 1003–1013
- Green PB (1962). Mechanism for plant cellular morphogenesis. Science 138: 1404-1405
- Gutierrez R, Lindeboom JJ, Paredez AR, Emons AM, Ehrhardt DW (2009) Arabidopsis cortical microtubules position cellulose synthase delivery to the plasma membrane and interact with cellulose synthase trafficking compartments. Nat. Cell Biol. 11: 797-806
- Hamant O, Traas J, Boudaoud A (2010) Regulation of shape and patterning in plant development. Curr. Opin. Genet. Dev. 20: 454-459
- Hamant O, Heisler MG, Jönsson H, Krupinski P, Uyttewaal M, Bokov P, Corson F, Sahlin P, Boudaoud A, Meyerowitz EM, Couder Y, Traas J (2008) Developmental patterning by mechanical signals in Arabidopsis. Science 322: 1650-1655
- Herth W (1985) Plasma-membrane rosettes involved in localized wall thickening during xylem vessel formation of *Lepidium sativum* L. Planta 164:12-21
- Kennedy CJ, Cameron GJ, Sturcova A, Apperley DC, Altaner C, Wess TJ and Jarvis MC (2007) Microfibril diameter in celery collenchyma cellulose: X-ray scattering and NMR evidence. Cellulose 14: 235-246.
- Ketelaar T, de Ruijter NC, Emons AM (2003) Unstable F-actin specifies the area and microtubule direction of cell expansion in Arabidopsis root hairs. Plant Cell 15: 285-292
- Ketelaar T, Anthony RG, Hussey PJ (2004) Green fluorescent protein-mTalin causes defects in actin organization and cell expansion in Arabidopsis and inhibits actin depolymerizing factor's actin depolymerizing activity in vitro. Plant Physiol. 136: 3990-3998
- Kimura S, Laosinchai W, Itoh T, Cui X, Linder CR, Brown RM Jr. (1999) Immunogold labeling of rosette terminal cellulose-synthesizing complexes in the vascular plant *Vigna angularis*. Plant Cell 11: 2075-2085
- Mueller SC, Brown RM Jr. (1980) Evidence for an intramembrane component associated with a cellulose microfibril-synthesizing complex in higher plants. J. Cell Biol. 84: 315-326
- Nakamura M, Yagi N, Kato T, Fujita S, Kawashima N, Ehrhardt DW, Hashimoto T (2012) Arabidopsis GCP3-interacting protein 1/MOZART 1 is an integral component of the γ-tubulin-containing microtubule nucleating complex. Plant J. 71: 216-225
- Nicol F, His I, Jauneau A, Vernhettes S, Canut H, Höfte H (1998) A plasma membrane-bound putative endo-1,4-β-D-glucanase is required for normal wall assembly and cell elongation in Arabidopsis. EMBO J 17: 5563–5576
- Paredez AR, Somerville CR, Ehrhardt DW (2006) Visualization of cellulose synthase demonstrates functional association with microtubules. Science 312: 1491-1495
- Persson S, Paredez A, Carroll A, Palsdottir H, Doblin M, Poindexter P, Khitrov N, Auer M, Somerville CR (2007) Genetic evidence for three unique components in primary cell-wall cellulose synthase complexes in Arabidopsis. Proc. Natl. Acad. Sci. USA 104: 15566-15571
- Schindelman G, Morikami A, Jung J, Baskin TI, Carpita NC, Derbyshire P, McCann MC, Benfey PN (2001) COBRA encodes a putative GPI-anchored protein, which is polarly localized and necessary for oriented cell expansion in Arabidopsis. Genes Dev. 15: 1115-1127
- Stoppin-Mellet V, Gaillard J, Vantard M (2006) Katanin's severing activity favors bundling of cortical microtubules in plants. Plant J. 46: 1009-1017
- Sugimoto K, Williamson RE, Wasteneys GO (2000) New techniques enable comparative analysis of microtubule orientation, wall texture, and growth rate in intact roots of Arabidopsis. Plant Physiol. 124: 1493-1506
- Tindemans SH, Hawkins RJ, Mulder BM (2010) Survival of the aligned: ordering of the plant cortical microtubule array. Phys. Rev. Lett. 104: 058103

- Uyttewaal M, Burian A, Alim K, Landrein B, Borowska-Wykręt D, Dedieu A, Peaucelle A, Ludynia M, Traas J, Boudaoud A, Kwiatkowska D, Hamant O (2012) Mechanical stress acts via katanin to amplify differences in growth rate between adjacent cells in Arabidopsis. Cell. 149: 439-451
- Wasteneys GO, Ambrose JC (2009) Spatial organization of plant cortical microtubules: close encounters of the 2D kind. Trends Cell Biol. 19: 62-71
- Wei L, Zhang W, Liu Z, Li Y (2009) AtKinesin-13A is located on Golgi-associated vesicle and involved in vesicle formation/budding in Arabidopsis root-cap peripheral cells. BMC Plant Biol. 9:138
- Wu X, Xiang X, Hammer JA 3rd (2006) Motor proteins at the microtubule plus-end. Trends Cell Biol. 16: 135-143
- Zhong R, Kays SJ, Schroeder BP, Ye ZH (2002) Mutation of a chitinase-like gene causes ectopic deposition of lignin, aberrant cell shapes, and overproduction of ethylene. Plant Cell 14: 165-179

Supplemental data
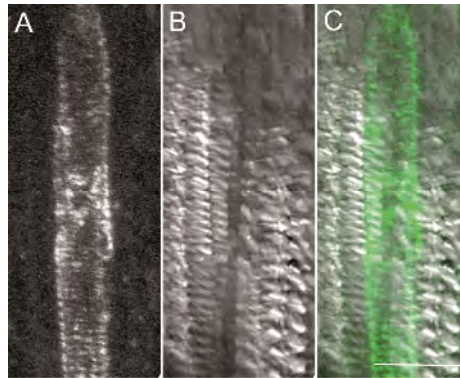
Figure 1. The CESA antibody labels bands in the plasma membrane of developing root xylem cells.
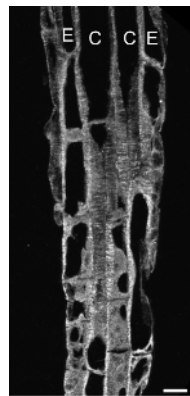
Figure 2. Microtubule organization in an immunolabeled section through the root elongation zone. Microtubules in different root cell types all are transversely oriented to the long axis of the root. This image shows both cortical (indicated with a C) and epidermal (indicated with an E) cell files. Bar: 10 μm.

Supplemental movie 1 and 2: CESA complexes in GFP::CESA3 expressing root epidermal cells (1 in the root elongation zone; 2 in the root hair zone).

Chapter 5

General discussion

Ying Zhang, Anne Mie Emons, Tijs Ketelaar

Laboratory of Cell Biology, Wageningen University,
The Netherlands.

Introduction

In this thesis, we have focused on two aspects related to plant cell growth and cell wall formation: the role of the exocyst in targeting exocytotic events to (polarized) locations and the regulation of the orientation of cellulose microfibril deposition by cortical microtubules. Firstly, we will discuss the results that we obtained from our work on the exocyst, and in particular the exocyst subunit that functions as a landmark protein in fungi and vertebrates (Finger et al., 1998; Wiederkehr et al., 2003; He and Guo, 2009; Hutagalung et al., 2009). Using these data and other data from the literature, we will identify possible functions of the exocyst in plant development and homologies between the function of the plant and fungal exocyst during polarized secretion during cytokinesis. Then, we will move the focus to cortical microtubules and their role in cell wall deposition. We will focus on root hair cells, the cells that we used to decipher the regulation of the orientation of cellulose microfibril deposition by cortical microtubules. Finally, we will integrate the results that we obtained and explore possible relationships between cortical microtubules, cellulose synthase complexes, cellulose microfibril orientation and exocyst mediated polarized secretion.

The exocyst in plant cells: possible functions

The exocyst is an octameric protein complex that was first identified in budding yeast, where it was identified as a tethering factor essential for vesicle fusion during polarized secretion of materials during bud growth and cytokinesis (Hsu et al., 2004; Munson and Novick, 2006; Zhang et al., 2005; Zhang et al., 2008; Songer and Munson, 2009). The polarized localization of the exocyst during cytokinesis in yeast is also observed in plant cells, where all studied exocyst subunits localize to the early developing cell plate (Fendrych et al., 2010; Chapter 2 of this thesis). Interestingly, the exocyst subunits dissociate from the cell plate before cytokinesis has completed, indicating that the exocyst could play a role in setting up polarized transport of vesicles to the cell plate, but not in maintaining this polarized transport during cell plate formation. During or just after cell plate attachment to the existing cell walls, the exocyst reappears at the newly formed cytokinetic wall (Fendrych et al., 2010; Chapter 2 of this thesis). As the resolution of the current studies (Fendrych et al., 2010; Chapter 2 of this thesis) is hampered by the accessibility of meristematic cells for fluorescence microscopy, it is not clear whether the exocyst reappears on the cell plate before or after cell plate completion. The exocyst localization to the whole cell plate during this later stage and the absence of a preferential localization to the

attachment sites suggests that it is not the attachment of the cell plate to the daughter cells that is mediated by the exocyst, but a post-cytokinetic process that occurs specifically on the newly formed cell wall. Before we speculate about the role of the exocyst during this stage of the cell cycle, we will discuss knowledge about the function and localization of the exocyst in interphase plant cells and plant development.

As stated above, in bud forming interphase yeast cells, the exocyst localizes polarly to the bud tip (Munson and Novick, 2006). In interphase plant cells, where obviously no bud formation occurs, but other different types of polar expansion, the situation is less clear. We show that in tips of growing root hairs, locations of highly polarized secretion that could be compared to polarized secretion during bud formation in yeast, SEC3 does not accumulate strongly (Chapter 2 of this thesis). The localization of several other exocyst subunits (SEC6, SEC8 and EXO70A1) has been investigated in tip-growing pollen tubes by immunofluorescence (Hála et al., 2008). Although there appears to be a strong accumulation of these subunits in the apices of pollen tubes, unfortunately the resolution of micrographs in this study is not sufficient to determine whether these subunits have a membrane localization or whether they are enriched in the cytoplasmic dense apical area of pollen tubes. The localization of other exocyst subunits has been investigated in diffusely growing Arabidopsis and Tobacco Bright Yellow 2 cells, where SEC5A, SEC15A, SEC15B and EXO84B fused to GFP localized to globular structures in the perinuclear cytosol (Chong et al., 2010), and the subcellular localization of EXO70 proteins differed depending on the isoform; they either show a cytoplasmic organization or localize to smaller or larger cell compartments. These compartments have different degrees of co-localization with snares specific for early endosomes, late endosomes and the trans Golgi network (Chong et al., 2009; Wang et al., 2010). Unfortunately, the fixation steps of the immunolocalization studies of Chong et al. (2009) are poor, yielding plasmolyzed and collapsed cells, and the functionality of genetic fusions of exocyst subunits with GFP was not tested by complementation analysis of mutants in which these genes are disrupted. However, Wang et al. (2010) show that EXO70E2 localizes to discrete punctate structures at the plasma membrane and cytosol of Arabiospis and Tobacco BY-2 cells. These structures represent secretory compartments that are contained by two membranes that are both decorated with EXO70E2. These organelles, of which the inner membrane is expelled into the apoplast, do not co-localize with known organelles and have been termed EXPO (Exocyst Positive organelles). The different, punctuate localizations in the cytoplasm that were observed in these studies were absent in our SEC3 localization

studies. The absence of this possible TGN/vesicle localization in our SEC3 localization experiments is consistent with a role for SEC3 as a landmark protein for exocytosis as has been described in budding yeast (Finger et al. 1998; Wiederkehr et al. 2003; He and Guo 2009; Hutagalung et al. 2009). Wang et al. (2010). In yeast, EXO70 has a dual localization, both to the bud site, like SEC3, but also to vesicles, like the other exocyst subunits. The localization of EXO70E2 to both cytoplasmic compartments and the plasma membrane of plant cells indicates that EXO70E2 behaves similarly as EXO70 in yeast, although no association with double membrane compartments has been reported in yeast. In future research, co-localization studies should reveal whether or not there is a relation between the SEC3 puncta that we observe and the EXPO organelles.

Besides localization of the exocyst, also mutants in which exocyst subunits have been knocked out should be discussed. Single copy exocyst mutants in Arabidopsis are gametophytically defective, which is caused by failure of pollen tube germination and/or growth (Cole et al. 2005; Hála et al. 2008). Plants that are homozygous for mutations in exocyst subunits that are encoded by multiple copies, show strong growth defects (EXO84B: is severely dwarfed and has compromised division in leaf epidermal and guard cells (Fendrych et al., 2010); EXO70A1: is disrupted in root hair growth, the formation of the stigmatic papillae, and had shortened hypocotyls in etiolated seedlings, smaller organs, loss of apical dominance and reduced fertility (Synek et al., 2001)). The sec3a mutant that we describe in Chapter 2 of this thesis is the only exocyst mutant defective in embryo development. This mutant could be useful in future work to decipher the role of the exoycst in plant development. Our sec3a mutant suggests that the exocyst plays a role in acquisition of polarity during embryo development, whereas the exo84b and the exo70a1 mutants show that the exocyst plays a role during sporophyte cell growth and differentiation (Synek et al., 2001; Fendrych et al., 2010). Besides a role in gamytophyte functioning/viability and sporophyte development, the exocyst subunits EXO70B2 and EXO70H1 have been implicated in resistence against plant pathogens (Pecenková et al., 2011).

The pertinent question about the plant exocyst is: what does it exactly do during plant development? Why is it so important? Our data show that the exocyst, or at least SEC3, is not polarly localized in polarly expanding interphase cells and that the presence of SEC3A puncta on the plasma membrane does not correlate with cell growth. However, this does not exclude a role in polarized plant cell growth. If the membrane localized SEC3 puncta are scaffolds that can be used by vesicles equipped with the other

exocyst subunits for exocytosis, not SEC3, but other exocyst subunits could determine the polarity targeting of exocytotic events. This is unlikely, since yeast SEC3 can directly bind phosphatidylinositol 4,5-biphosphate ($PI(4,5)P_2$) of the inner plasma membrane leaflet (He et al., 2007; Liu et al., 2007; Zhang et al., 2008) and interact with Rho GTPases that are likely to be the regulator of polar localization to the bud tip in yeast since SEC3 is a downstream effector of CDC2 and RHO1 (Guo et al. 2001; Zhang et al. 2001). In plants, the exocyst can be recruited to the plasma membrane by Rho Of Plants (ROP) through interaction of SEC3A with the adaptor protein ICR1 (Lavy et al., 2007; Hazak et al. 2010), suggesting regulation of the plant exocyst, albeit in a different fashion than the fungal exocyst, by Rho GTPases.

As discussed above, in yeast SEC3 is the protein that provides a spatial landmark on the plasma membrane to which the remainder of the exocyst is targeted. If Arabidopsis SEC3 has a similar function in interphase cells, (exocytotic) events of unknown nature should be targeted to the SEC3 puncta on the plasma membrane. We show that SEC3 puncta do not preferentially co-localize with cortical microtubules and are unlikely to be involved in insertion of CESA complexes into the plasma membrane. This suggests that the exocyst is mediating an (exocytotic) event not related to cell growth or cellulose microfibril deposition. Thus, it is likely that the exocyst mediates another, unidentified type of exocytosis in plant cells of for example ion-channels, water-channels, PIN proteins or receptors involved in plant defense. The accumulation of the exocyst at the plasma membrane that surrounds the newly formed post-cytokinetic wall may play a role in equipping the membrane at this location with integral proteins that were not present yet during its formation, for example because their presence may interfere or even counteract with the formation of the cell plate. The localization to the early cell plate may have a similar function, but the proteins that are inserted may differ depending on the stage of the cell cycle (telophase versus interphase). The auxin efflux carrier PIN could be a candidate for exocyst-mediated polar targeting, as ICR1 is required for recruitment of PIN proteins to polar domains at the plasma membrane (Hazak et al., 2010). Through interaction with this protein (Lavy et al. 2007), the exocyst may well be involved in the polarized positioning of PIN proteins. It remains to be determined whether this is the case, and if so, whether this is relevant only when the exocyst localization is polarized to the cell plate, or also in non-dividing interphase cells.

The role of cortical microtubules in root hair morphology and cellulose microfibril deposition alignment

Plant cells have a large variety of shapes to perform their specific functions. For example, pollen tubes are long and thin to deliver the sperm cells to the embryo sac and trichomes possess spike-shaped extensions to provide protection against invertebrate herbivores.   To understand plant cell morphogenesis, it is important to realize that plant cells are walled and under turgor pressure during normal conditions. Since the turgor exerts equal forces in all directions, cell growth is controlled by local differences in cell wall flexibility; areas with flexible cell wall will expand, whereas areas that are less flexible withstand the turgor pressure and do not expand (Ketelaar and Emons., 2001). As cells expand, the cell wall stretches. At the same time synthesis of new cell wall takes place to maintain cell wall thickness. Important load bearing polymers of the cell wall involved are the cellulose microfibrils (Lindeboom et al., 2007). In axially, also termed diffuse or intercalary, growing cells, for example root epidermal cells that we used in Chapters 2 and 4 of this thesis, cellulose microfibrils are aligned transversely to the longitudinal growth axis of these cells, which is thought to provide the force that resists expansion in the transverse direction (Lindeboom et al., 2007). In these cells, the movement of CESA complexes that contain the cellulose synthase enzymes, which synthesize cellulose microfibrils (Paredez et al., 2005), is guided by cortical microtubules. The spacing between cortical microtubules is at any moment much larger than the spacing of the cellulose microfibrils observed in the cell wall. In Chapter 4 of this thesis, we show that a possible explanation for this discrepancy is that over time cortical microtubules reorganize and that this reorganization is sufficient for cortical microtubules, and thus cellulose deposition, to cover the cell cortex. In time projections of 3 subsequent frames collected with 10 minutes intervals, we observed that a much higher percentage of the cell cortex was covered by microtubule fluorescence than in single frames. This shows that in a 20 minutes interval, during which a CESA complex produces a cellulose microfibril of approximately 6 μm, cortical microtubule reorganization may be sufficient to obtain an evenly spaced layer of cellulose microfibrils.

In Chapter 3 of this thesis, we focus on root hairs, tip growing cells. Tip growth differs from axial growth in that cell expansion only takes place at the one site of cell surface (review Arabidopsis: Ketelaar and Emons, 2001). Root hair cells are a well-characterized cell type. In expanding root hairs, two areas can be defined: the growing tip and the non-expanding tube. In the growing tip, cellulose microfibrils are arranged randomly (Arabidopsis: Akkerman et al., 2012), and cortical microtubules are absent (Arabidopsis: van Bruaene et al., 2004). Insertion of CESA complexes in the plasma

membrane occurs in tip and tube of growing as well as of fully-grown hairs (Chapter 3 of this thesis). Since root hairs elongate at a faster rate (Arabidopsis root hairs elongate at speeds of ± 1 µM per minute) than the movement velocity of CESA complexes in these cells (284 ± 53 nm.min^{-1}), it is not possible that a CESA complex that is inserted into the plasma membrane of the tube of a growing root hair reaches the growing tip. This implies that cortical microtubules, which are absent from the tip, are not involved in the guidance of the randomly oriented cellulose microfibrils in the tips of these hairs.

We show that in root hair tubes cortical microtubules are involved in guiding CESA complexes (Chapter 3 of this thesis). When compared to axially expanding cells, cellulose microfibril deposition in the non-expanding root hair tube is comparable to that in fully-grown root hair cells. Growth termination of axially expanding cells is marked by reorientation of the cortical microtubule array from transverse to longitudinal or oblique to the long axis of the cell (Arabidopsis: Sugimoto et al., 2000). After growth termination, cellulose microfibril deposition continues in the orientation of the reorganized cortical microtubules (Lloyd and Chan, 2004). In root hair tubes, upon cessation of cell elongation cortical microtubules do not adopt a different angle but become less dense, while CESA complexes continue for some time to deposit cellulose microfibrils after root hair growth termination (Chapter 3 of this thesis). The gradual decrease in cortical microtubule density in ageing root hairs allowed us to study the role of CMTs in targeting insertion and guiding movement of CESA complexes. In Chapter 3 of this thesis we show that, independent of the density of cortical microtubules (41.6% in tubes of growing and 20.0% in tubes of fully-grown root hairs), the percentage of CESA complexes that are inserted into the plasma membrane on the microtubules remains similar (in the range of 62-64%). This indicates a stronger preference for CESA complex insertion on cortical microtubules when their density is lower. Gutierrez et al. (2009) found that 78% of the CESA insertion events occurred on cortical microtubules in elongating etiolated hypocotyl cells that had a cortical microtubule density of approximately 50%. In contrast to insertion of CESA complexes, the percentage of CESA complexes tracking cortical microtubules dropped when microtubule density decreased; at low microtubule densities, CESA complexes still preferentially coincided with cortical microtubules, but unlike CESA complex insertion, co-localization with cortical microtubules depended on the microtubule density (Chapter 3 of this thesis). Since insertion occurs preferentially on cortical microtubules, the occurrence of CESA complexes in between them may simply be a consequence of the dynamic instability of cortical microtubules;

when a microtubule depolymerizes and the CESA complexes that were tracking this microtubule continue to produce a cellulose microfibril, it will take longer before it runs into another microtubule when there are less cortical microtubules. In the mor1 mutant, in which the density and organization of cortical microtubules are decreased (Whittington et al., 2001), a similar increase of CESA complexes that do not track cortical microtubules has been observed (Fujita et al., 2011). However, if this is the case in fully-grown root hairs with low microtubule densities, it does neither explain the larger variation in the movement direction of CESA complexes that move in between cortical microtubules than those tracking cortical microtubules nor the difference in movement direction of CESA complexes tracking microtubules (5.7 ± 9.6°) and those in between microtubules (-18.4 ± 20.9°) in fully grown root hairs. This suggests that the CESA complexes moving in between and those tracking cortical microtubules obey different orientation regulations. Those in between the cortical microtubules may just move forward in a straight line unless obstructed by a cortical microtubule (Lindeboom et al., 2007). Interestingly, the orientation of CESA complexes in the absence of cortical microtubules, after their depolymerization with oryzalin (-16.7 ± 21.0°), resembles that of those in between cortical microtubules when cortical microtubules are present. Although the reason for the different movement direction with a larger variation of complexes remains unclear, our results show that cortical microtubules do have a function in the orientation of cellulose deposition in root hair tubes.

We were able to calculate an average lifetime, i.e. residency time, of CESA complexes in the plasma membrane of root hair tubes. This lifetime is remarkably short, 12.8 minutes, a time during which cellulose microfibrils with an average length of 3.6 μm are produced. The lifetime is independent of the density of the cortical microtubule array, but dependent on the presence of cortical microtubules; in the absence of cortical microtubules, the lifetime increases to 22.3 minutes, which results in longer cellulose microfibrils with an average length of 6.3 μm. The relevance of the increased lifetimes is not clear; however, it implies that there is a feedback mechanism between CESA complex insertion, which decreases in the absence of cortical microtubules (Chapter 3 of this thesis), and CESA complex lifetime, which was not observed by Gutierrez et al. (2007). More research will be required to understand the nature of the feedback loop.

What could be the functional relevance of the guidance of CESA complexes by cortical microtubules during root hair growth? Depolymerization of microtubules causes a

wavy root hair phenotype (Bibikova et al., 1999; Ketelaar et al., 2001). This indicates that microtubules guide the orientation of root hair growth. Since cortical microtubules are absent from the tip of growing root hairs, but form a dense array with an axial orientation just below the dome (Van Bruaene et al., 2004), a possible way they could do this is by focusing the CESA complex movement in the subapex of the hair in the axial orientation and changing the movement direction of CESA complexes that are inserted into the plasma membrane of the dome of growing root hairs from random to longitudinal. This longitudinal cellulose microfibril alignment may contribute to obtaining straight root hairs.

CESA complex insertion and tethering of exocytotic events by SEC3 of the exocyst are unrelated processes and not all Golgi vesicles contain CESA complexes in their membranes.
Before we started our work on the exocyst, we hypothesized that it could play a role in polarized secretion of cell wall matrix material for root hair growth. As discussed above, this hypothesis is not supported by our data. In addition, we were able to show that the exocyst subunit SEC3 is not involved in the insertion of CESA complexes into the plasma membrane. In contrast to our expectations that both targeting of CESA complex insertion and exocyst mediated exocytosis could play a role in root hair tip growth, both events are likely unrelated and not the primary events leading to tip growth. Tip growth involves exocytosis of cell wall matrix contained in Golgi vesicles locally at the cell tip, and indeed Golgi vesicles do accumulate in tips of all tip-growing cells studied (Arabidopsis root hairs: Galway, 2000). Since CESA does not accumulate in the hair tip (Chapter 3 of this thesis), CESA complex insertion and cell wall matrix containing Golgi vesicle insertion are separate processes, and only a subclass of Golgi vesicles contains one or a few CESA complexes in their membrane.

This thesis has led to a better understanding of both exocyst functioning and the role of cortical microtubules in orienting cellulose microfibril production. The lack of a relation between the two subjects is part of this understanding…

References

- Akkerman M, Franssen-Verheijen M., Immerzeel P, Hollander LD, Schel JH, and Emons AM (2012). Texture of cellulose microfibrils of root hair cell walls of Arabidopsis thaliana, Medicago truncatula, and Vicia sativa. J Microsc. 247, 60-67.
- Bibikova TN, Blancaflor EB, Gilroy S (1999) Microtubules regulate tip growth and orientation in root hairs of Arabidopsis thaliana. Plant J.17: 657-665.
- Chong YT, Gidda SK, Sanford C, Parkinson J, Mullen RT, Goring DR. 2009. Characterization of the Arabidopsis thaliana exocyst complex gene families by phylogenetic, expression profiling, and subcellular localization studies. New Phytologist 185, 401-419.
- Cole RA, Synek L, Zarsky V, Fowler JE (2005) SEC8, a subunit of the putative Arabidopsis exocyst complex, facilitates pollen germination and competitive pollen tube growth. Plant Physiol. 138:2005-2018.
- Fendrych M, Synek L, Pecenková T, Toupalová H, Cole R, Drdová E, Nebesarová J, Sedinová M, Hála M, Fowler JE, Zárský V. 2010. The Arabidopsis exocyst complex is involved in cytokinesis and cell plate maturation. Plant Cell 22: 3053-3065.
- Finger FP, Hughes TE, Novick P (1998) Sec3p is a spatial landmark for polarized secretion in budding yeast. Cell 92, 559–571.
- Fujita M, Himmelspach R, Hocart CH, Williamson RE, Mansfield SD, Wasteneys GO (2011) Cortical microtubules optimize cell-wall crystallinity to drive unidirectional growth in Arabidopsis. Plant J. 66, 915-928.
- Galway ME (2000) Root hair ultrastructure and tip growth. In: Ridge RW, Emons AMC, eds. Root hairs: cell and molecular biology, Springer, Tokyo, 1-15.
- Guo W, Tamanoi F, Novick P (2001) Spatial regulation of the exocyst complex by Rho1 GTPase. Nat Cell Biol. 3, 353-360.
- Gutierrez R, Lindeboom JJ, Paredez AR, Emons AM, Ehrhardt DW (2009) Arabidopsis cortical microtubules position cellulose synthase delivery to the plasma membrane and interact with cellulose synthase trafficking compartments. Nat. Cell Biol. 11, 797-806.
- Hála M, Cole R, Synek L, Drdova E, Pecenkova T, Nordheim A, Lamkemeyer T, Madlung J, Hochholdinger F, Fowler JE, Zarsky V (2008) An exocyst complex functions in plant cell growth in Arabidopsis and tobacco. Plant Cell 20, 1330–1345.
- Hazak O, Bloch D, Poraty L, Sternberg H, Zhang J, Friml J, Yalovsky S (2010)A rho scaffold integrates the secretory system with feedback mechanisms in regulation of auxin distribution. PLoS Biol. 8, e1000282.
- He B, Guo W (2009) The exocyst complex in polarized exocytosis. Curr. Opin. Cell Biol. 21, 537–542.
- He B, Xi F, Zhang X, Zhang J, Guo W (2007) Exo70 interacts with phospholipids and mediates the targeting of the exocyst to the plasma membrane. EMBO J. 26, 4053–4065.
- Hsu SC, TerBush D, Abraham M, Guo W (2004) The exocyst complex in polarized exocytosis. Int. Rev. Cytol. 233, 243–265.
- Hutagalung AH, Coleman J, Pypaert M, Novick PJ (2009) An internal domain of Exo70p is required for actin-independent localization and mediates assembly of specific exocyst components. Mol. Biol. Cell 20, 153–163.
- Ketelaar MJ, Emons AMC (2001) The cytoskeleton in plant cell growth: lessons from root hairs. New Phytol. 152, 409-418.
- Lavy M, Bloch D, Hazak O, Gutman I, Poraty L, Sorek N, Sternberg H, Yalovsky S (2007) A Novel ROP/RAC effector links cell polarity, root-meristem maintenance, and vesicle trafficking. Curr. Biol. 17, 947–952.
- Lindeboom J, Mulder BM, Vos JW, Ketelaar T, Emons AM (2008) Cellulose microfibril deposition: coordinated activity at the plant plasma membrane. J Microsc. 231, 192-200.
- Liu J, Zuo X, Yue P, Guo W (2007) Phosphatidylinositol 4,5-bisphosphate mediates the targeting of the exocyst to the plasma membrane for exocytosis in mammalian cells. Mol. Biol. Cell 18, 4483–4492.

- Lloyd C, Chan J (2004) Microtubules and the shape of plants to come. Nat. Rev. Mol. Cell Biol. 5, 13–22.
- Munson M, Novick P (2006) The exocyst defrocked, a framework of rods revealed. Nat. Struct. Mol. Biol. 13, 577–581.
- Pecenková T, Hála M, Kulich I, Kocourková D, Drdová E, Fendrych M, Toupalová H, Zársky V. (2011) The role for the exocyst complex subunits Exo70B2 and Exo70H1 in the plant-pathogen interaction. J Exp Bot. 62:2107-2116.
- Songer JA, Munson M (2009) Sec6p anchors the assembled exocyst complex at sites of secretion. Mol. Biol. Cell 20, 973–982.
- Sugimoto K, Williamson RE, Wasteneys GO (2000) New techniques enable comparative analysis of microtubule orientation, wall texture, and growth rate in intact roots of Arabidopsis. Plant Physiol. 124: 1493–1506.
- Synek L, Schlager N, Eliás M, Quentin M, Hauser MT, Zársky V (2006) AtEXO70A1, a member of a family of putative exocyst subunits specifically expanded in land plants, is important for polar growth and plant development.. Plant J. 48, 54-72.
- Van Bruaene N, Joss G, Van Oostveldt P (2004) Reorganization and in vivo dynamics of microtubules during Arabidopsis root hair development. Plant Physiol. 136, 3905-3919.
- Wang J, Ding Y, Hillmer S, Miao Y, Lo SW, Wang X, Robinson DG, Jiang L (2010) EXPO, an exocyst-positive organelle distinct from multivesicular endosomes and autophagosomes, mediates cytosol to cell wall exocytosis in Arabidopsis and tobacco cells. Plant Cell 22, 4009-4030.
- Whittington AT, Vugrek O, Wei KJ, Hasenbein NG, Sugimoto K, Rashbrooke MC, Wasteneys GO (2001) MOR1 is essential for organizing cortical microtubules in plants. Nature 411, 610-613.
- Wiederkehr A, Du Y, Pypaert M, Ferro-Novick S, Novick P (2003) Sec3p is needed for the spatial regulation of secretion and for the inheritance of the cortical endoplasmic reticulum. Mol. Biol. Cell 14, 4770–4782.
- Zhang X, Bi E, Novick P, Du L, Kozminski KG, Lipschutz JH, Guo W (2001) Cdc42 interacts with the exocyst and regulates polarized secretion. J. Biol. Chem. 276, 46745–46750.Zhang X, Zajac A, Zhang J, Wang P, Li M, Murray J, TerBush D, Guo W (2005) The critical role of Exo84p in the organization and polarized localization of the exocyst complex. J. Biol. Chem. 280, 20356–20364.
- Zhang X, Orlando K, He B, Xi F, Zhang J, Zajac A, Guo W (2008) Membrane association and functional regulation of Sec3 by phospholipids and Cdc42. J Cell Biol. 180, 145-158.

Summaries and Acknowledgements

Summaries, Samenvatting, and Acknowledgements

Summary

The work presented in this thesis covers aspects of exocytosis, plant cell growth and cell wall formation. These processes are strongly linked as cell growth and cell wall formation occur simultaneously and exocytosis is the process that delivers cell wall components to the existing cell wall and integral membrane proteins to the plasma membrane. The chapters in this thesis describe work on the exocyst, a group of proteins thought to be involved in polarized secretion, the regulation of CESA complex mediated cellulose microfibril deposition by cortical microtubules, and the organization of cortical microtubules.

Chapter 1 is a review in which research on the plant exocyst is discussed. We compare the literature about the plant exocyst with knowledge about well-studied yeast and mammalian exocysts and explore which aspects of exocyst functioning are conserved in plants and which aspects are not. We propose that the plant exocyst has acquired distinct functions and mechanisms in exocytosis for plant cell growth, based on the fact that each subunit of the exocyst in yeast and mammals is encoded by one gene, whereas some exocyst subunits in plants, particularly EXO70, are encoded by multiple genes.

In **Chapter 2,** we presented experimental data on the exocyst. Using a yeast two hybrid based approach we present novel interactions between different exocyst subunits. We continue by focusing on the exocyst subunit SEC3, which functions as a landmark protein in yeast and mammalian cells. We show that both SEC3 genes in Arabidopsis are essential for plant development; A T-DNA insertion in the *SEC3A* gene causes embryo development to arrest at the globular stage and a T-DNA insertion in the *SEC3B* gene causes gametophytic lethality. We were able to complement the sec3a mutant by introducing a pSEC3A::SEC3A:GFP construct and used the resulting lines to study the subcellular localization of SEC3A. The fusion protein shows a similar localization to cytokinetic cell plates as has been shown for other exocyst subunits. In interphase cells SEC3A:GFP localizes to the cytoplasm and to the plasma membrane, where it forms immobile, punctuate structures with discrete average lifetimes of 6-12 seconds. These puncta are equally distributed over the cell surface of root epidermal cells and tip growing root hairs and the density of puncta does not decrease after growth termination of these cells. Either SEC3a puncta may not participate in exocytosis for polarized cell expansion, or the plasma membrane recruitment of SEC3 is a default process that requires other, polarly localized factors to mediate exocytotic events.

Chapter 3 focused on the role of cortical microtubules in the insertion, guidance and occurrence in the plasma membrane of cellulose microfibril producing CESA complexes. We characterized a wide range of parameters that give insight in CESA complex behavior, such as velocity, density and movement angles in the expanding tip and non-expanding tube of growing root hairs and the same areas in fully-grown root hairs. Then we performed co-localization studies of CESA complexes with cortical microtubules. In tubes of both growing and fully-grown root hair cells CESA complex insertion occurred preferentially on cortical microtubules. Part of the population of CESA complexes that were moving in the plasma membrane was tracking cortical microtubules, whereas others were moving in between cortical microtubules. CESA complexes tracking cortical microtubules had a slightly different movement direction, but also a much lower variation in movement direction than the CESA complexes that were moving in between cortical microtubules. When microtubules are absent, all CESA complexes move in the same direction as those that do not track cortical microtubules in the presence of microtubules, and the variation in the movement direction is similar to that of CESA complexes moving in between cortical microtubules. This shows that CMTs in root hairs focus CESA complex movement, by which they order cellulose microfibrils into a tighter helix.

In the absence of microtubules, the average lifetime of CESA complexes increases from 12.8 minutes to 22.3 minutes, showing that there is a feedback mechanism between CESA complex insertion and CESA complex lifetime. Since their velocity of movement in the plasma membrane does not change, they produce longer cellulose microfibrils in the absence of cortical microtubules

In **Chapter 4**, we addressed the question how CESA complexes that are guided by widely spaced cortical microtubules can produce a uniform layer of cellulose microfibrils with a much smaller spacing in axially growing root epidermal cells. We studied the orientation, density, alignment and movement of cortical microtubules and CESA complexes using immunocytochemistry and live cell imaging of root epidermal cells. The CMTs, the rows of CESA complexes and the innermost CMFs lay in the same orientation, approximately transverse to the elongation axis in both the inner and outer periclinal cell face in the elongation zone and root hair zone. CESA complexes predominantly move in rows along CMTs in both directions. Analysis of timelapse movies of CMTs revealed that the position shifting of cortical microtubules accounts for how the uniform layer of cellulose microfibrils can be formed.

Chapter 5 is the general discussion of the thesis, where we provide a framework in which the results presented in the previous chapters fall.

Samenvatting

Het werk beschreven in dit proefschrift heeft betrekking op exocytose, plantencelgroei en celwandvorming. Deze processen zijn sterk gekoppeld omdat celgroei en celwandvorming gelijktijdig plaats vinden, en voor celgroei aanmaak van nieuwe celwand noodzakelijk is. Exocytose is het proces dat celwandbestanddelen toevoegt aan de bestaande celwand en integrale membraaneiwitten aan de plasmamembraan. De verschillende hoofdstukken van dit proefschrift beschrijven werk aan i. de exocyst, een eiwittencomplex dat vermoedelijk betrokken is bij polaire exocytose, ii. de rol van corticale microtubuli tijdens cellulose microfibrilvorming door CESA-complexen, en iii. de organisatie van corticale microtubuli.

In **hoofdstuk 1** bediscussiëren we het onderzoek dat gedaan is aan de exocyst in planten. We vergelijken de literatuur over de exocyst in planten met kennis over de goed onderzochte exocyst in gist en dierlijke cellen, waarbij we vooral kijken naar aspecten die geconserveerd of juist anders zijn in planten. We hypothetiseren dat de exocyst in planten verschillende functies heeft verworven die specifiek zijn voor exocytose in planten, gebaseerd op het feit dat, in tegenstelling tot in planten, alle exocyst subunits in gist en zoogdieren worden gecodeerd door een gen. In planten worden sommige exocyst subunits, met name EXO70, gecodeerd door meerdere genen.

In **hoofdstuk 2** presenteren we experimentele data over de exocyst in planten. Gebruik makend van 'yeast two hybrid' technologie tonen we nieuwe interacties aan tussen verschillende eiwitten van de exocyst. Vervolgens focusseren we op het exocyst eiwit SEC3, dat een bakenfunctie heeft in gist en zoogdieren. We tonen aan dat beide Arabidopsis *SEC3* genen essentieel zijn voor de ontwikkeling van de plant; een T-DNA insertie in het *SEC3A* gen leidt tot een remming van embryo-ontwikkeling tijdens de globulaire fase en een T-DNA insertie in het *SEC3B* gen leidt tot gametofytische letaliteit. De *sec3a* mutant kon gecomplementeerd worden door introductie van een pSEC3A::SEC3A:GFP construct. We hebben lijnen met dit construct gebruikt om de subcellulaire lokalisatie van SEC3A te bestuderen. Het fusie-eiwit decoreert cytokinetische celplaten net als eerder aangetoond voor een aantal andere exocyst-eiwitten. In interfase cellen heeft SEC3A:GFP een cytoplasmatische lokalisatie, en aan de plasmamembraan vormt het immobiele punten, die een gemiddelde levensduur hebben van 6 tot 12 seconden. Deze punten zijn gelijkmatig verdeeld over het celoppervlak van wortelepidermiscellen, inclusief in top-groeiende

wortelharen. Ook in deze laatste cellen neemt de dichtheid van de punten niet af na het beëindigen van de celgroei. Dit suggereert dat de SEC3A punten niet betrokken zijn bij exocytose voor polaire celgroei, of als alternatief, dat de SEC3A punten standard worden gerekruteerd waarna andere factoren met een polaire lokalisatie exocytose activeren.

In **hoofdstuk 3** richten we ons op de rol van corticale microtubuli in de insertie, geleiding en aanwezigheid van cellulose microfibril-producerende CESA-complexen. We hebben een set parameters gekarakteriseerd die inzicht geven in het gedrag van CESA complexen, zoals snelheid, dichtheid en bewegingsrichting in de groeiende top en de niet-groeiende buis van groeiende wortelharen en in dezelfde gebieden van volgroeide wortelharen. Vervolgens hebben we co-lokalisatie studies uitgevoerd van CESA complexen met corticale microtubuli. In de buizen van zowel groeiende als volgroeide wortelharen werden CESA complexen preferentieel geïnserteerd in de plasmamembraan boven corticale microtubuli. Een deel van de populatie CESA complexen die bewogen in de plasmamembraan volgde corticale microtubuli, terwijl anderen CESA complexen bewogen tussen corticale microtubuli in. CESA complexen die corticale microtubuli volgden hadden een andere bewegingsrichting, maar ook een veel kleinere variatie in bewegingsrichting, dan de complexen die tussen corticale microtubuli bewogen. In de afwezigheid-van microtubuli bewogen alle CESA complexen in dezelfde richting als die van complexen die bewogen tussen corticale microtubuli in de aanwezigheid van microtubuli. Ook de variatie in bewegingsrichting was vergelijkbaar met die van CESA complexen die bewogen tussen corticale microtubuli. Dit toont aan dat corticale microtubuli in wortelharen CESA complex beweging focussen, waardoor de cellulose microfibrillen in een strakkere helix geordend worden. In de afwezigheid van microtubuli neemt de gemiddelde levensduur van CESA complexen toe van 12.8 tot 22.3 minuten. Dit laat zien dat er terugkoppeling is tussen CESA complex insertie en levensduur. Omdat de bewegingssnelheid in de plasmamembraan niet verandert worden er dus langere cellulose microfibrillen geproduceerd in de afwezigheid van corticale microtubuli.

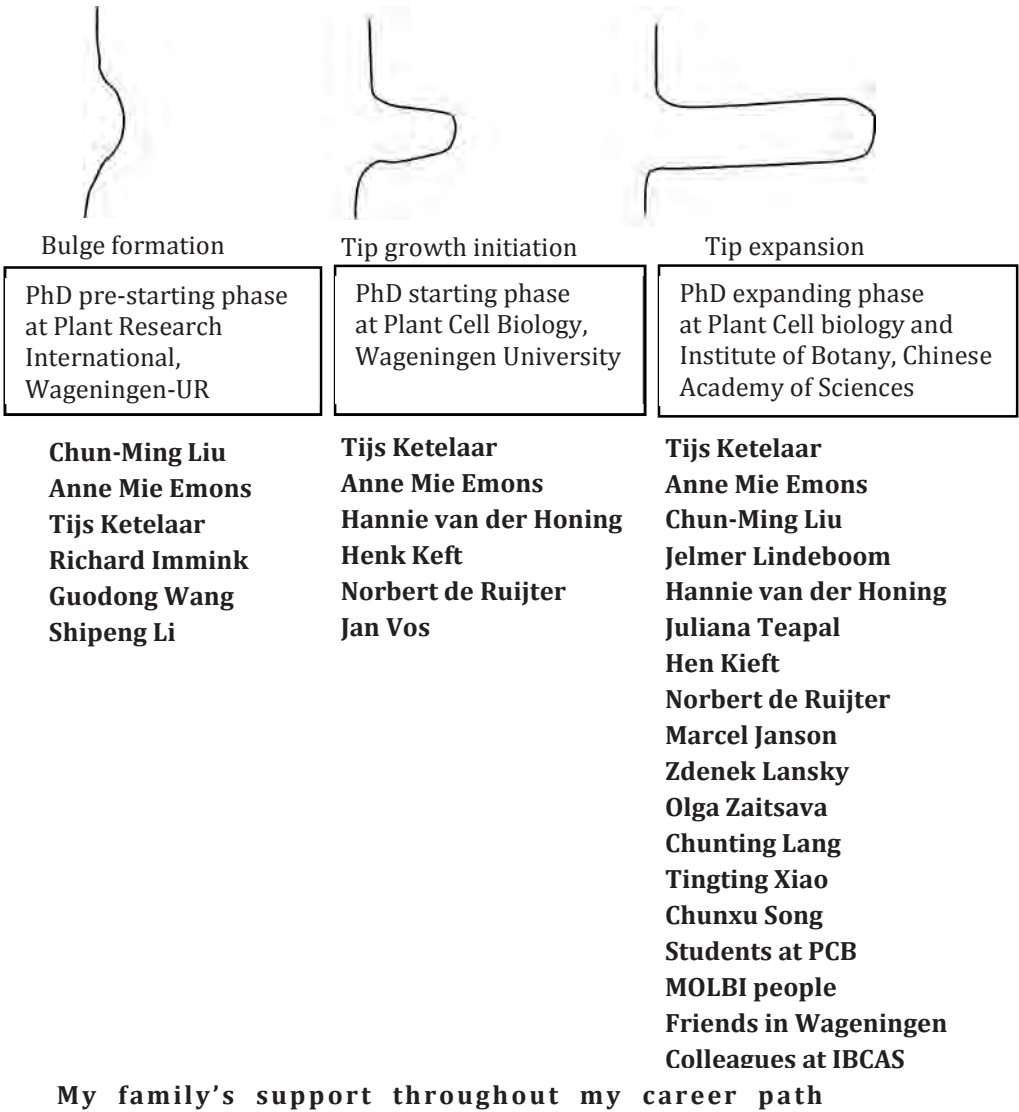In **hoofdstuk 4** geven we antwoord op de vraag hoe CESA complexen die geleid worden door corticale microtubuli die ver uit elkaar liggen een uniforme laag cellulose microfibrillen kunnen afzetten in intercalair groeiende wortelepidermiscellen in plaats van een lokale ophoping van microfibrillen op de plaats van de microtubuli. We hebben de oriëntatie, dichtheid en beweging van corticale microtubuli en CESA

complexen bestudeerd door middel van immunocytochemie en in levende cellen. De corticale microtubuli, de rijen CESA complexen en de binnenste cellulose microfibrillen liggen in dezelfde oriëntatie, ongeveer dwars op de strekkingsrichting, in zowel de binnenste als buitenste periclinale celcortices van cellen in de strekkingszone en wortelhaarzone. Een ruime meerderheid van de CESA complexen beweegt in rijen in beide richtingen langs corticale microtubuli. Analyse van timelapse filmpjes laat zien dat het veranderen van de positie van corticale microtubuli een verklaring kan zijn voor het vormen van een uniforme laag cellulose microfibrillen.

Hoofdstuk 5 is de discussie van dit proefschrift, waarin we een kader geven waarin de experimentele resultaten uit de voorgaande hoofdstukken te plaatsen zijn.

Acknowledgements

The growth in my career path during the PhD period somehow resembles the root hair development, which requires well-coordinated components and signaling molecules from both the inner and outer environment. I'd like to thank all the people at different stages for helping and supporting me to grow toward one direction: a good scientist.

Bulge formation	Tip growth initiation	Tip expansion
PhD pre-starting phase at Plant Research International, Wageningen-UR	PhD starting phase at Plant Cell Biology, Wageningen University	PhD expanding phase at Plant Cell biology and Institute of Botany, Chinese Academy of Sciences

Chun-Ming Liu
Anne Mie Emons
Tijs Ketelaar
Richard Immink
Guodong Wang
Shipeng Li

Tijs Ketelaar
Anne Mie Emons
Hannie van der Honing
Henk Keft
Norbert de Ruijter
Jan Vos

Tijs Ketelaar
Anne Mie Emons
Chun-Ming Liu
Jelmer Lindeboom
Hannie van der Honing
Juliana Teapal
Hen Kieft
Norbert de Ruijter
Marcel Janson
Zdenek Lansky
Olga Zaitsava
Chunting Lang
Tingting Xiao
Chunxu Song
Students at PCB
MOLBI people
Friends in Wageningen
Colleagues at IBCAS

My family's support throughout my career path

About the Author

Curriculum Vitae, List of publications, Education statement

Curriculum Vitae

Ying Zhang was born on the 13th of August, 1977 in Xi'an, Shaanxi province, in China. She performed her undergraduate studies between 1996 and 2000 in Shaanxi Normal University, where she majored in biology. In 2000, she began her master studies in cell biology in the School of Life Sciences in East China Normal University in Shanghai. Afterwards, she continued as a PhD student in the same school until 2005. Because of family issue, she abandoned her PhD studies and moved to the Netherlands. From August 2006, she participated in a 5-month research training at Plant Research International, part of Wageningen University and Research center in Wageningen, The Netherlands. In January of 2007, she started a sandwich PhD program co-proposed by dr. Tijs Ketelaar (laboratory of Plant Cell Biology, Wageningen University) and Professor Chun-Ming Liu (Institute of Botany, Chinese Academy of Sciences) in the Laboratory of Plant Cell Biology of Wageningen University, From July 2011 to January 2012 she was employed by the Institute of Botany, Chinese Academy of Sciences, in Beijing, China, where she worked as cell biologist in prof. Chun-Ming Liu's laboratory. From February 2012 onwards, she joined Dr. Juan Dong's lab at the Rutgers University, USA as a post-doctoral researcher.

List of Publications

- Zhang Y , Liu CM, Emons AM, Ketelaar T (2010) The plant exocyst. J Integr Plant Biol 52: 138- 146.

- Zhang Y, Immink R, Liu CM, Emons AMC, Ketelaar T. The exocyst subunit SEC3A is essential for embryo development and accumulates in transient puncta at the plasma membrane. (Submitted)

Education Statement of the Graduate School

Experimental Plant Sciences
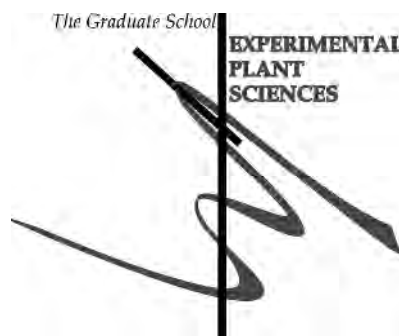
Issued to: Ying Zhang

Date: 14 November 2012

Group: Laboratory of Cell Biology, Wageningen University

1) Start-up phase	date
► **First presentation of your project**	
Oral presentation at Plant Cell Biology "Regulation and functioning of the putative plant exocyst complex"	16 Mar 2007
► **Writing or rewriting a project proposal**	
► **Writing a review or book chapter**	
A review " The plant exocyst", published in Journal of Integrative Plant Biology 2010, 52 (2): 138-146	13 Mar 2009
► **MSc courses**	
► **Laboratory use of isotopes**	
Subtotal Start-up Phase	*7,5 credits**

2) Scientific Exposure	date
► **EPS PhD Student Days**	
EPS PhD student day (3x), Wageningen University, Leiden University, Utrecht University	Sep 2007, Feb 2009 & Jun 2009
EPS the first joint retreat PhD students, Wageningen, The Netherlands	02 - 03 Oct 2008
The 2nd joint retreat of PhD students in Plant Sciences, Cologne, Germany	15 - 17 Apr 2010
► **EPS Theme Symposia**	
EPS theme 1 'Developmental Biology of Plants', Wageningen University	11 Oct 2007
EPS theme 1 'Developmental Biology of Plants', Leiden University	30 Jan 2009
EPS theme 1 'Developmental Biology of Plants', Wageningen University	28 Jan 2010
EPS theme 1 'Developmental Biology of Plants', Leiden University	20 Jan 2011
► **NWO Lunteren days and other National Platforms**	
ALW meeting 'Experimental Plant Sciences', Lunteren (5x)	Apr 2007, 2008,2009,2010 & 2011
Annual Dutch Meeting on Molecular and Cellular Biophysics (2x)	Sep 2009 & Oct 2010

► **Seminars (series), workshops and symposia**

EPS symposium on the plant endomembrane system, VU, Amsterdam	02 Jul 2010
Seminars (Gijsje Koenderink, Anja Geitmann, Lacey Samuels (2x), Staffan Persson, Koen Visscher)	Mar - Dec 2007
Flying seminar (Prof Scott Poethig, Prof Hiroo Fuduka)	Sep -Nov 2007
Seminar Michael Lampson	01 Feb 2008
Flying seminar Dr. Rick Vierstra	14 Apr 2008
Semina Dr. Chris Hawes	20 Aug 2010
Seminars in Beijing (Liwen Jiang, Pascal Genschik, Asaph Aharoni)	Nov - Dec 2011

► **Seminar plus**

Flying seminar (Prof. Hiroo Fuduka, Zhenbao Yang)	Nov 2007 & Jun 2008

► **International symposia and congresses**

EU COST E50 Workshop 'Systems Biology for Plant Design'	08 - 11 Jul 2009
Gordon conference: Plant and Microbial Cytoskeleton, Andover, the US	08 - 13 Aug 2010
National conference of plant biology, Tianjin, China	18 - 22 Jul 2010
9th International Botanical microscopy meeting	16 - 21 Apr 2011
2nd International symposium on Integrative Plant Biology, Lanzhou, China	26 - 28 Aug 2011

► **Presentations**

EPS theme 1 meeting (poster)	02 Apr 2007
ALW meeting 'Experimental Plant Sciences (2x poster)	Apr 2008 & Apr 2010
Gordon conference:Plant and Microbial Cytoskeleton, USA (poster)	08 - 13 Aug 2010
2nd International symposium on Integrative Plant Biology, China (poster)	27 Aug 2011
EPS theme 1meeting : 'Developmental Biology of Plants' (2x oral)	Jan 2009 & Jan 2011
the 2nd Joint Retreat of PhD students in Plant Sciences (oral)	16 Apr 2010
Annual Dutch Meeting on Molecular and Cellular Biophysics (oral)	05 Oct 2010
9th International Botanical Microscopy Meeting (oral)	18 Apr 2011
2nd International Symposium on Integrative Plant Biology, China (oral)	26 Aug 2011
China Agriculture University (oral)	21 Sep 2011

► **IAB interview**	04 Dec 2009
► **Excursions**	

Subtotal Scientific Exposure   *28,7 credits**

3) In-Depth Studies	*date*

► **EPS courses or other PhD courses**

PhD Summerschool, "Environmental signaling: Arabidopsis as a model"	27 - 29 Aug 2007

	PhD course, Gateway to gateway technology	17 - 21 Nov 2008
►	**Journal club**	
	Paticipation of PCB Journal club	2007-2011
►	**Individual research training**	
	Subtotal In-Depth Studies	*5,1 credits**

4) Personal development		*date*
►	**Skill training courses**	
	Ph.D competence assessment	30 Jan 2007
	Techniques for writing and presenting a scientific paper	11 - 14 Dec 2007
	Career perspectives	Oct - Nov 2010
►	**Organisation of PhD students day, course or conference**	
►	**Membership of Board, Committee or PhD council**	
	Subtotal Personal Development	*3,0 credits**

	TOTAL NUMBER OF CREDIT POINTS*	**44,3**

Herewith the Graduate School declares that the PhD candidate has complied with the educational requirements set by the Educational Committee of EPS which comprises of a minimum total of 30 ECTS credits

* A credit represents a normative study load of 28 hours of study.